Erasmus Mundus MSc Programme

Coastal and Marine Engineering and Management

CoMEM

Wave Attenuation by Global Coastal Salt Marsh Habitats

Delft University of Technology
June 2016

Gerald Songy
4434455

The Erasmus Mundus MSc Coastal and Marine Engineering and Management is an integrated programme organized by five European partner institutions, coordinated by Norwegian University of Science and Technology (NTNU).

The joint study programme of 120 ECTS credits (two years of full-time study) has been obtained at three of the five CoMEM partner institutions:

- Norges Teknisk – Naturvitenskapelige Universitet (NTNU) Trondhiem, Norway
- Technische Universiteit (TU) Delft, The Netherlands
- City University London, Great Britain
- Universitat Politècnica de Catalunya (UPC), Barcelona, Spain
- University of Southampton, Southampton, Great Britain

The first year consists of the first and second semesters of 30 ECTS each, spent at NTNU, Trondheim and Delft University of Technology respectively. The second year allows for specialization in three subjects and during the third semester courses are taken with a focus on advanced topics in the selected area of specialization:

- Engineering
- Management
- Environment

In the fourth and final semester an MSc project and thesis must be completed. The two year CoMEM programme leads to three officially recognized MSc diploma certificates. These will be issued by the three universities which have been attended by the student. The transcripts issued with the MSc Diploma Certificate of each university include grades/marks for each subject. A complete overview of subjects and ECTS credits is included in the Diploma Supplement, as received from the CoMEM partner university, Delft University of Technology (TU Delft).

Information regarding the CoMEM programme can be obtained from the programme coordinator and director:

Dr. ir. øivind A. Arntsen
Associate Professor in Marine Civil Engineering
Deputy Head, Department of Civil and Transport Engineering
NTNU Norway
Telephone: +4773594625 Cell: +4792650455 Fax: +4773597021
Email: oivind.arntsen@ntnu.no

Wave Attenuation by Global Coastal Salt Marsh Habitats

Gerald M. Songy

A thesis presented in partial fulfillment of the requirements for the degree of Master of Science in Civil Engineering within the Coastal and Marine Engineering and Management (CoMEM) program

Delft University of Technology

Delft, the Netherlands

Submitted for approval on

June 20, 2016

Graduation Committee:

Prof.Dr.Ir. Reniers, A.J.H.M.	Delft University of Technology (Chairman)
Dr. van Wesenbeeck, B.K.	Deltares/Delft University of Technology
Dr.Ir. Dijkstra, J.T.	Deltares
Ir. Vuik, V.	Delft University of Technology

TU Delft

Deltares
Enabling Delta Life

Preface

This thesis concludes my MSc studies in the Coastal and Marine Engineering and Management program where I studied at the Norwegian University of Science and Technology (first semester), The University of Southampton (third semester), and Delft University of Technology (second and fourth semesters). I would like to thank those involved in the organization and administration of this program, since it provided me with such a great experience and opportunity to learn about coastal engineering and different cultures both in Europe and worldwide.

I would also like to thank all of my CoMEM classmates: Alejandra, Ana, Athul, Dennis, Ilija, John, Kyle, Said, Stuart, Thevaher, and Yahia, for the many good memories over the duration of this program. Special thanks goes to Stuart, for his willingness to assist me with many different components of my thesis work and studies during the duration of the program; and to John, for deciding to accompany me and leave Louisiana in order to obtain a graduate degree in coastal engineering in Europe.

I would like to thank Deltares for giving me the opportunity to perform this research as an intern at their facilities for the past several months. I was fortunate to be selected for a research topic that I could perform abroad while being highly relevant and applicable to the coastline of my home, Louisiana. I would additionally like to thank Alessio Giardino and Kees den Heijer of Deltares for their assistance and advice on Bayesian Networks and the Netica program; and Robert McCall, for his assistance with the XBeach modeling software.

I would also like to thank my graduation committee for their valuable feedback, patience, and encouragement throughout the duration of this research. Professor Reniers, Bregje, Jasper, and Vincent formed an intelligent and well-rounded committee who I enjoyed learning from. A special thanks to Jasper, who was very patient with me and always provided assistance whenever I had any questions regarding modeling or programing. I would also like to thank Vincent for sharing data from the BE SAFE study for the calibration phase of my research; and Bregje, for sharing data from the Hannover flume study which was used for additional model testing.

In addition, I would like to thank those individuals who introduced me to the field of coastal engineering and who motivated me to obtain a graduate degree in this field of study - especially my father, Ron Rodi, Dr. Clint Willson, Dr. Ranjit Jadhav and all of the individuals who I worked under and alongside at the Coastal Protection and Restoration Authority (CPRA) of Louisiana.

I would like to thank my family and especially my parents for their encouragement, support, and for always believing in me. Lastly, I would like to thank Meg for her patience, understanding, good attitude, and support from many miles away throughout the duration of this program.

Gerald Songy
Delft, June 2016

Abstract

Across the world, the presence of humans in coastal regions is constantly increasing. Today, approximately half of the world's population lives within 60 kilometers of the ocean, and three fourths of the large cities in the world are located on the coast (UNEP, 2016). Based on IPCC predictions (2013), sea level rise is projected to increase by at least 0.28 – 0.61 meters by the year 2100. This poses a serious threat for the global population inhabiting these coastal regions, since they will be more prone to coastal erosion and catastrophic flooding as a result (Gedan *et al.*, 2011). In many of these coastal locations, vegetation is present, and often times acts as a buffer zone between hard (man-made) defense structures (Spalding *et al.*, 2014). The presence of these vegetation forms could greatly reduce maintenance costs for coastal defense structures, and be more adaptive to changing local conditions. In addition, the idea of incorporating more "hybrid" flood defense measures around the world is valued because a vegetated foreshore can greatly reduce wave energy by depth-induced wave breaking, bottom friction, and attenuation by the vegetation itself (Vuik *et al.,* 2016).

In this study, a numerical model (XBeach-vegetation) and statistical Bayesian Network (Netica) was developed for the simulation and quantification of wave attenuation for various combinations of global salt marsh characteristics and extreme hydraulic conditions. The purpose of this modeling effort was to test the ability of the numerical model and statistical model in properly simulating salt marsh-hydraulic interactions which occur around the world. Additionally, testing of the ability of this model to quantify wave attenuation over salt marsh habitats while under extreme hydraulic conditions (high wave heights and water levels) was performed. First, the numerical model was calibrated, tested, and validated based on both a field and flume study which measured wave attenuation over natural salt marsh. Next, the numerical model was used to produce many results for wave heights at various locations over a salt marsh platform. These results produced a dataset which was input into a Bayesian Network (BN) for further organization and quantification of wave attenuation by global salt marshes. Finally, the salt marsh components were tested for their influence on the BN, and the results were compared to the Xbeach-vegetation results for several cases in order to provide an example of how each method produces results.

Initially, the numerical model was calibrated and validated based on wave data which was provided by members of the BE SAFE study and was recorded during a winter storm in 2015 at Hellegat Polder, Western Scheldt, the Netherlands. The numerical model simulated the recorded wave heights accurately, and proved to be effective in reproducing results for extreme hydraulic conditions recorded at Hellegat. Additionally, the numerical model was tested on the conditions of the Hannover wave flume study, which generated extreme waves in one of the largest wave flumes around the world, in order to measure wave attenuation by a 40 meter section of natural salt marsh at the end of the flume.

Once the model was calibrated and validated, the set-up for a batch of numerical model simulations took place. In order to assign inputs which were representative of global coastal salt marsh habitats, data was collected from many sources to form a database. Next, the numerical model was set-up in order to simulate waves occurring over an arbitrary salt marsh platform for many different salt marsh characteristics and hydraulic conditions. Wave heights were obtained at five distances across the salt marsh platform, and the results were input into a BN for further data handling.

The BN (Netica) was used to structure and organize the data into a compiled network, which was completed before the network could be used further. Once the network was compiled, the various salt marsh characteristics and hydraulic conditions were varied within the network in order to see which characteristics and conditions were most likely to produce certain wave heights at various distances throughout the salt marsh platform. The influence of each characteristic and parameter could additionally be quantified in a probabilistic manner using the network. In selecting the various

values within each node of the BN separately, an assessment could be performed in order to see the influence of each salt marsh component on the resulting wave heights. The results produced by both the Netica program and the Xbeach-vegetation model were presented in order to show a comparison of how each method presents the results. Finally, a sensitivity analysis of the various salt marsh characteristics was performed to obtain knowledge on how these components influenced resulting wave heights. Once all of this was completed, conclusions were made based on the results, and recommendations were provided for the improvement of future research efforts within this field.

Table of Contents

1 Introduction

1.1 Background

Across the world, the presence of humans in coastal regions is constantly increasing. Today, approximately half of the world's population lives within 60 kilometers of the ocean, and three fourths of the large cities in the world are located on the coast (UNEP, 2016). Based on IPCC predictions (2013), sea level rise is projected to increase by at least 0.28 – 0.61 meters by the year 2100. This poses a serious threat for the global population inhabiting these coastal regions, since they will be more prone to coastal erosion and catastrophic flooding as a result (Gedan *et al.*, 2011).

The increase in population density around the world means that the impact of sea level rise will also significantly increase the maintenance costs of coastal infrastructure, which traditionally relied on hard structures for flood defense. In recent years, attention has been given to the idea of combining coastal ecosystems (soft measures) with traditional hard structures (e.g. seawalls) to form a "hybrid" coastal defense (Figure 1). The potential for this exists across the world, since low lying coastal ecosystems commonly contain vegetation between the open ocean and hard defense structures (Spalding *et al.*, 2014). Coastal ecosystems can not only contain coarser sediment of sandy foreshores and dunes that grow vegetation, but also finer sediments that typically promote the growth of mangroves, sea grasses, and salt marshes. The idea of incorporating more "hybrid" flood defense measures around the world is valued because a vegetated foreshore can greatly reduce wave energy by depth-induced wave breaking, bottom friction, and attenuation by the vegetation itself (Vuik *et al.,* 2016). In Figure 1, examples of coastlines having minimal, natural, managed realignment, and hybrid coastal defense schemes are displayed.

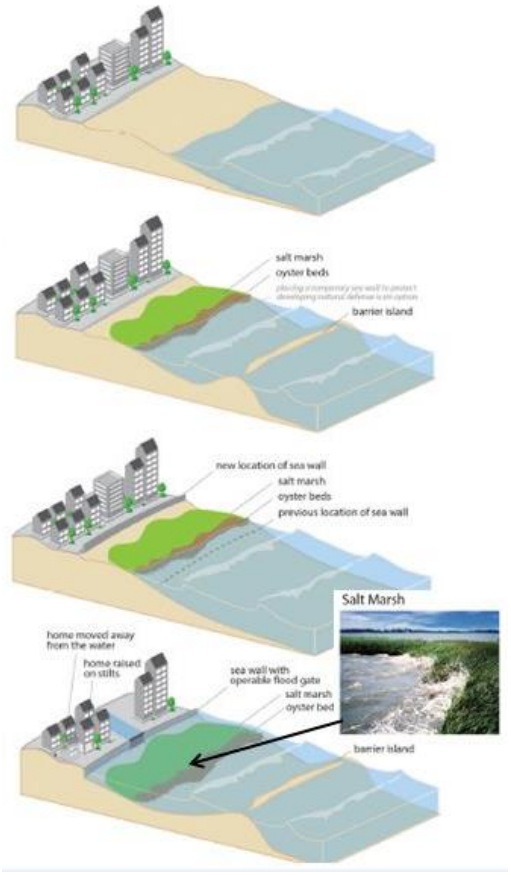

Figure 1: Coastal defense examples which include minimal defense (top), natural measures (second from top), managed realignment (third from top), and hybrid defense measures (bottom) (modified from Sutton-Grier *et al*., 2015).

The hybrid defense method, which is the method displayed at the bottom of Figure 1, has become increasingly popular in recent years. This is because when hard and soft defense elements are combined, the resulting costs are lower and the defense measure is more adaptable to changing conditions (i.e., sea level rise, increasing storminess, land subsidence) (Möller *et al.*, 2014). In addition, coastal ecosystems containing vegetation serve several functions, such as: providing habitat for numerous species, creating sheltered environments for sediments to settle and accrete, and reducing the risk of flooding by reducing wave heights (van Rooijen, *et al.*, 2015). Since it is widely known that these vegetated foreshores have the ability to attenuate waves, more research effort has been made in recent years to quantify this ability so that it can be included in flood defense measures.

The focus of this research will involve global salt marsh habitats and their ability to attenuate waves. Salt marshes have the potential to serve as a buffer zone, which can reduce the impacts of waves for anything that exists behind them. In Figure 2, a global salt marsh and mangrove distribution is displayed.

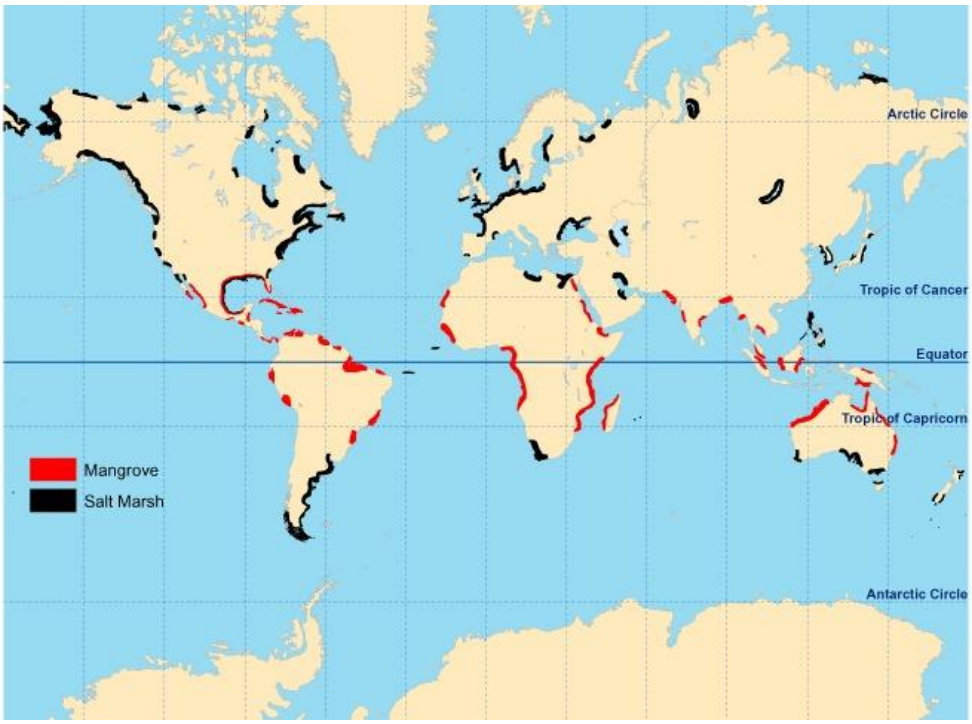

Figure 2: Global salt marsh distribution with areas of mangrove existence in red and areas containing salt marshes in black (Research Gate, 2016).

Figure 2 displays the wide range of locations where salt marsh habitats can be found around the world. Although salt marshes are abundant in many locations, little quantitative data is currently available that provides information on their physical properties and their interaction with extreme storm events and hydraulic conditions.

1.2 Motivation and Research Goal

1.2.1 Problem Statement

Hydraulic forcing and flooding from extreme storm events is a large risk for coastlines around the world. These regions are often times exposed and of low elevation, which makes them vulnerable to even small storm events. Some coastal regions do have hard protection measures such as seawalls and levees, but these structures can fail if storm conditions surpass the local design threshold (Anderson *et al.*, 2011).

It is known that coastal salt marsh habitats around the world have the ability to attenuate waves and reduce storm surge, but efficient and accurate analysis of global salt marshes and their ability to be incorporated into flood defense measures is currently lacking on a large scale. Additionally, the ability of marshes to protect a coastline while under stress during extreme storm events while high waves and water levels occur is not well known. The complexity of salt marsh habitats makes it difficult to have a standard approach for analyzing them and incorporating them into coastal flood defense measures, especially since their characteristics vary from one location to another. Additionally, conditions from one location to another can be different (e.g., tidal range, climate, storminess, sediment type, etc.). One additional impact is the varying state of the marsh from summer to winter, which is particularly prominent for areas located in higher latitudes.

Increasing understanding of how coastal salt marsh characteristics (i.e., slope of marsh platform, stem: height, density, diameter) play a role in reducing wave heights during extreme storm events around the world is necessary for moving forward in this research area. If more knowledge can be gained on which salt marsh characteristics enable a coastline to be effective in reducing wave heights and quantifying how effective a certain coastline is at attenuating wave heights, then perhaps the role of salt marsh and other coastal vegetation species in nature-based or hybrid flood defense measures could be increased.

1.2.2 Objective

The objective of this thesis is to improve understanding of how effective various salt marsh species around the world are at attenuating waves while being impacted by extreme hydraulic conditions, such as high water levels (e.g., storm surge[1]) and extreme wave heights. The following main research question will be answered through the research of this topic:

- Can wave attenuation by global coastal salt marsh habitats be efficiently quantified for extreme hydraulic conditions?

In addition, an attempt will be made to answer the following sub-questions:

- Is the XBeach-vegetation model in combination with a statistical Bayesian Network (Netica) an effective and efficient method to quantify wave attenuation by global coastal salt marshes?
- Can relationships be made between various salt marsh characteristics, hydraulic conditions, and wave attenuation?

1.2.3 Research Approach

A model quantifying wave attenuation by coastal salt marshes for global application will be developed. Available recorded wave data which recorded wave heights at various distances over a salt marsh during both a field study and a wave-flume study will be used to calibrate, test, and validate the numerical model (XBeach). The numerical model will then be used to produce results based on many simulations to obtain wave heights at various cross-shore locations over a salt marsh profile for a range of values for various global salt marsh characteristics and hydraulic conditions. The results of the numerical model will be input into a Bayesian Network (BN) using the Netica program. The discussion will focus on which characteristics of a coastline contribute to the most wave attenuation, so that connections can be made for application on other coastal salt marsh habitats around the world. The results obtained from the numerical model will be compared both before and after input into the BN in order to gauge how well the BN represents and quantifies the wave height results from the dataset. The method used for this research will also be analyzed to ensure that the physical processes are properly incorporated while simultaneously providing results

[1] Storm surge is when water can build up at a given coastline during a storm and elevate the still water level without the effect of waves (Bosboom and Stive, 2015).

to end-users (e.g., governmental agencies, NGOs, industry consultants, and citizens) in a clear manner.

1.2.4 Report Structure

In this initial chapter, information on the background of salt marshes and the research objective were discussed. Chapter 2 of this report reviews prior work on salt marsh ecology and existence around the world, and studies on wave attenuation by salt marshes (laboratory, field, and modeling efforts). Chapter 3 discusses the set-up of a numerical model used for simulating wave attenuation by salt marsh. In chapter 4, the model calibration, testing, and validation will be discussed, and some model results will be presented. Chapter 5 describes the statistical BN(Netica) model set-up, which includes sections on BN theory, data collection, XBeach-vegetation simulations (for BN input), and BN results. Finally, discussion of the results will occur in Chapter 6, followed by conclusions and recommendations for the improvement of future research efforts within this field in Chapter 7.

2 Literature Review

2.1 Salt Marsh Ecology and Presence Around the World

Salt marshes rest in the intertidal region between high and low tide levels (Figure 6), and are often fronted by a mudflat. Their formation can occur in several ways, which include: forming over terrestrial habitats as sea levels rise, expanding over previous sub-tidal habitats by capturing sediments, and being raised into the intertidal zone. They can form in coastal regions of almost all latitudes, but in the tropical regions mangrove forests mostly replace them (Pennings and Bertness, 1999). However, this does not mean that salt marshes cannot exist in these regions. For instance, in tropical regions salt marshes can be located inland from mangrove species in northern Australia and beside mangroves in the coastal regions of Mexico. They can exist as far north as the subarctic and are widespread especially near the James and Hudson Bays of Canada, covering roughly 300,000 km^2. They have a range of different stem properties (height, diameter, density, stiffness) which are all important when studying their ability to attenuate waves and reduce storm surge.

In coastal areas, salt marshes are typically protected from direct wave impact by the presence of barrier islands or because of their location within an estuary or a bay. Some coastal salt marshes can however be directly impacted by ocean waves in locations such as the Gulf of Mexico coast, Louisiana, west Florida, the coast of the Netherlands, and the north Norfolk coast of Britain.

Salt marshes encounter daily and seasonal water level changes from tides, freshwater sources (e.g., rivers and precipitation), and storm surge. In North America, salt marshes are primarily located on the Atlantic coast and the Gulf of Mexico. In the North Atlantic coastal region (i.e. coasts of Labrador, Nova Scotia, and Newfoundland), salt marshes can be found within river deltas and in locations where the wave energy is low (less than 2 meters amplitude). When looking south of this region located on the continent of North America, salt marshes can be classified based on three main types:

1. The Bay of Fundy marshes in Canada: Influenced hydrologically by rivers and a high tidal range of up to 11 meters that has a foundation composed of red silt.
2. The New England marshes (Maine to New Jersey): Foundation composed of marsh peat and marine sediments.
3. The Coastal Plain marshes: Extend from New Jersey in the southern direction, along the Atlantic and Gulf of Mexico, and ending at the coast of Texas. The tidal range experienced by these marshes is lower than those experienced by the two previously mentioned salt marsh types. Additionally, the source of silt in this region is much higher. The Mississippi River delta wetlands, which contain the largest area of salt marshes in the U.S., are also included in this classification.

All three of the previously mentioned salt marsh types are mostly composed of *Spartina alterniflora*, which can be viewed in Figure 3. This marsh type mostly exists on the seaward edge of salt marsh habitats, since it has the ability to withstand high water salinity levels, and longer periods of inundation.

Figure 3: *Spartina alterniflora* (cordgrass), the typical species of salt marsh found along many U.S. east coast and Gulf of Mexico salt marshes (Cronk and Fennessy, 2001).

The *S. alterniflora* can often be found in two different forms that are present in the same salt marsh habitat: short and tall forms. The short form (10 to 80 cm) typically grows inland from the tall form (1 to 3 m), which exists along tidal creeks and is situated closest to the sea, in the lowest areas of the marsh.

In many coastal regions of the eastern U.S. and Gulf coast, salt marsh habitats have a layer of *Spartina patens* (salt marsh hay), that is located inland from the zone of *S. alterniflora.* Additional salt marsh species can exist along the east coast of the U.S., such as: *Juncus gerardii* (rush), *Distichlis spicata* (spike grass), and *Salicornia europaea* (glasswort)(Cronk and Fennessy, 2001). In Figure 4, an approximate distribution of various types of *Spartina* found in the U.S. is provided.

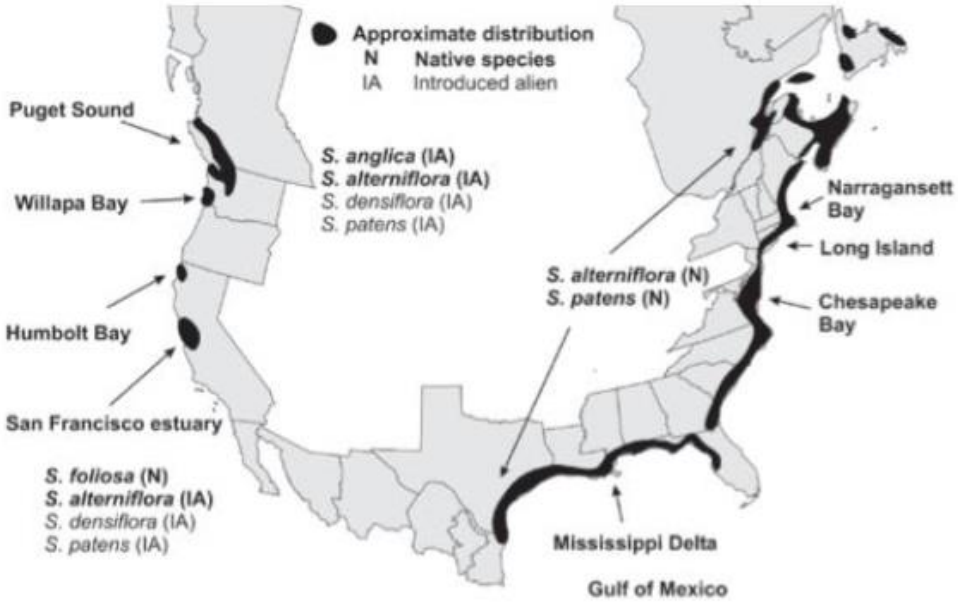

Figure 4: Approximate distribution of *Spartina* salt marshes in the U.S. (Doody, 2008)

In viewing Figure 4, it is evident that the U.S. has potential for incorporating hybrid flood defenses in many coastal locations, especially since many of these areas have a large population density within the coastal zone.

In the Pacific coastal region of the U.S. and Canada, salt marshes are less abundant, and this is mostly due to the geophysical conditions being unsuitable for the formation of salt marsh habitats (e.g., heavy surf, narrow continental shelf, mountainous terrain). In addition, the shoreline in this region is rising, and few river deltas and estuaries are present to provide good conditions for salt marsh formation. Many of the salt marsh habitats that previously existed have been filled for land development. However, some salt marshes habitats do still exist in protected bays and estuaries along the Pacific coast such as: Tijuana Estuary near San Diego, the northern region of San Francisco Bay, Tamales Bay north of San Francisco, Nehalem Bay in northern Oregon, Puget Sound in Washington, at the head of fjords and on the Queen Charlotte Islands in British Columbia, and in Cook Inlet close to Anchorage, Alaska (Cronk and Fennessy, 2001). The locations of some of the previously mentioned salt marsh habitats can be found in Figure 4.

In northern and Western Europe, salt marshes are located along the Atlantic coasts of Ireland, France, Portugal, Spain, and additionally the North and Baltic Seas. In the southern region of Europe, salt marshes can be found in the watershed of the Mediterranean Sea and the Rhone River delta. Additional locations of salt marshes in the Mediterranean include: the Tunisian, Moroccan, and Algerian coasts on the coast of Northern Africa. In Europe, the seaward zones of salt marsh habitats commonly are fronted by a tidal mudflat containing little vegetation. In Figure 5, the distribution of *Spartina Anglica* around Europe can be found.

Figure 5: Distribution of *Spartina Anglica* in Europe (http://www.europe-aliens.org/pdf/Spartina_anglica.pdf)

The reasoning for the difference between salt marsh characteristics in the U.S. and Europe is mainly due to the differences in tidal range. In Europe, tidal ranges can reach 15 meters, so some areas of marshes in Europe are seldom flooded with their highest marshes only being flooded during spring tides. For the eastern coast of North America, however, the salt marshes are mostly flooded twice per day by a much lower tidal range. This difference in tidal range between the U.S. and Europe causes the lower areas of salt marsh habitats in Europe to contain different species, which include: *Spartina maritima* (Portugal), *Salicornia europaea* and *Spartina anglica* in France and the United Kingdom, and *Salicornia dolichostachya* in the Netherlands (Cronk and Fennessy, 2001). For a better understanding of the typical zonation of salt marsh species, refer to Figure 6.

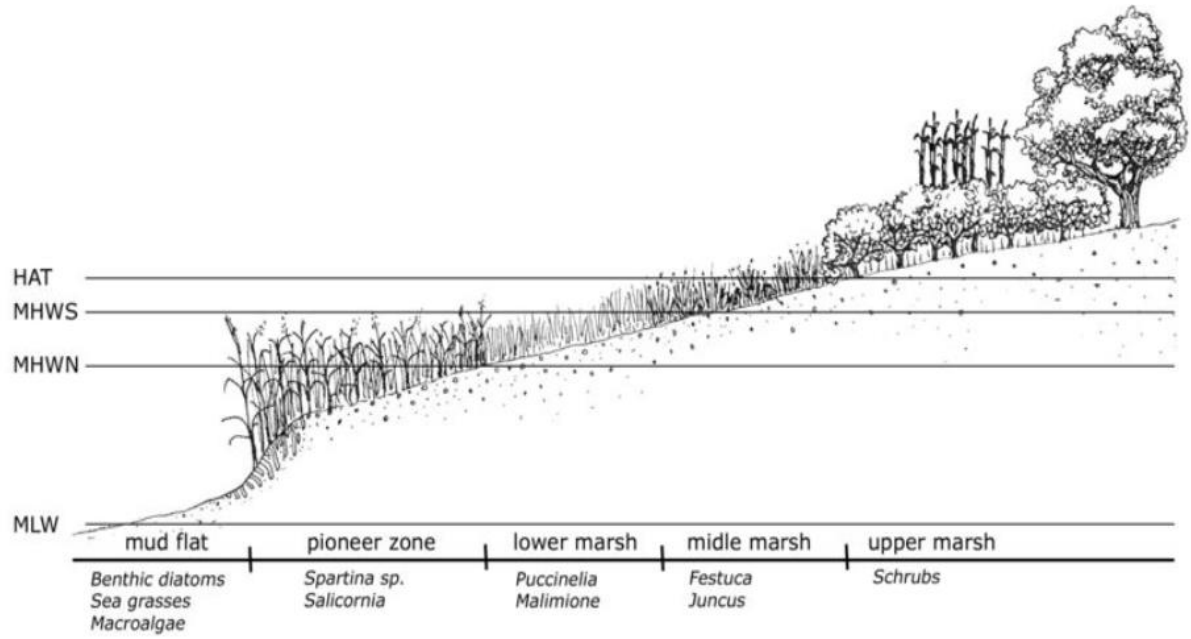

Figure 6: Typical zonation of salt marsh species (http://www.theseusproject.eu/wiki/File:Figure_salt-marsh_zonation.JPG).

Based on Figure 6, it can be noticed that salt marshes interact with changing water levels constantly. Salt marshes are able to withstand high salinity, tidal flooding, and limited wave forces. Additional natural disturbances can include: ice, herbivores, nutrient input, floating debris, fire, and sediments. At higher latitudes, marshes experience severe disturbances, because winter ice can erode marsh soils and highly seasonal climate produces plant debris (called wrack) that can smother and kill marsh plants (Figure 7). For instance, in southern New England (USA), ice sheets of up to 30 cm thick can cover intertidal marsh habitats during severe winters. These ice sheets can freeze water-logged, low-marsh soils which may be lifted up in large, intact sections during high tides. Ice damage to salt marsh structure can also occur in Arctic Alaska and Atlantic Canada, and it is so severe in these locations that it limits the development of low marsh. At lower latitudes, ice disruption is not a large factor, and therefore sediment deposition is mostly uninterrupted (Pennings and Bertness, 1999).

Figure 7: Wrack, which is dead floating plant material, commonly settles on salt marshes during high spring tide events. This process harms the section of a salt marsh plants that are situated under the newly deposited wrack material (NOAA, 2008).

In addition to salt marshes being impacted by the previously mentioned disturbances, the seasonal variability can have a great impact on a given salt marsh habitat around the world. Evidence of seasonal impacts this can be seen when looking at the variation between the two different states of a salt marsh in Bath, Western Scheldt, the Netherlands (Figure 8). Additional information on the general location of this salt marsh can be seen in Figure 14.

Figure 8: The seasonal variability of a salt marsh coastline composed of the species *Scirpus maritimus* in Bath, Western Scheldt, the Netherlands in July of 2014 (left) and November of 2014 (right) (Vuik *et al*., 2016)

In some regions of the world, such as Bath, the winter season can be harsh on salt marsh habitats, causing their stem heights and densities to decrease significantly. This means that their ability to attenuate waves is lessened in the winter months, which can be an important consideration when attempting to incorporate salt marshes into flood defense design in the future.

2.2 Wave Attenuation by Salt Marshes and Other Vegetation

In addition to salt marshes being valued and studied for their ecological benefits, they have also been studied to better understand their ability to attenuate waves. By studying wave height reduction over salt marshes through laboratory, field, and modeling work, knowledge has been gained on the physical interaction between waves and vegetation. The purpose of these studies was to make a quantified connection between different properties of salt marshes (plant stem: density, height, and diameter) and wave attenuation so that salt marshes could serve a role in future flood defense efforts.

2.2.1 Laboratory Studies

The interaction between vegetation and waves has been studied in laboratory conditions by using both natural and artificial plants. Natural salt marsh was used in three studies found in literature (Fonseca and Cahalan, 1992; Tschirky *et al*., 2000, Möller *et al.*, 2014) while several have used artificial elements to represent vegetation (Dubi and Tørum, 1996; Løvås and Tørum, 2000; Lima *et al.,* 2006; Augustin *et al.*, 2009; Cavallaro *et al.*, 2010). A list of these various studies performed along with the type of vegetation can be seen in Table 1. Generally, the idea behind these experiments is to vary only one parameter at a time and keep all others constant in order to clearly show the result of varying the desired parameter of study.

Table 1: Various flume experiments and their vegetation types (modified from Anderson *et al.*, 2011).

Reference	Element
Fonseca and Cahalan (1992)	harvested *Halodule wrightii, Syringodium filiforme, Thalassia testudinum, Zostera marina* (all sea grass species)
Dubi and Tørum (1996)	plastic *Laminaria hyperborea*
Tschirky *et al.* (2000)	harvested *Scripus americanus*
Løvås and Tørum (2000)	plastic *Laminaria hyperborea*
Lima *et al*. (2006)	flexible nylon rope for *Brachiaria subquadripara*
Augustin *et al.,* (2009)	cylindrical wooden dowels for *Spartina alterniflora*
Cavallaro *et al.*(2010)	polyethylene (*Posidonia oceanica*)
Möller *et al.,* (2014)	*Puccinellia, Elymus*

In reviewing these laboratory experiments, many things can be learned and are worth mentioning regarding their findings. Fonseca and Cahalan (1992) looked at four species of sea grasses and evaluated them for their ability to reduce wave energy for various combinations of stem density, and water depths over a 1 meter test section in a wave tank. They found that the percent wave energy reduction per meter due to sea grasses equaled 40 %. They also concluded that a low rate of wave attenuation over a vegetation field can be significant when occurring over large distances. Lima *et al.* (2006) found that increasing stem density greatly increases attenuation percentage per meter.

Several of the studies used relative stem length as a reference, which is the portion of the water column where vegetation is present (ratio of the stem length (l_s) to water depth (h). It was found repeatedly that as this ratio exceeded 1 (emergent conditions), wave attenuation increased, and as the relative stem length decreased below 1 (submerged conditions) wave attenuation decreased (Anderson *et al.*, 2011). Tschirky *et al.* (2000) concluded with five main points regarding their research. These include: 1) wave attenuation increased as plant beds increased, 2) more wave attenuation occurred for higher stem densities, 3) attenuation was larger for larger incident waves, 4) attenuation changed inversely with water depth, 5) a clear relation between wave attenuation and wave period could not be made.

The study performed by Möller *et al.* (2014) used one of the largest wave flumes in the world in order to measure wave attenuation for storm surge conditions. The study used natural vegetation that was excavated from the coast of northern Germany, and generated waves of up to 0.9 meters and water depths of up to 2 meters over the base of the marsh plant stems. For even the most extreme conditions, the salt marsh was found to decrease the incident wave heights by approximately 20% over a span of 40 meters (see Figure 20). The findings of this study advanced understanding on the performance of salt marshes under extreme hydraulic conditions (storm conditions), which is when knowledge on wave attenuation by salt marshes is most important. In the following section, the relevant field studies found in the literature which researched wave attenuation will be provided.

2.2.2 Field Studies

Several field studies have been performed in order to build on knowledge gained from flume studies. The majority of the field studies performed in the past involve measuring wave attenuation for mild and low-wave conditions (wind-generated waves). In recent years, there has been an attempt to record extreme wave conditions in the field so that the presence of salt marshes can be incorporated into flood defense schemes. Listed in Table 2 are relevant field studies which measured wave attenuation in the past.

Table 2: The various field studies found in the literature which focus on wave attenuation by vegetation (modified from Anderson *et al.*, 2011)

Reference	Transect Length (m)	Dominant Plant Species
Wayne (1976)	20	*Spartina Alterniflora*
Knutson *et al*., (1982)	30	*Spartina Alterniflora*
Möller and Spencer (2002)	163	*Aster, Suaeda, Puccinellia, Salicornia, Limonium spp.*
	10	*Aster, Suaeda, Puccinellia, Salicornia, Limonium spp.*
Cooper (2005)	300	*Puccinellia maritima, Salicornia europaea*
	250	*Atriplex portulacoides, Spartina alterniflora*
	110	*Atriplex portulacoides, Salicornia europaea*
Möller (2006)	10	*Spartina anglica, Salicornia spp.*
	10	*Spartina anglica, Salicornia spp.*
	10	*Salicornia spp.*
Lövstedt and Larson (2010)	10	*Phragmites australis (reeds)*
Yang *et al.,* (2012)	50	*Scirpus & Spartina alterniflora*
Jadhav and Chen (2013)	28	*Spartina Alterniflora*
Vuik *et al.*, (2016)	50	*Spartina Anglica*

The majority of the studies in Table 2 studied wave attenuation by salt marshes for mild hydraulic conditions, while in recent years more extreme conditions have been researched (Yang *et al.,* 2012; Jadhav and Chen, 2013; Vuik *et al.*, (2016)).Yang *et al.* (2012) quantified wave attenuation at an exposed macro tidal coast in the Yangtze Estuary, China. The marsh transect was roughly 50 meters in length, and wave heights observed at this location reached 0.73 meters, with over-marsh water depths up to 1.61 meters. The study performed by Jadhav and Chen (2013) measured wave attenuation during a tropical storm over a 28-meter transect of marsh situated on the northern shore of Terrebonne Bay in Louisiana, USA. Wave heights of nearly 0.4 meters were recorded, with over-marsh water depths reaching 0.8 meters. Vuik *et al*. (2016) measured wave attenuation over a marsh transect of roughly 50 meters at Hellegat Polder, Western Scheldt, the Netherlands. Significant wave heights of up to 0.69 meters were recorded at this site, with over-marsh water depths reaching 1.86 meters.

Figure 9 shows the wave attenuation rate (*r*) for several different studies that have measured attenuation related to the distance across which it was measured. This value can be found by calculated using the following equation:

$$r = \frac{(\frac{h_1 - h_2}{h_1})}{x} \quad (1)$$

where *r* is the rate of attenuation, h_1 is the initial height of the wave, and h_2 is the height of the wave after crossing distance *x*. The majority of the studies performed have looked at attenuation due to wind waves, while some others have looked at attenuation for more extreme waves produced by

storm events. In Figure 9, the wave attenuation rates calculated for several studies involving wave attenuation by vegetation for both wind waves and storm surge waves is provided.

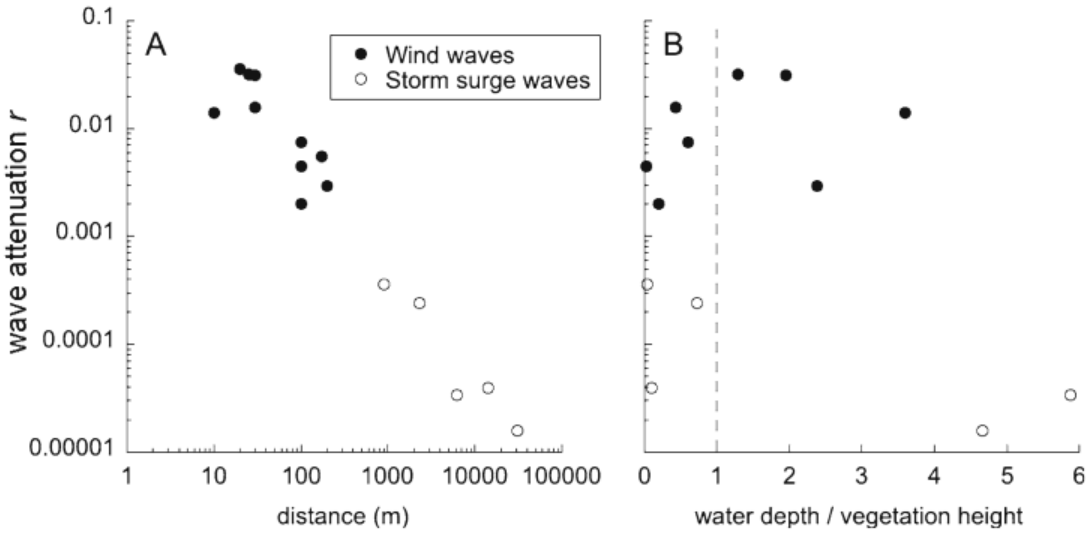

Figure 9: Measured wave attenuation *r* related to the distance across which it was measured (A) and in (B) the ratio of water depth to vegetation height (Gedan *et al.,* 2011).

Figure 9 shows that storm surge waves can be attenuated by salt marshes, but longer distances of salt marsh are needed to account for the larger waves and water levels[2]. In the following section, modeling efforts that have been performed for studying wave attenuation by vegetation are reviewed.

2.2.3 Modeling Wave Attenuation by Vegetation

The incorporation of vegetation into numerical models is a young field, but has become more common recently and has proved to be effective. Most of the models used for this purpose incorporate an empirical drag coefficient (C_D) in order to estimate drag forces caused by waves on the plant stem. Although in nature salt marshes are known to have flexibility and sway, when modeling the physical interaction between waves and salt marshes such as *Spartina alterniflora* it is necessary to consider the plant stems as rigid, vertical cylinders. In Figure 10, a schematic is shown of the typical parameters used for wave-vegetation modeling. The parameters include: average stem spacing (Δs), average stem diameter (d), average stem length (l_s), average stem density (N, [stems/m^2]), and the total horizontal force per unit volume on a stem array (F_x), and the water depth (h).

[2] This idea is especially relevant for low-lying coastal areas containing gradual slopes that are prone to storm surges.

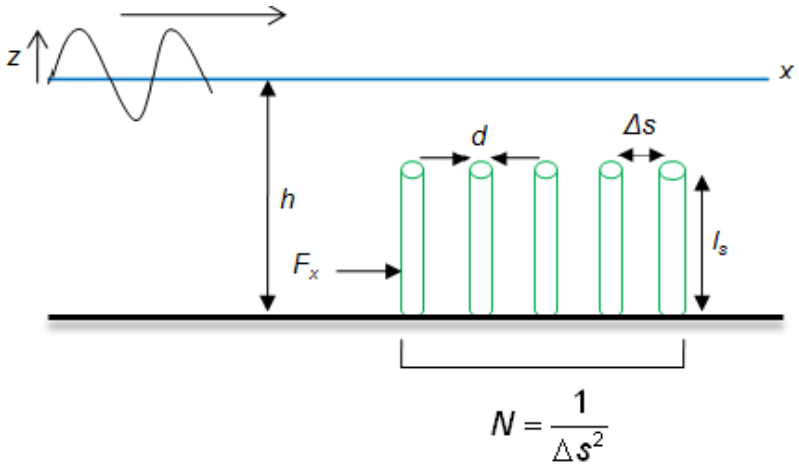

Figure 10: Model input parameters for vegetation (Anderson *et al.*, 2011).

Using the parameters in Figure 10, the wave attenuating ability of a salt marsh can best be estimated through modelling efforts. Now that a general description on modelling wave-vegetation interaction has been provided, the equations used to compute the physical processes involved in this interaction will be listed below.

The wave energy equation of conservation through a vegetation field can be listed as:

$$\frac{\partial E c_g}{\partial x} = -\varepsilon_v \tag{1}$$

Where *E* represents the wave energy density, c_g is the group velocity of the wave, and ε_v is the time-averaged rate of energy reduction caused by vegetation per unit of horizontal area (van Rooijen *et al.*, 2015). A common practice is to use the time-averaged wave energy loss as the work that is performed by the waves on the vegetation as a function of the wave-induced drag force:

$$\varepsilon_v = \overline{\int_{-h}^{-h+\alpha h} F(z)u(z)dz} \tag{2}$$

Where *h* is the water depth, αh is the vegetation height, *F* is the horizontal component of the force that acts on the vegetation per unit of volume, and *u* is the horizontal velocity. The over-bar means that this equation is averaged over time. Since the plant swaying motion and inertial forces are neglected for these calculations, the force induced by plants can be written as:

$$F = \frac{1}{2}\rho C_D b_v N u|u| \tag{3}$$

Where ρ is the water density, C_D is a drag coefficient, b_v is the vegetation stem diameter, *N* is the vegetation density, and *u* is the orbital velocity. Linear wave theory can be applied to solve for the horizontal velocity component, which is an expression created by Dalrymple *et al.* (1984) for the time-averaged energy dissipation for regular waves travelling through a vegetation field on a uniform bed. This formulation was modified by Mendez and Losada (2004) to account for random waves, and waves travelling over a sloping bed, listed as:

$$\langle \varepsilon_v \rangle = \frac{1}{2\sqrt{\pi}} \rho \tilde{C}_D b_v N \left(\frac{kg}{2\sigma}\right)^3 \frac{\sinh^3 k\alpha h + 3\sinh k\alpha h}{3k\cosh^3 kh} {H_{rms}}^3 \quad (4)$$

Where k is the wave number, g is the gravitational acceleration, σ is the wave frequency, h is the water depth, C_D is the (bulk) drag coefficient and H_{rms} is the root mean square wave height (van Rooijen, 2015). Several studies performed in recent years have attempted to model hydraulic-vegetation interactions, and their results have proven that current modeling methods are effective in simulating this physical process. Two additional studies performed in recent years which modeled wave-vegetation interactions but using the SWAN (Simulating WAves Nearshore) program include: a) the study performed by Suzuki (2011), who used SWAN with multiple vertical vegetation layers over several different vegetation fields, and b) Vuik *et al.* (2016) who used SWAN with multiple vertical vegetation layers to calculate run-up on a dike at Hellegat polder, Western Scheldt, the Netherlands.

One final modeling study worth mentioning was performed by van Loon-Steensma (2015) in the Netherlands, and simulated wave attenuation over a salt marsh foreshore which measured 200 meters in width. In looking at Figure 11, the wave height reduction over a 200-meter salt marsh section can be viewed based on two different storm extremities (1/10000 per year and 1/10 per year storm) and two different salt marsh heights (high and low) in the Netherlands.

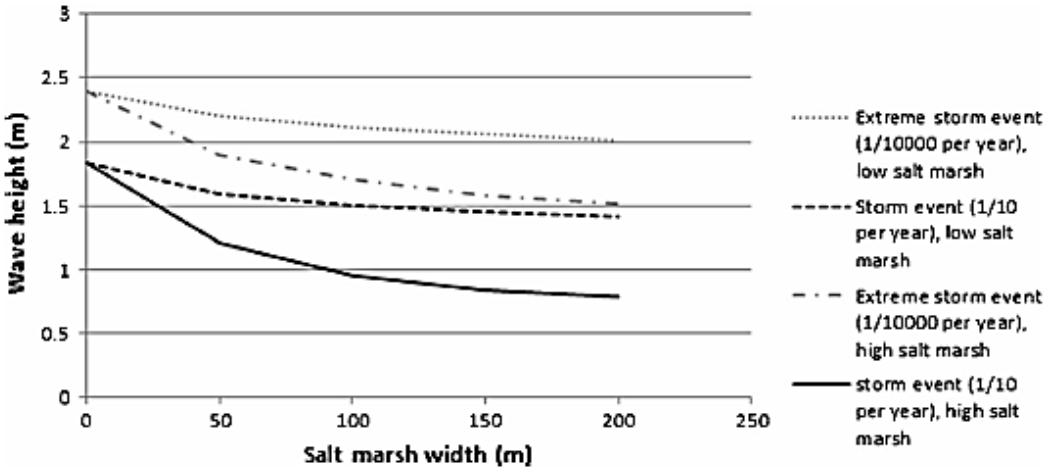

Figure 11: Modelled wave height in the Netherlands over a salt marsh foreshore for both a high and low salt marsh when simulating a 1/10 and a 1/10000-year storm condition (van Loon-Steensma, 2015).

Figure 11 shows that even for extreme storm surge levels (1/10000 per year) and for a low-lying salt marsh, a 200-meter width of salt marsh can reduce a wave height by nearly 0.5 meters. Now that the relevant modeling information has been explained, background information and theory will be presented on the empirical drag coefficient in the following paragraph.

Vegetation Drag Coefficients

The vegetation drag coefficient is an important component of modelling wave attenuation by salt marshes and other forms of vegetation. It is a component that is still very much empirical (based on experimental studies), and no single equation exists that can solve the drag coefficient for any given salt marsh or other vegetation type. As a result of this, it is necessary to calculate the drag coefficient based on both the local stem properties and hydraulic conditions at the study location.

The drag coefficient enables the entire drag force on a vegetation field to be an aggregate of the drag forces produced by individual stems in the vegetation field. It is not possible to assign a generalized value for all plant-produced drag forces, because C_D is dependent on mainly plant and hydraulic characteristics. The vegetation bulk drag coefficient can however be approximated by the use of empirical formulas. These formulas predict C_D values for various plant types by calculating the C_D as a function of non-dimensional flow parameters (Anderson *et al.*, 2011). One common method used to estimate the bulk drag coefficient is to calculate the stem Reynolds number,

$$\mathrm{Re_d} = \frac{u_c d}{v} \tag{5}$$

where $\mathrm{Re_d}$ is the stem Reynolds number, u_c is the maximum orbital velocity, and d represents the representative stem diameter. To solve for the maximum orbital velocity, Kobayashi *et al.* (1993) used the maximum horizontal velocity solved by linear wave theory for u_c,

$$u_{\max} = \frac{gHk}{2\omega}\frac{\cosh k(h+z)}{\cosh kh} \tag{6}$$

Where g is the acceleration of gravity, H is the local wave height, k is the wave number, h is the water depth, z the distance along vertical axis, and ω the wave angular frequency which is defined by $\omega = (2\pi/T)$. As the local wave height increases, the orbital velocity and the Reynolds number also increase, which decreases the effectiveness of drag resistance by vegetation. This results in a decrease of the drag coefficient for conditions of extremity. In Figure 12, the impact of the vegetation on the flow velocity profile can be viewed.

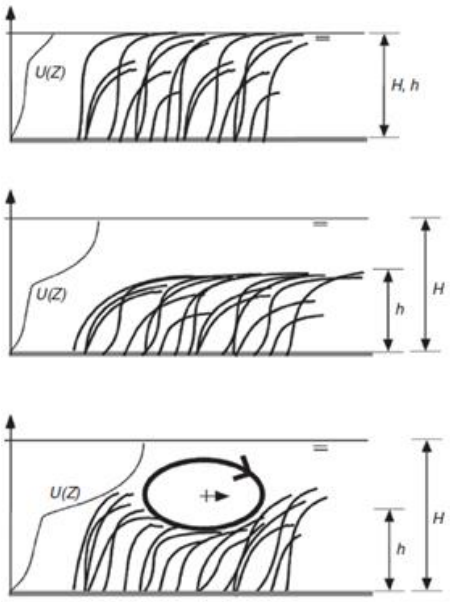

Figure 12: An overview of the flow velocity profile as the flow magnitude increases (from top image to bottom image) when vegetation occupies the entire water column for weak flow and near-emergent vegetation (top image), for increased flow and when the top of the vegetation bends to protect the inside of the canopy (middle image), and as flow becomes extreme and accelerates over the canopy and forcing the canopy blades to be displaced (bottom image) (Nepf, 2011).

As seen in Figure 12, the flow velocity near the bed is low, and therefore the Reynolds number must be calculated at the top of the vegetation canopy (where the highest turbulent stress occurs) for an accurate representation of the physical processes which occur in nature. Although Figure 12 displays the interaction between flow and vegetation in the water column, the process is similar for the interaction between waves and vegetation in the water column.

Figure 13 shows the relationship between the Reynolds number and the drag coefficient, which has mostly been used in the past as a means for estimating a representative value for the drag coefficient (C_D).

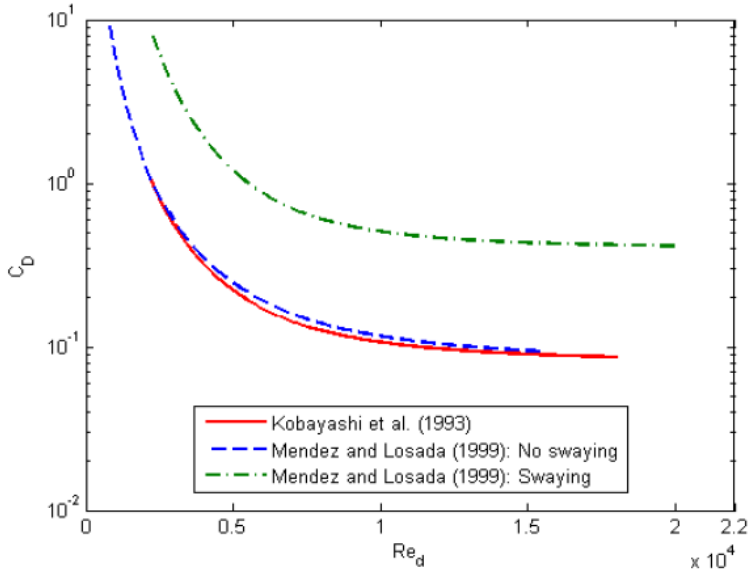

Figure 13: Empirical relationships between the Reynolds number and drag coefficient (Anderson *et al.*, 2011).

Mendez and Losada (1999) looked at this relationship for both swaying vegetation and non-swaying vegetation. It can be seen that the incorporation of swaying causes the drag coefficient to be increased. This is because for the same stem Reynolds number, the velocity input into the drag formulation is lower when plant motion is incorporated (Anderson *et al.*, 2011). It is also important to note that turbulence is increased on two different levels: One related to the wakes that occur behind individual plant stems, and the other for larger eddies that occur in the shear layer above the vegetation canopy. The latter occurrence of turbulence can also impede the vegetation canopy, however the degree of encroachment depends on the plant stem spacing (Dijkstra, 2012).

2.2.4 Conclusion

Good research has been performed to date, however much of it is site specific, and a system does not exist for dynamic applicability which has studied wave attenuation by global coastal salt marshes. In addition, there is no method currently which looks at salt marsh coastlines on a large scale to assess wave attenuation ability for extreme hydraulic conditions, since many of the previous studies were limited to measuring wave attenuation under mild conditions (wind waves). Perhaps if such a model were to be developed which uses numerical model results based on extreme hydraulic conditions and combinations of salt marsh characteristics (marsh platform slope, stem: height, density, diameter) as inputs for a statistical network, then potentially an efficient and effective tool could be created for quantifying the physical processes which occur for a given global coastal salt marsh.

3 Numerical (XBeach-Vegetation) Model Set-Up

3.1 XBeach-Vegetation

In order to quantify wave attenuation by vegetation for a given salt marsh coastline, the numerical modeling software XBeach was used. Xbeach is a depth-averaged, two-dimensional process-based model that solves the time dependent short wave action balance for the entire wave group. When using the XBeach model, there are three processes which occur on a short wave scale that are able to be incorporated in simulations, and these are: dissipation due to wave breaking (D_w), dissipation due to bottom friction (D_f), and dissipation due to vegetation (D_v) (Roelvink *et al.*, 2015).

This numerical modeling software was chosen for simulating wave attenuation by salt marshes for several reasons. First, it has the ability to incorporate salt marsh properties (stem height, stem density, stem diameter, and drag coefficient (C_D)) and calculate the resulting wave height at each grid cell within the computational domain. Second, this model has been calibrated and validated recently during a study performed by van Rooijen *et al.* (2015) using flume data from Kansy (1999). The data from the Kansy (1999) experiment measured wave attenuation over a kelp bed in a flume (submerged vegetation), however for this thesis work wave attenuation by both emergent and submerged salt marsh will be studied. Lastly, the XBeach software is valued for this application due to its computational efficiency when run in its 1-D form.

For this the purposes of this research, both the surf beat and the stationary modes within XBeach were used. The surf beat mode was used for the model calibration and validation, and it calculates the total wave energy dissipation that is directionally integrated due to wave breaking. The stationary mode was used to produce the model results used as inputs for the statistical BN in stationary mode, wave averaged equations are solved, but infragravity waves are neglected (Chapter 5.2).

Surf Beat Mode

The surf beat mode, which was the method used for the calibration and validation model simulations, is an instationary method that resolves the short wave variations on the scale of the wave group and the long waves with them. This mode uses the equation of Roelvink (1993), which calculates the dissipation with a fraction of breaking waves multiplied by the dissipation per breaking event (Roelvink *et al.*, 2015).

The incorporation of vegetation in the XBeach model is made possible by using the formulation from Mendez & Losada (2004). Their expression can be viewed below:

$$\frac{\partial A}{\partial t} + \frac{\partial c_g A}{\partial x} = \frac{D_{break} + D_{veg}}{\sigma} \tag{7}$$

Where $A = E_w/\sigma$, E_w is the wave energy, D_{break} is the wave dissipation due to breaking and D_{veg} is the wave energy dissipation from vegetation which can be solved using equation (8), and the root mean square wave height is given by:

$$H_{rms} = \sqrt{\frac{8E_W}{\rho g}} \tag{8}$$

The ability to vary the vegetation properties in the vertical direction is also possible, however this is mostly desirable for modeling mangrove species, and so this method will not be included for the purposes of this research.

Stationary Mode

The stationary mode of XBeach solves the wave-averaged equations and neglects infragravity waves and wave-group variations. For the batch of XBeach simulations which produced results for input into the BN, the XBeach stationary mode was used. The mode specifies a constant and uniform wave energy (a stationary, non-spectral wave boundary condition), which is based on the given values of T_{rep}, H_{rms}, direction and power of the directional distribution function. In this way, only the wave attenuation by vegetation (in this case salt marsh) can be the main focus. For this study, the XBeach-vegetation mode was used and only takes into consideration the wave travel in the cross-shore direction. Hence, all models are run in 1D.

Initially, the surf beat mode of XBeach was used for calibration since accurate field data was recorded over the salt marsh transect at Hellegat Polder. Once calibration was completed, originally the methodology called for incorporating both the offshore slope and the salt marsh platform slope. However, the methodology was modified since data was found which proved there is a large difference in steepness between the offshore slope and the salt marsh platform slope (see Figures 31 and 32). By using the stationary mode of XBeach, a stationary boundary condition could be defined at the marsh edge, and the impacts of infragravity waves, shoaling, and refraction were excluded.

3.2 Assumptions and Limitations

For this report, the model formulations only focus on the wave propagation in the cross-shore direction. As a result, all of the formulations are used in their 1D form (van Rooijen *et al.*, 2015). This also means that only normally incident waves are included (waves propagating perpendicular to the shore at 90°) while in nature the angle of wave approach varies. Another assumption when modeling with XBeach-vegetation is that the spatial variation in salt marsh and elevation only change in the cross-shore direction. For example, in nature the properties of a salt marsh field (stem: height, density, and diameter) will vary in the alongshore direction (parallel to the coastline) along with the elevation. Additionally, wave growth is neglected for these model simulations.

As mentioned previously, the numerical model is based on the physics of the vegetation (stem: height, density, diameter), but not the swaying motion of the plants while being impacted by waves and flow velocity are used for basis of the XBeach vegetation model (van Rooijen *et al.*, 2015). It is assumed that the salt marsh plant stems act as a rigid cylinder, where the wave dissipation depends on the plant structure (relative to the water depth). The relative stem length can change over time as the water depth changes (from storm surge or tides) from the swaying and flexing of the vegetation (Anderson *et al.*, 2011). In addition, the calculation of the drag coefficient is based on linear wave theory, when in reality the waves will not follow this identically when propagating over salt marshes.

It is also important to mention that based on equations (2) and (3), XBeach uses a vegetation factor when incorporating the vegetation properties into its calculations. The equation for the vegetation factor can be seen below:

$$\text{Vegetation factor} = (C_D)(N)(b_v) \tag{9}$$

Where C_D represents the (bulk) drag coefficient, N is the plant stem density, and b_v is the plant stem diameter.

This is important to realize when performing many simulations, because for instance if C_D is kept constant, a salt marsh platform with a stem density of 1000 stems per meter and stem diameter of 2 mm will yield the same results as one with 200 stems and a plant stem diameter of 10 mm. A table composed of vegetation factor values for the various combinations in the batch of XBeach-vegetation simulations can be found in Appendix B.

One final important assumption that is noteworthy is the exclusion of infragravity waves and wave group variations for the results of the batch of XBeach simulations used as inputs for the statistical BN. Since the stationary mode of XBeach was used, the vegetation only influences the wave action balance.

3.3 Grid and Boundaries

For all simulations, a non-varying grid size was used meaning that the grid size stayed constant from between both boundary conditions at each end of the model domain. A grid size of 0.3 meters was used for calibration and validation simulations based on the recorded data at Hellegat polder in order to properly account for the effects of the marsh cliff located at the marsh edge. For the Hannover flume simulations, a grid size of 0.5 meters was used, and finally for the simulations performed for the BN, the grid size varied depending on the slope used as an input. For example, grid sizes (dx) of 2, 5, 10, and 25 meters were used for slopes of 1/20, 1/100, 1/500, and 1/2000, respectively. These values were used because using a steep slope such as 1/20 would not produce good results if a coarse grid size of 25 meters was defined.

3.4 Boundary Conditions

3.4.1 Available Data

The data recorded at Hellegat polder was provided by members participating in the BE-SAFE study (Vuik *et al*., 2016). This study analyzed the effects of vegetation on wave damping for severe storm conditions (recorded significant wave heights up to 0.69 m) in the Netherlands, and used both field measurements and numerical modeling. For testing the numerical model based on the conditions of the Hannover flume study, data was provided by a participant of the flume study.

The data obtained for the batch of XBeach simulations was based on collected data (see Chapter 5.1 and Appendix B). The boundary conditions for the calibration effort were set 5 meters left of the wave sensors for both the Hellegat polder and Hannover flume studies. For the batch of XBeach simulations used as input for the BN, the incoming boundary condition was set at the marsh edge while the ending boundary condition was set at a level located at the water level (z_{s0}) plus 2 meters for run-up. The simulations where structured in such a way so that the computational domain only spanned the distance which corresponded to the location where the water level reached z_{s0} + 2.In doing this, unnecessary computations were avoided (See Chapter 5.2 for more information).

4 Numerical Model (XBeach-vegetation) Calibration and Validation

4.1 General

In order to prepare the numerical model for application on other locations, the model must be calibrated using data sources of good quality that also include extreme hydraulic conditions. The calibration process is necessary to see how the model performs using the conditions and parameters that were recorded in field and flume studies. For this research, the numerical model is tested to ensure that it is capable of handling both high wave heights and water levels so that it can be applied to other coastal regions around the world which contain salt marshes.

Calibration, testing, and validation of the numerical model used for this research was performed based on data from both a field study and a flume study. The field study was performed on a salt marsh platform in the Netherlands, where wave measurement sensors were deployed along a transect of a marsh platform. Vegetation properties were additionally recorded which were used as inputs for the numerical model. Contrary to the field study, the flume study was performed in a 300-meter-long wave tank that used natural salt marsh that was excavated from a coastal region in Northern Germany. The salt marsh was reassembled to form a vegetated section in the wave flume, where wave sensors were placed both before and after the vegetated section in order to measure wave attenuation. Additionally, vegetation properties were recorded in the field and in the flume, and the flume values were used as inputs for the numerical model simulations.

Both of the data sources used for this calibration include both extreme wave heights and extreme water levels that are near the highest found in current literature (up to approximately 1 meter) for studies which measured wave heights over salt marshes. These datasets provide an opportunity to minimize knowledge gaps in literature since the numerical model simulations can be compared with recorded extreme hydraulic conditions to check the accuracy of the XBeach-vegetation model when simulating extreme hydraulic conditions. In nature, marshes are likely to interact with water levels and waves of even higher extremity (see Figures 34, 35, and 36), however, recorded wave height data available for calibration could not be obtained for heights above 1 meter. Therefore, it is not possible to calibrate and validate the model for conditions above this height.

4.2 Calibration Using Field Data

The field site used for this calibration is located near Hellegat Polder in the Western Scheldt, The Netherlands (Figure 14). The wave data used has been provided by the research programme BE SAFE, which is financed by the Netherlands Organisation for Scientific Research (NWO). Field measurements at Hellegat Polder recorded wave heights over a 200-m natural salt marsh foreshore during extreme storm conditions from November 2014 to January 2015, as part of the BE-SAFE research programme (Vuik *et al.,* 2016). The vegetated foreshore at Hellegat is dominantly composed of cordgrass (*Spartina anglica*), and has a slope of roughly 1:40.

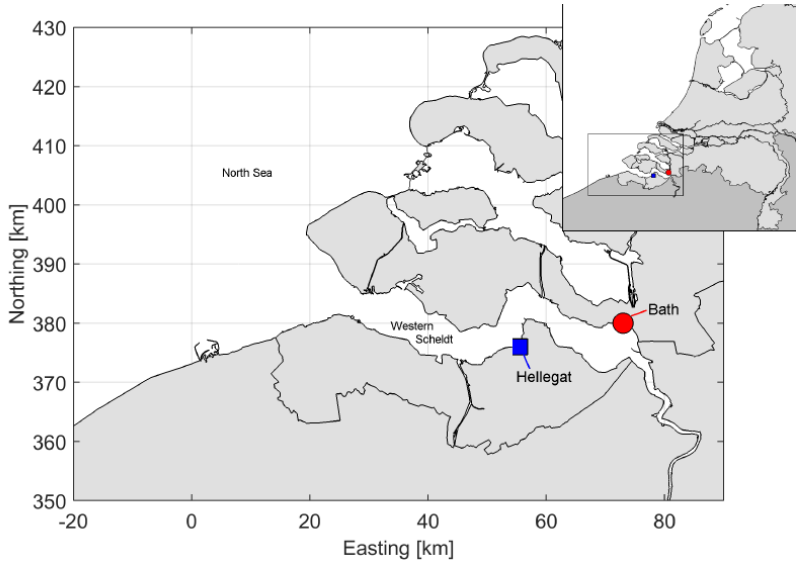

Figure 14: Location of the Hellegat salt marsh in the Western Scheldt estuary, the Netherlands (Vuik *et al.*, 2016).

From Figure 14 the location of Bath can also be noticed, however this site was not incorporated into calibration or validation efforts. In Figure 15, the bathymetry and locations of both the salt marsh and wave gauges can be viewed. Four wave sensors were deployed perpendicular to the marsh platform. The first wave sensor (S1) was placed on a mudflat section 2.5 meters in front of the seaward edge of the vegetation, with the second (S2), third (S3) and fourth (S4) wave sensors being placed approximately 5, 15, and 50 meters into the vegetation (Vuik *et al.*, 2016). In addition, elevation heights (also provided by a member of the BE SAFE study) were recorded by using an RTK-GPS surveying device. Based on the recorded elevation survey, a grid size of 0.3 meters was used in order to attempt to effectively simulate waves over the marsh edge cliff.

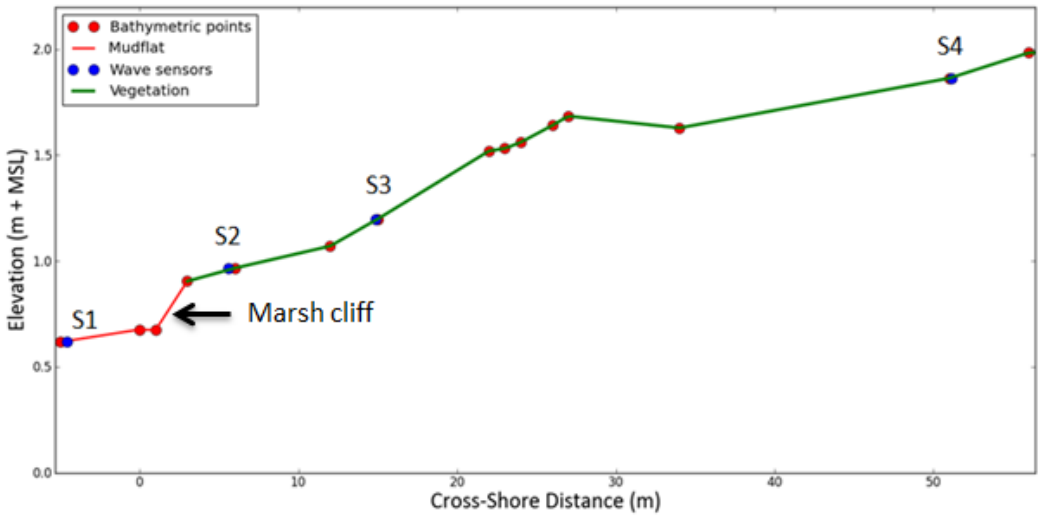

Figure 15: Bathymetry and locations of the salt marsh and four wave sensors

In addition to the recording of elevation points and the deployment of wave sensors, the recording of vegetation parameters was also performed during the BE-SAFE study and the data was made available for this report. The vegetation data used as model input for this calibration can be viewed in Table 3. Mean stem height (h_{mean}), near-bottom stem density ($N_{v,0}$), and near-bottom stem diameter ($b_{v,0}$) were all recorded and provided for each of the three sections falling between the four wave sensors.

Table 3: Mean plant height h_{mean}, near-bottom stem density $N_{v,0}$, mean near-bottom stem diameter $b_{v,0}$, for the three segments of the marsh transect at Hellegat.

Section	h_{mean} (m)	$N_{v,0}$ (m^{-2})	$b_{v,0}$ (mm)
S1-S2	0.20	944	3.0
S2-S3	0.29	1136	3.4
S3-S4	0.27	1520	2.7

The mean stem height and mean near-bottom stem diameter follow similar trends from the seaward edge of the marsh to the landward end, increasing until the third wave sensor (S3) and then decreasing again in the last section. On the other hand, the near-bottom stem density increases at each section from the seaward edge until the landward edge of the salt marsh platform.

In order to investigate which C_D value to use based on both the salt marsh properties and the hydraulic conditions, four equations were used from the literature which relates the drag coefficient to the Reynolds number (R_e). These equations are listed in Table 4, along with the vegetation properties used for each study, and a range for the Reynolds number that they were based on.

Table 4: Relationship between Reynolds number Re and bulk drag coefficient C_D using equations in the literature.

Publication	Vegetation Properties	Description of C_D	Based on range
Möller et al. (2014)	*Elymus athericus*, l_v=0.70 m, b_v=1.3 mm, h=2.0 m, H_s=0.1-0.9 m	$C_D = (227/R_e)^{1.62} + 0.16$	$100< R_e<1100$
Paul and Amos (2011)	*Zostera noltii*, sea grass, l_v=0.13 m, h=1.5-3.5 m, H_s=0.10-0.18 m	$C_D = (153/R_e)^{1.45} + 0.06$	$100< R_e<1000$
Jadhav and Chen (2012)	*Spartina Alterniflora*, l_v=0.63 m, b_v=8 mm, h=0.4-0.6 m, $H_s \leq 0.4$ m	$C_D = 2600/R_e+0.36$	$600< R_e<3200$
Anderson and Smith (2014)	Synthetic Spartina, l_v=0.42 m, b_v=6.4 mm, h=0.31-0.53 m, H_s=0.05-0.19 m	$C_D = (744/R_e)^{1.27}+0.76$	$500< R_e<2300$

Two of these equations are based on studies on natural salt marsh (Möller *et al.* 2014; Jadhav and Chen, 2012), while one was based on synthetic salt marsh (Anderson and Smith, 2014) and finally the last one was based on sea grass (Paul and Amos, 2011). The results of the calculations using the above equations and based on all of the recorded wave heights at Hellegat reaching wave sensors 3 and 4 are plotted in Figure 16.

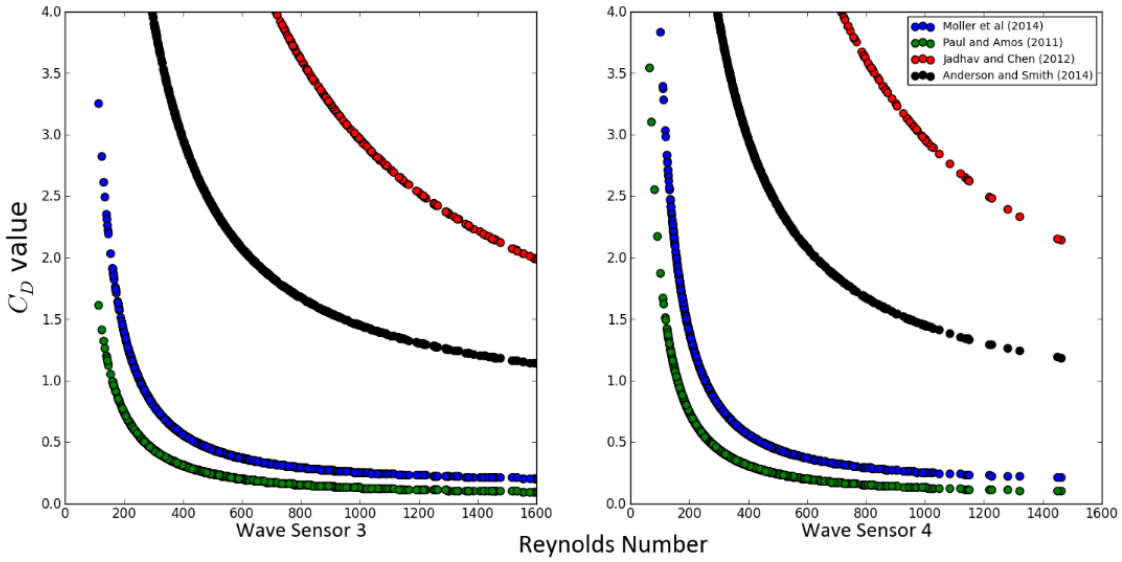

Figure 16: Relationship between drag coefficient (C_D) and the Reynolds number at wave sensor 3 and 4 for various C_D equations in the literature.

It can be seen that the equations of Jadhav and Chen (2013) and Anderson and Smith (2014) yield higher values for C_D than the equations of Möller *et al*. (2014) and Paul and Amos (2011) at both of the wave sensors. Additional data can be found in Appendix A for the plotted relationship between the drag coefficient and the significant wave height-water depth ratio (H_{mo}/h) calculated for all four equations.

The calculated C_D values at wave sensors 3 and 4 are plotted in relation to a common value found in the literature for an effective drag coefficient (Figure 17). The results of van Rooijen *et al.* (2015), which used the XBeach-vegetation model to simulate wave attenuation over kelp and Vuik *et al.* (2016), which used SWAN to measure wave run-up over salt marsh, both found a value of 0.4 to be a satisfactory value for C_D while performing calibration efforts for their respective studies.

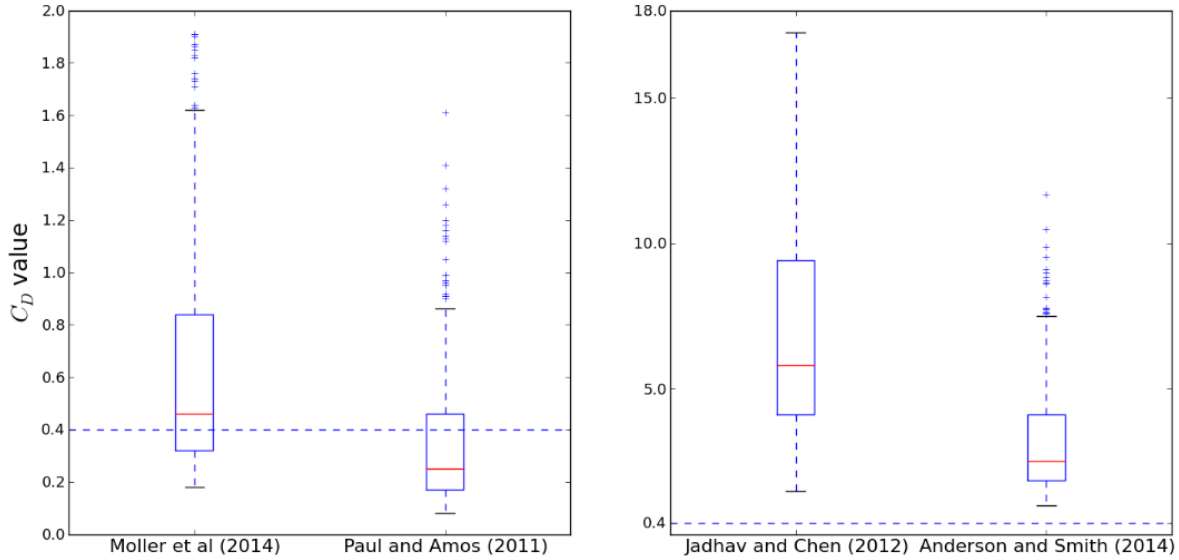

Figure 17: Calculated C_D values at sensor 3 (S3) from equations in the literature based on the recorded wave heights at Hellegat.

Based on Figure 17, it can be seen that the Möller *et al* (2014) and Paul and Amos (2011) equations give reasonable values which represent the C_D value well at wave sensor 3, while the Jadhav and

Chen (2012) and the Anderson and Smith (2014) equations yield higher values for the drag coefficients. A plot of the calculated C_D values at sensor 4 can also be seen in Figure 18.

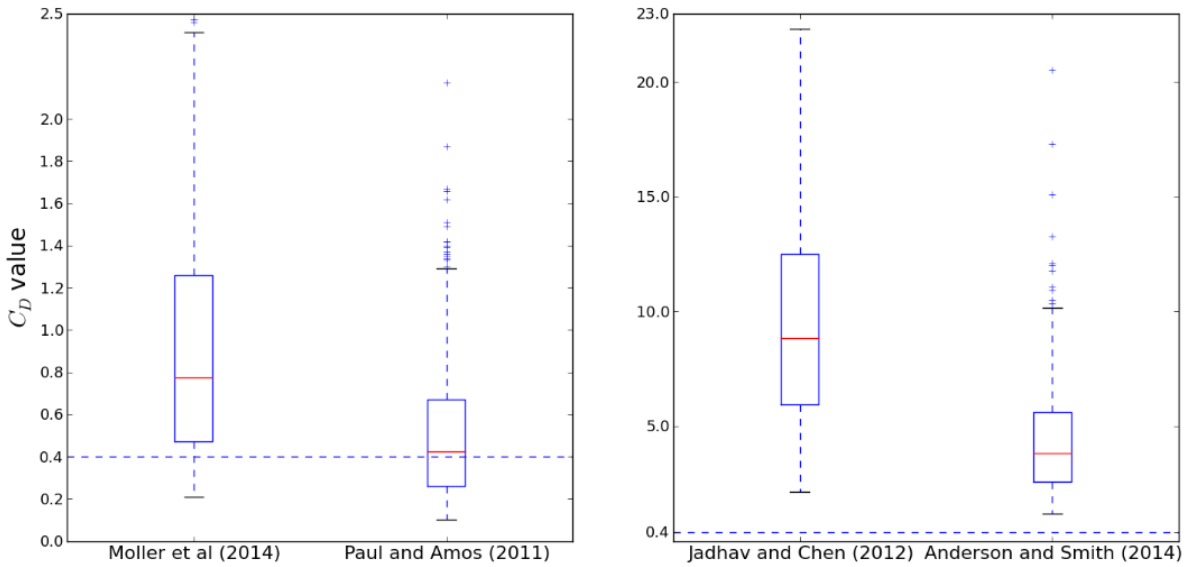

Figure 18: Calculated C_D values at sensor 4 (S4) from equations in the literature based on the recorded wave heights at Hellegat.

The Möller *et al.* (2014) gives a larger mean value at wave sensor 4 for the drag coefficient, while the equation of Paul and Amos (2011) produces a good mean value for the drag coefficient at sensor 4. This could be attributed to the fact that the Paul and Amos (2011) equation was based on calm conditions (H_s = 0.10-0.18), and for this case by the time the waves reach sensor 4 many of them are almost fully attenuated. Additionally, the reasoning for this occurrence could be that it is coincidental. Based on these values obtained for the drag coefficient at wave sensors 3 and 4, it was decided that the Möller *et al*. (2014) equation and the Paul and Amos (2011) equation would further be tested while performing XBeach simulations. For the purposes of the XBeach-vegetation model, these two equations produce drag coefficient values that are more characteristic than the other two equations that were analyzed based on all of the bursts recorded at Hellegat polder.

In order to test the numerical model, the most extreme hydraulic conditions were tested rather than simulating all of the recorded bursts at Hellegat. Only these conditions were used since the scope of this research is to study wave attenuation over salt marshes for extreme hydraulic conditions. The highest recorded significant wave height (H_{mo}) along with the fourth and fifth-highest recorded waves were used for calibration, while the second and third highest waves were used for model validation (Chapter 4.3). In addition, the second and third highest recorded water levels (z_{s0}) were simulated for calibration, while the fourth and fifth-highest water levels were used in model validation. The hydraulic conditions used in the simulations can be viewed in Table 5.

Table 5: Recorded significant wave height (H_{mo}), wave period (T_p), water level (z_{s0}), and water depth (h) at Hellegat used as inputs for the numerical model calibration. The water level value represents the height above MSL, while the water depth is the water level minus the bed height.

	H_{mo} (m)	T_p (s)	z_{s0} (m)	h (m)
First, fourth, and fifth-highest recorded wave heights	0.69	4.03	2.50	1.90
	0.51	2.68	2.79	2.19
	0.48	3.88	2.59	1.99
Third highest water level	0.46	3.08	2.96	2.36

The hydraulic conditions listed in Table 5 are among some of the most extreme data found in the literature for measuring wave attenuation over salt marshes. For these simulations, the drag coefficient (C_D) was set in XBeach to a fixed value of 0.4. In addition, a gamma value of 0.45 and a bed friction value (f_w) of 0.1 were used as model input. The results from using these hydraulic inputs can be viewed in Figure 19, where the numerical model results for wave height are shown in comparison with the recorded wave heights at Hellegat for those conditions.

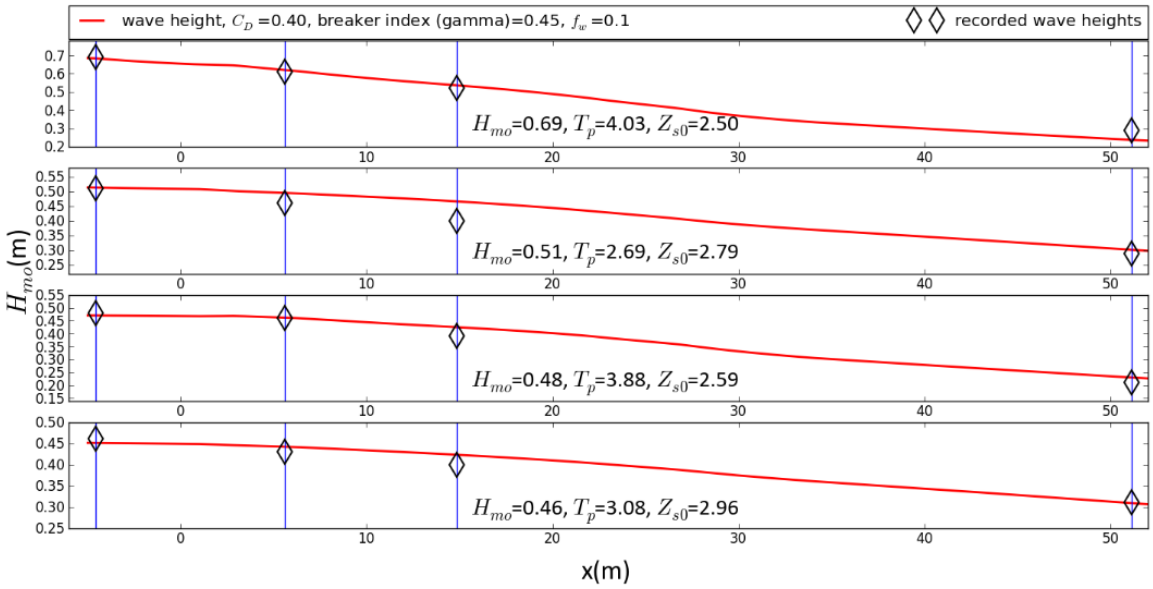

Figure 19: Calibration results for the first, fourth, and fifth-highest recorded waves at Hellegat. The recorded wave heights are represented by the diamonds, while the simulated wave heights for various hydraulic conditions are represented by the solid red lines.

Using a constant C_D value of 0.4 produced good results for the varying water level and wave height conditions. The numerical model was run for other various C_D values, which can be found in the Appendix A. These values fell in the range of C_D values that were calculated based on empirical equations found in the literature (Möller *et al.*, 2014; Paul and Amos (2011)). In addition to the numerical model being calibrated based on the conditions which occurred at Hellegat Polder, the model was tested based on conditions from the Hannover flume study.

4.3 Calibration Using Flume Data

Wave attenuation data from the flume study performed in Hannover, Germany was also used to test the numerical model. A 300-m-long, 5-m-wide and 7-m-deep wave flume was used to generate the waves. For vegetation, sections of *Elymus* from the northern German Wadden Sea were excavated and transported to the wave flume site. The natural salt marsh was reassembled into adjacent blocks and placed 108 meters from the wave generator and spanning 40 meters in length. Wave gauges were placed both before and after the 40-m salt marsh section in order to measure wave attenuation across the salt marsh. Tests were conducted for both regular and irregular waves reaching heights of 0.9 meters and water depths of up to 2 meters above the base of the vegetation. For this testing, only the irregular conditions were simulated. A general experimental set-up of the flume can be seen in Figure 20.

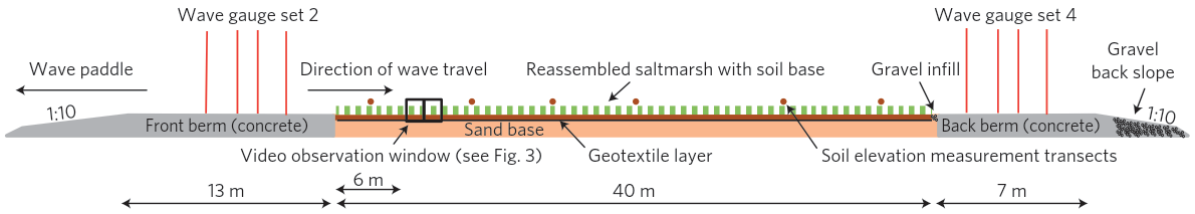

Figure 20: A general overview of the experimental wave flume set-up for the study performed in Hannover, Germany (Möller *et al.*, 2014).

Wave sensors were placed approximately 3 meters before the vegetated section and 2.2 meters behind the vegetated section in order to capture the wave dissipation over the salt marsh. In Figure 21, the flume geometry can be viewed. The origin was set at the starting point of the vegetation section.

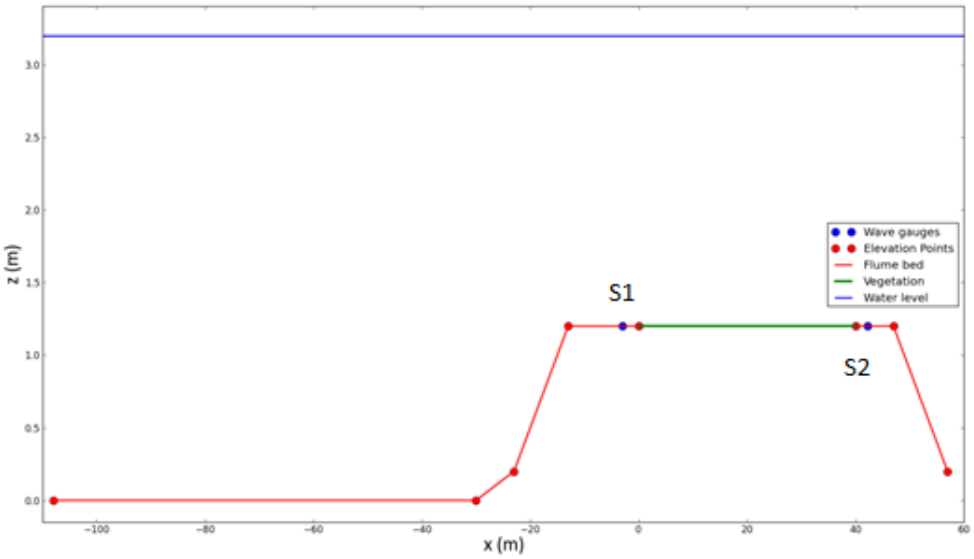

Figure 21: The flume set-up in the numerical model for the irregular wave conditions which were simulated based on data from the study performed in Hannover, Germany.

For these calibration simulations, a water level of 2 meters (over-marsh depth) was used. The model domain used for the simulations was set 5 meters to the left of the first wave sensor (S1) where wave data was recorded until the second wave sensor (S2). The vegetation inputs used for the numerical model can be seen in Table 6.

Table 6: Measured vegetation properties of the Elymus salt marsh present in the wave flume in Hannover, Germany (Möller *et al.*, 2014).

Section	h_{mean} (m)	$N_{v,0}$ (m^{-2})	$b_{v,0}$ (mm)
S1-S2	0.70	1225	1.3

The values in Table 6 were obtained by measurements of the vegetation in the flume setting. In Table 7, the hydraulic conditions used as input for the numerical model testing are listed.

Table 7: Hydraulic conditions at sensor 1 from the Hannover flume study used for testing of the numerical model.

Case	H_{mo} (m)	T_p (s)	Z_{s0} (m)	h (m)
1	0.20	2.10	3.2	2.0
2	0.29	2.50	3.2	2.0
3	0.29	3.60	3.2	2.0
4	0.40	4.10	3.2	2.0
5	0.58	3.60	3.2	2.0
6	0.62	5.10	3.2	2.0
7	0.75	4.10	3.2	2.0
8	0.90	6.20	3.2	2.0

Using the conditions above, drag coefficients were calculated and plotted based on the formulation for C_D produced by the members of this study (Möller *et al.*, 2014), and an additional study found in the literature (Paul and Amos, 2011). Both formulations calculate the drag coefficient based on the Reynolds number, but the formulations were produced based on different hydraulic conditions and vegetation properties. The difference is probably attributed to the varying extremity of the hydraulic conditions and the vegetation characteristics for the two studies. Paul and Amos (2011) studied less extreme conditions over sea grass, while Möller *et al.* (2014) studied wave dissipation by salt marsh for some of the most extreme hydraulic conditions in the literature. In Figure 22, a graph is provided which shows the relationship between the C_D and the wave height to water depth ratio at the start of the vegetation in the flume.

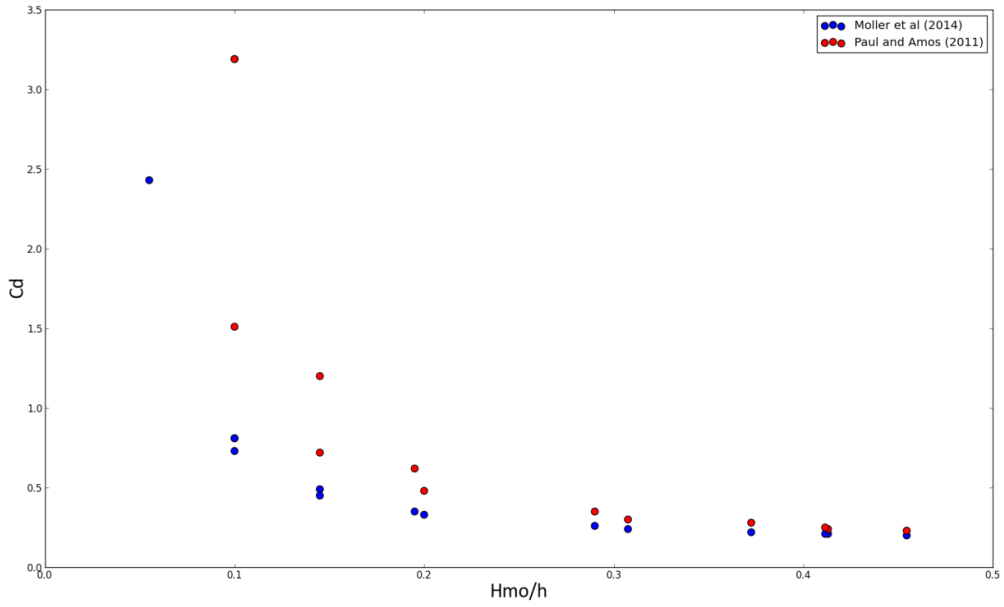

Figure 22: Calculated drag coefficients for the Hannover flume wave conditions at wave sensor 1 based on the formulations produced by Möller *et al* (2014) and Paul and Amos (2011).

Additionally, the numerical model was simulated for the previously listed hydraulic conditions using calculated drag coefficients from both the Möller *et al.* (2014) and the Paul and Amos (2011) studies. Various drag coefficient values were calculated for the different simulations based on the varying

hydraulic conditions in the flume for each case. The Paul and Amos (2011) equation was used to calculate these values based on the Reynolds number (see Table 4). The results of these simulations can be seen in Figure 23 and Figure 24.

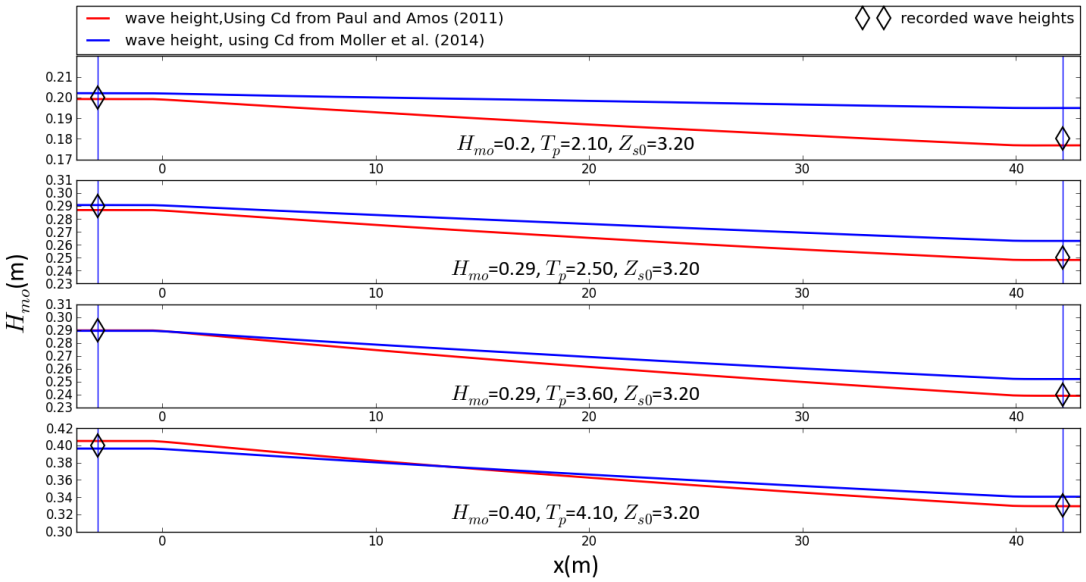

Figure 23: Calibration results for the lower four wave heights produced in the Hannover wave flume for two different calculated drag coefficients.

The model overestimated the wave height for the lower wave height simulations when the drag coefficient based on the Möller *et al.* (2014) equation was used. Using the drag coefficient of Paul and Amos (2011) resulted in producing more accurate results for the lower wave conditions. Overall, the model reproduced the wave height values fairly well for the four lower wave conditions that were simulated. The results from the four higher wave conditions that were simulated can be viewed in Figure 24.

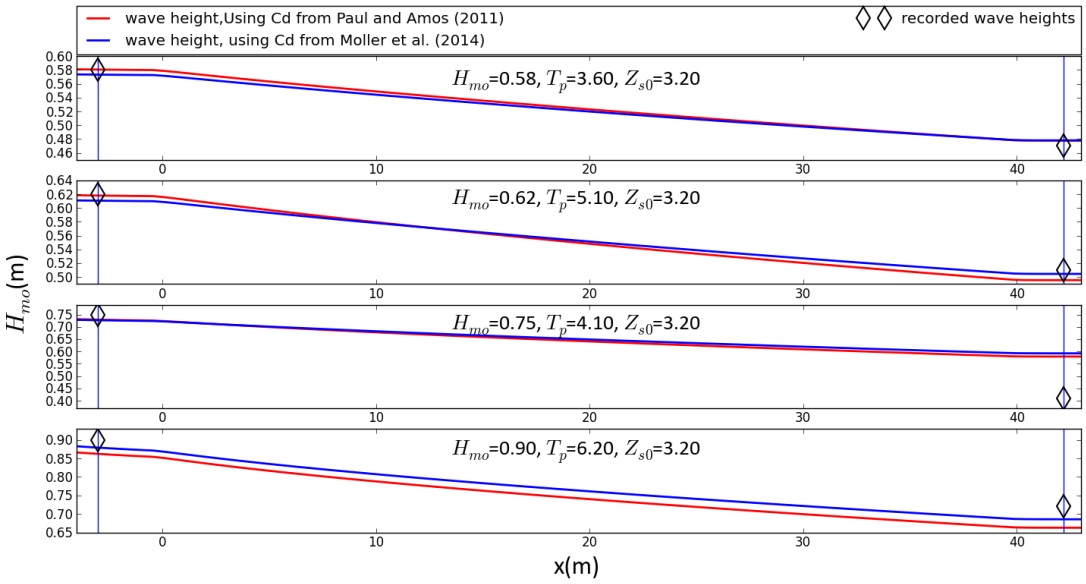

Figure 24: Calibration results for the four higher wave conditions simulated based on data recorded at the Hannover wave flume and using two different calculated drag coefficients.

For both drag coefficients, the model produced accurate results when simulated for a wave height of 0.58 and 0.62. When the wave height was raised to 0.75, however, the model overestimated the wave height at wave sensor 2. For the last case, the wave height was raised to 0.9 meters, and the model underestimated the wave height at the second wave sensor. In order to visualize further the performance of the model when compared to the recorded data in the flume, a plot was made to relate the recorded wave height-modelled wave height ratio to the wave height-water depth ratio (Figure 25).

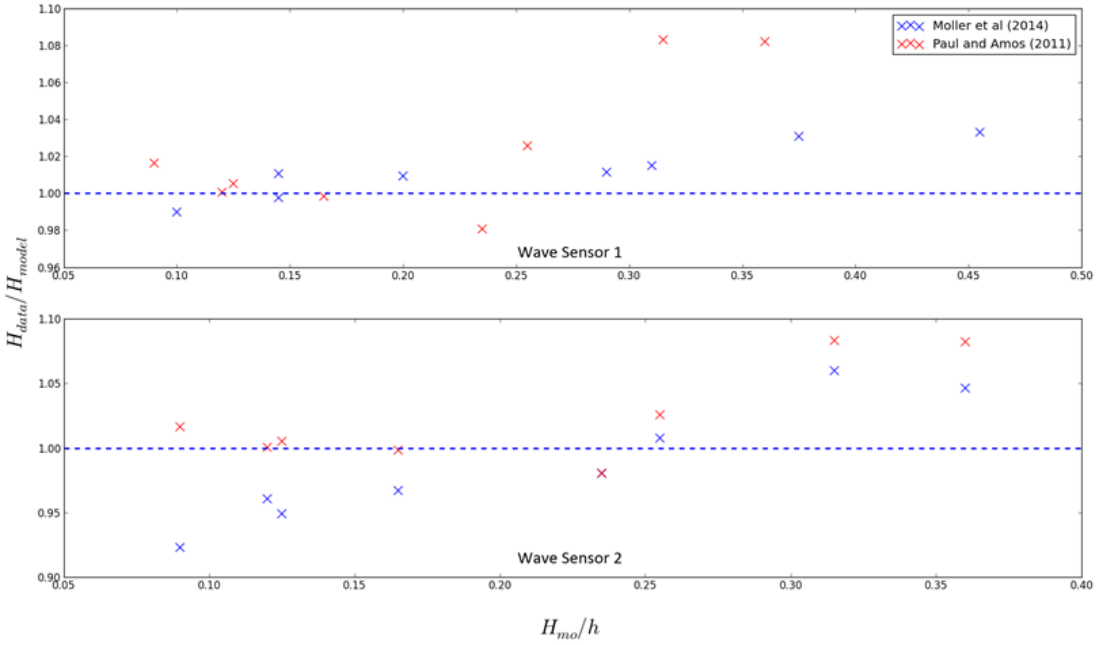

Figure 25: The relationship between the recorded wave height-simulated wave height ratio and the wave height-water depth ratio. The dashed line at y=1 represents a perfect fit between recorded and simulated wave heights.

Figure 25 shows that the drag coefficient equations produced by both Paul and Amos (2011) and Möller *et al*. (2014) show good agreement with the model results for the low to medium waves, however, when the waves surpass a certain height the model becomes less accurate and underestimates the wave height at the two wave sensors. Once the numerical model was calibrated and tested, it was validated based on a different set of hydraulic conditions.

4.4 Validation

The numerical model was validated using data from a less extreme storm event that occurred at Hellegat roughly 20 days before the storm event used for calibration. Based on the results of the calibration, a drag coefficient (C_D) of 0.4 was used to validate the model for further application. For validation, all model parameters used in the calibration simulations are left unchanged. In doing this, only the hydraulic conditions are varied, and the adaptability of the model can be checked and validated.

The hydraulic conditions used for validation are listed below in Table 8. These conditions include the second and third-highest wave heights recorded at Hellegat, along with the fourth and fifth-highest recorded water levels.

Table 8: Hydraulic conditions recorded from Hellegat used for validation of the numerical model. The significant wave height (H_{mo}), peak period (T_p), water level (z_{z0}) and water depth (h) are listed for each condition.

	H_{mo} (m)	T_p (s)	z_{s0} (m)	h (m)
second and third highest recorded wave heights	0.53	2.76	2.55	1.95
	0.52	2.76	2.89	2.29
fourth and fifth highest recorded water levels	0.38	2.76	2.94	2.34
	0.34	2.69	2.93	2.33

The highest wave heights used for validation are approximately 0.5 meters, while the highest water levels are just below 3 meters. The results of the validation simulations are presented in Figure 26.

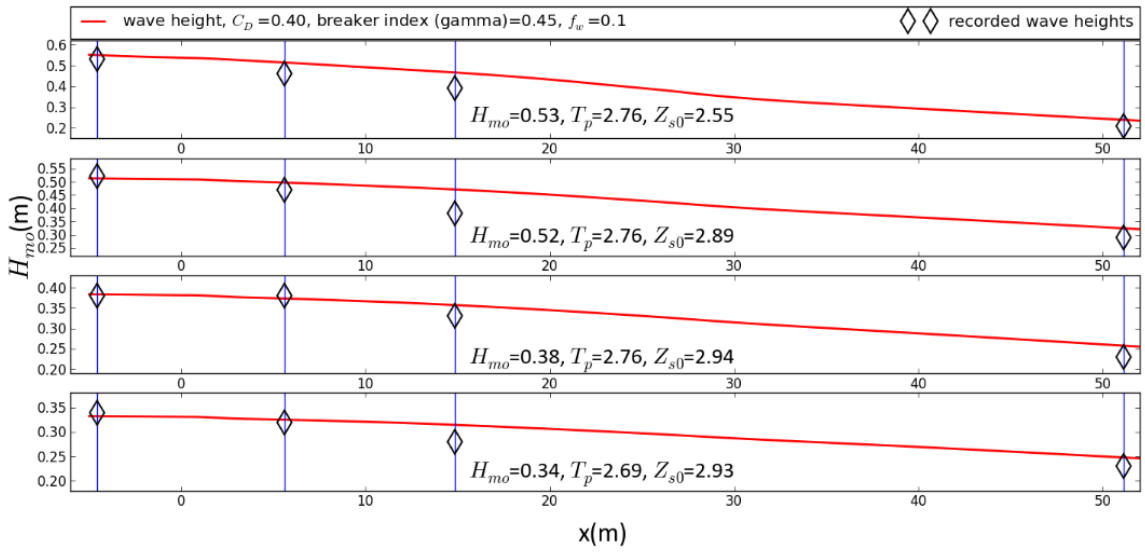

Figure 26: The model results for the validation compared to the recorded wave attenuation data at Hellegat.

Based on the results of the validation simulations in Figure 26, it can be seen that a drag coefficient value of 0.4 represents the recorded wave heights well, and should prove to be applicable on other locations with similar conditions. However, the use of an extrapolated C_D based on an equation from the literature could be considered to improve model accuracy if a wide range of salt marsh characteristics and hydraulic conditions were to be simulated.

To review the calculated mean difference (model minus recorded data) for the wave height at each wave sensor, an error plot was produced and can be seen in Figure 27. The mean difference was calculated for each of the hydraulic conditions used in calibration and validation at wave sensors 3 and 4. The calculated mean difference is denoted by the red line for each plotted box, with the standard deviation spanning from the mean value to the edge of each box.

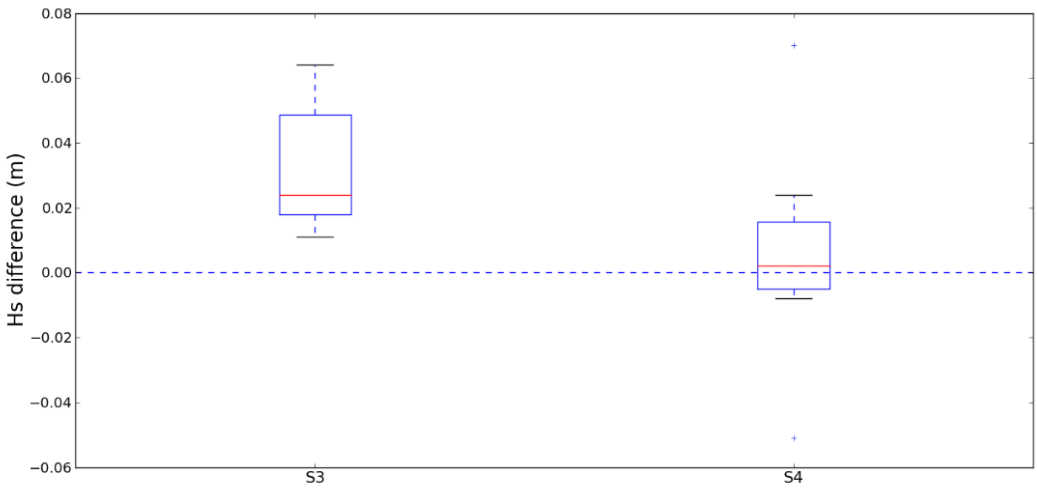

Figure 27: Difference in Hs (model minus data) for the calibration and validation simulations when compared to recorded data at wave sensors S3 and S4 at Hellegat.

In looking at the calculated mean difference, it can be seen that as a whole the model over-predicts the wave heights slightly. The maximum calculated mean difference occurs at sensor S3 with a value just above 2 cm, and ranging from approximately 1 to 7 cm. The validation simulations were less accurate than the calibration simulations, which is probably attributed to the use of a constant C_D while hydraulic conditions varied. It is known that the drag coefficient varies based on the Reynolds number (see Figure 16), so this is one disadvantage of using a constant value for all simulations. These calculated error results for calibration and validation based on the highest hydraulic conditions which occurred at Hellegat can be compared to a recent study that was performed using the SWAN vegetation model (Vuik *et al.*, 2016), which showed a mean error within 4 cm (model minus data) based on results from using all of the recorded bursts at Hellegat.

4.4 Sensitivity Analysis

In order to test the sensitivity of the input parameters for the numerical model, an analysis was performed separately for two different input parameters in XBeach, γ_{break} (breaker index, gamma), and f_w (bed friction). When testing these two parameters separately, all other values used as model input were kept constant so that the variations of these values were clearly shown in the results.

The default value of gamma is set automatically to 0.55 in XBeach, and this value produced results which over-estimated the wave heights at wave sensors 2 and 3 (see Figure A-3). As a result, a range of gamma values were tested from 0.4 to 0.7 to see the impact on the accuracy of the results when compared to the recorded wave heights.

A value of 0.45 gave the least error when comparing the wave attenuation slope of the model versus the recorded data from wave sensor 2 to wave sensor 3. Therefore, a gamma of 0.45 was chosen as input for the calibration and validation simulations. In Appendix A, a table is provided with these error calculations. Additionally, simulations were performed using various C_D values to see their impact on wave heights along the marsh transect at Hellegat. These results are additionally provided in Appendix A.

In addition to testing gamma, the bed friction parameter (f_w) was also varied to optimize the model results. The XBeach model did prove to be sensitive to the bed friction parameter when testing values in the range of 0.1 to 0.6. For calibration and testing, a value of 0.1 was used to account for low roughness due to the mudflat at Hellegat. In the following chapter, the framework for the statistical (BN) model set-up will be introduced and explained.

5 Statistical (Bayesian Network) Model Set-up

In order to attempt to predict wave attenuation by global salt marsh habitats efficiently, a statistical (BN) model was constructed. In this chapter, the different components of the BN are mentioned, and the required steps for the network construction are explained. These steps include: Theory on BNs, Data Collection, XBeach-Vegetation Simulations (for BN input), BN Construction and Training, and BN Results. In Figure 28, the complete structure of the combined numerical model (Xbeach-vegetation) and the statistical BN (Netica) can be viewed.

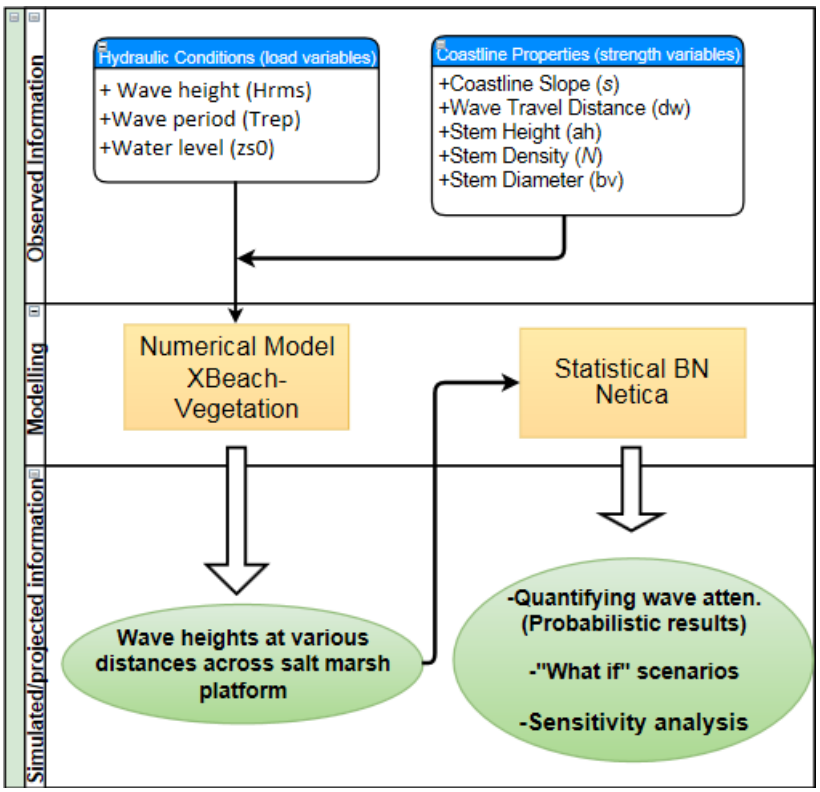

Figure 28: The entire model structure and flow information.

The idea behind this methodology is to produce many different simulations based on combinations of various hydraulic conditions and salt marsh characteristics and input the results from the simulations into a BN for data organization and quantification. By building a BN, the possibility of using prior numerical model data to forecast wave height reduction for a given set of hydraulic conditions and salt marsh characteristics is thought to be achievable. The BN is thought to be an effective and efficient method for quantifying a given salt marshes ability to attenuate waves, but also to show the influence that different salt marsh characteristics have on resulting wave heights.

5.1 Theory on Bayesian Networks

A BN is a probabilistic structure that produces a group of random variables and their dependence on each other through a graph network (van Verseveld *et al.*, 2015). The variables of the BN and their relationships are signified by using nodes and arrows (Figure 29). If an arrow is present between two nodes, it can be assumed that the parent node has an influence on the child node.

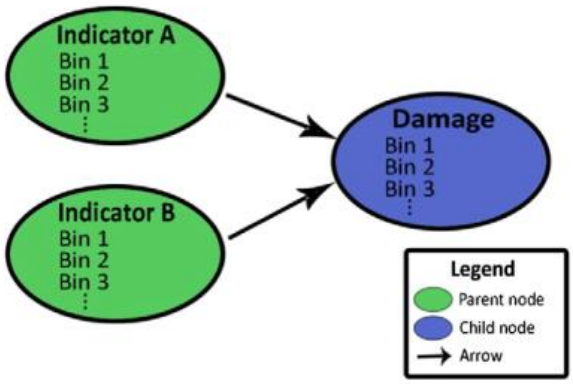

Figure 29: A basic BN example which relates two indicators to a result node. The indicator nodes are called parent nodes, while the result node is called a child node. Bins are necessary whenever a node represents a continuous parameter (van Verseveld, 2015).

This idea is all based on Bayes' rule, which states how current beliefs can be adjusted as new data or information becomes available. The BN is useful because it relies on existing data to make decisions while also accounting for uncertainty at the same time. The formulation based on Bayes' rule is:

$$p(F_i|O_j) = p(O_j|F_i)p(F_i/p(O_j)) \quad (10)$$

Where $p(F_i|O_j)$ is the updated conditional probability of a forecast F_i, when given a group of observations O_j. The prior probability of F_i, $p(O_j)$, and O_j are all represented by $p(F_i)$. Adding the probability $p(O_j|F_i)$ these likelihoods can be obtained from the data. It should also be noted that it is not possible for predictions to occur outside of the data ranges of the nodes, and additionally combinations cannot occur that do not exist in the dataset either (den Heijer *et al.*, 2012).

In order to create an effective BN, four steps must be performed, which include: data collection, network construction, network training, and validity check (den Heijer, 2012). For this thesis research, only the first three of the previously mentioned steps will be performed. The Netica software program (Norsys, 2014) will be used to construct and handle the BN. More details on the Netica program can be found later in this chapter.

5.2 Data Collection

In order to establish a guideline for the assignment of parameters to test for the batch of numerical model simulations using XBeach-vegetation, data was recorded for eight categories which were split into two sections: salt marsh characteristics, and hydraulic conditions. The salt marsh characteristics include: the cross-shore width of a salt marsh platform, the marsh platform slope, the average stem height, average stem density, and average stem diameter. The hydraulic conditions include: water level, wave height, and wave period. A more detailed description of these eight categories can be found in Chapter 5.3.

5.2.1 Salt Marsh Characteristics

The salt marsh data was collected from various sources (literature, National Wetlands Inventory, EU-FAST Project data; See Appendix B). Obtainable data was collected on the various characteristics of global salt marshes in order to obtain a sound basis for assigning representative values for the simulations.

An overview of the data obtained for the various salt marsh characteristics can be viewed in Figure 30. Once the data was recorded for the various parameters, it was plotted using a histogram for

each variable. Based on the histograms, values can be defined as input values for the batch of XBeach-vegetation simulations. The defined values can be found in Table 9 of Chapter 5.3.1.

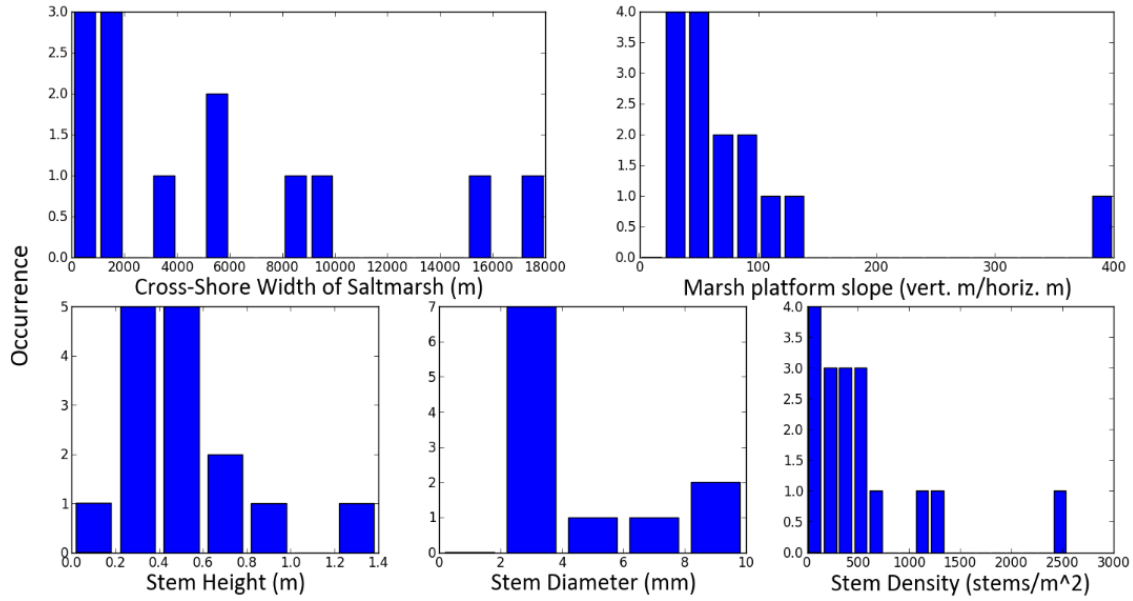

Figure 30: Overview of the salt marsh characteristic values obtained from various sources.

In reviewing the salt marsh data, it can be seen that certain values occur more frequently than others for the different salt marsh parameters. One interesting observation that is noteworthy to mention is the variation of slope steepness between open water and the salt marsh platform. In Figure 31, this variation is made clear.

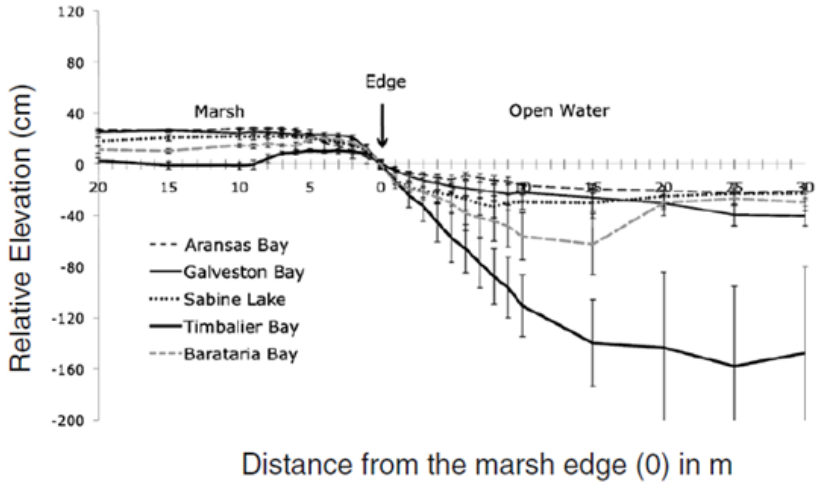

Figure 31: Example of the variation between the offshore slope and the marsh platform slope (modified from Minello *et al.*, 2012).

Based on the data from the study performed by Minello *et al.* (2012), the open water slopes show more steepness than those of the marsh platform. Additionally, the error bars produced for the slope profiles in the open water section have a higher range than those in the marsh section of Figure 31. This is the reasoning for assigning the incoming boundary at the marsh edge for the batch of XBeach-vegetation simulations, instead of at a certain distance offshore. By setting the incoming boundary condition at the marsh edge, the error due to a varying slope was minimized. A further analysis of the marsh platform slope steepness compared to the open water slope steepness is provided in Figure 32.

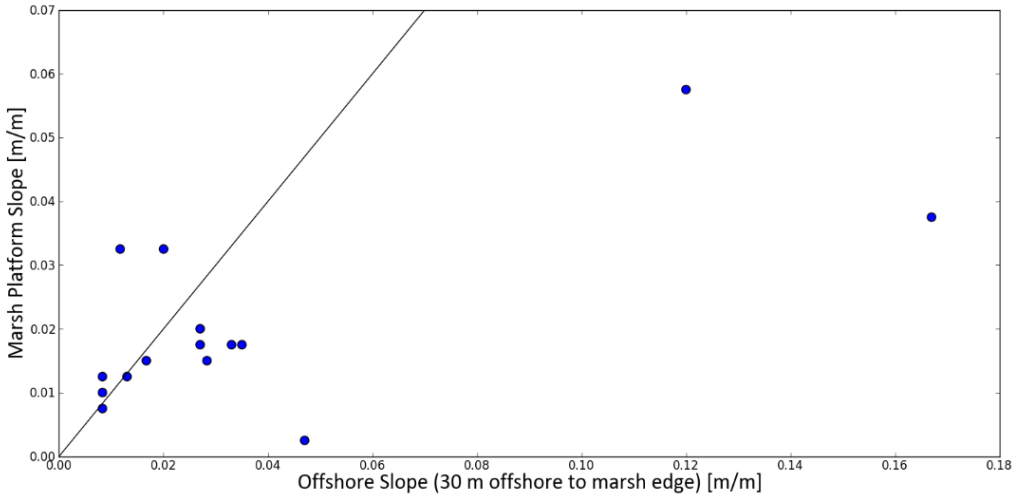

Figure 32: Plot of the marsh platform slope versus the offshore slope, based on the data from 15 different coastlines containing salt marshes in the USA.

Based on Figure 32, nine of the fifteen offshore slopes analyzed from Minello *et al.* (2012) show more steepness than the marsh slopes. The dots which are plotted to the right of the perfect fit line (signifying equal slope between offshore and marsh platform) contain offshore slopes which have more steepness than the marsh platform slopes. This is the reasoning for the decision to only consider the salt marsh platform slopes instead of the combined slope (offshore and marsh platform) in the numerical model simulations. In addition to studying the variations in slope, a relationship was also made between the data found for stem height and stem diameter (Figure 33).

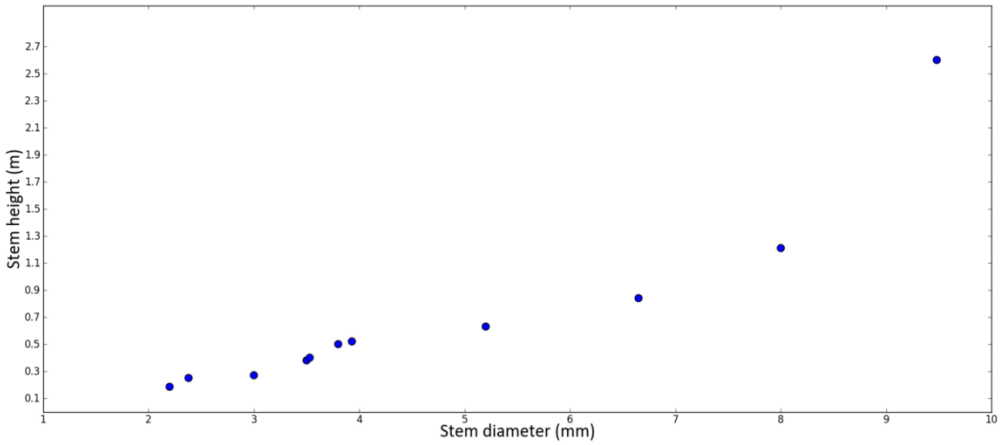

Figure 33: Relationship between stem height and stem diameter based on values found in the literature. The data used for this figure can be found in Appendix B.

It can be noticed from Figure 33 that as the stem diameter increases, so does the stem height. When looking at the wave attenuation attributed to the various stem height values versus the stem diameter values, a similar trend should result (Figure 41).

5.2.2 Hydraulic Conditions

In addition to the data collection of salt marsh characteristics, an overview of hydraulic parameters was additionally created. There was difficulty in finding data for extreme wave heights, however, extreme surge levels were fairly easy to obtain. Historic storm surge levels in the European region for both a 100-year and 1000-year return period are provided in Figure 34.

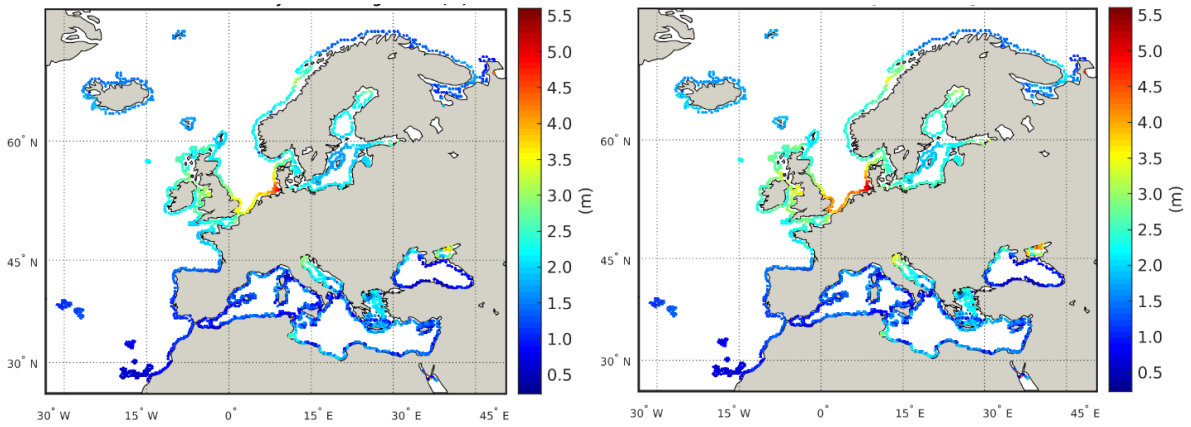

Figure 34: The European Extreme Storm Surge Level dataset including 100-yr storm surge level (left figure) and a 1000-yr storm surge level (right figure) (European Commission, Joint Research Centre, 2016).

Based on Figure 34, it can be seen that particularly on the east coast of England and from Belgium to Denmark, the surge levels can reach elevations of up to 5 meters. Recall from Chapter 2 that the modelling study performed by van Loon-Steenson (2015) in the Netherlands produced results which concluded that even waves produced by a 1/10000 year storm can be reduced by roughly 0.5 meters over a salt marsh width of 200 meters. It is important to mention that the surge levels in Europe are highest in the winter season (due to influence of winter storm behavior in the North Sea) while in the United States, surge levels are highest in early summer to early fall (due to the impact of Hurricanes[3] between these time periods). This is evident in Figure 36, which provides historical data for storm surge recordings based on forty different hurricanes from 1928 to 2008 at locations along the Gulf and Atlantic coasts of the U.S.

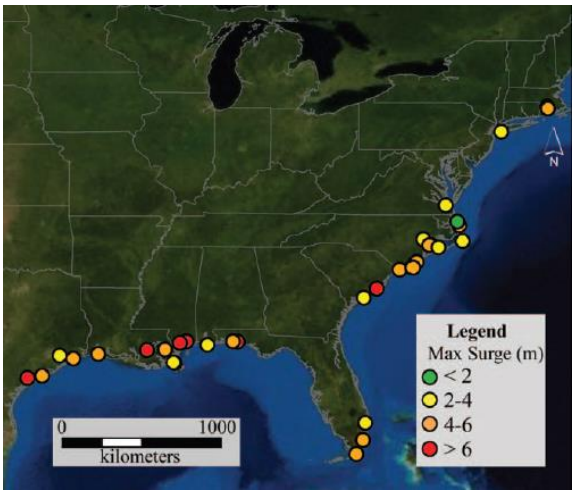

Figure 35: Maximum high water mark/storm surge recording for various hurricanes in the U.S. from 1928 to 2011 (Peek and Young, 2013).

In viewing Figure 35 it can be seen that many of the locations recorded a surge level reaching 4-6 meters, and even 7 locations recorded surge levels over 6 meters. This data reaffirms the idea that more knowledge is necessary regarding the interaction between salt marshes and extreme hydraulic conditions. Using Figures 34 and 36 as a reference for extreme surge levels in Europe and the U.S., water levels were defined for model input. The defined values can be seen in Table 9. Since wave heights and corresponding wave periods recorded at the seaward edge of salt marshes were difficult

[3] Atlantic Hurricane Season is officially from the 1st of June to the 30th of November (National Hurricane Center, 2016).

to obtain, the wave heights used for input were defined by the breaking condition and the wave periods were assigned using a relation to the wave height (See equations 11 and 12 below). Figure 36 provides an overview of the hurricane surge data recorded in the U.S. from Peek and Young (2011).

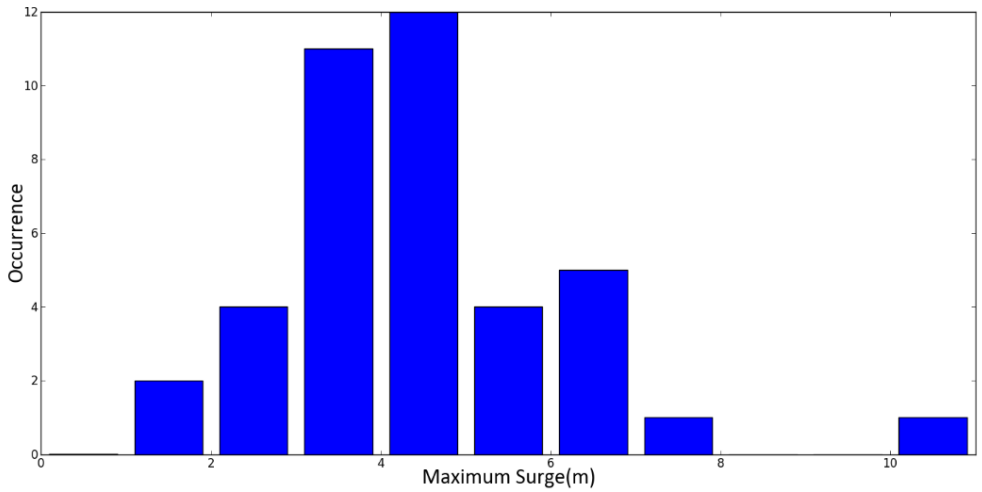

Figure 36: The maximum surge levels of 40 hurricanes which made landfall on the Gulf and Atlantic coasts of the U.S. from 1928 to 2011. (based on the data collected from Peek and Young (2011))

Based on the water levels assigned in Table 9, the wave heights were defined by using the maximum wave height to water depth ratio, which can be explained by equation 11 (below). The highest wave height (2.5 m) was checked with the lowest water level (3.20 m) to ensure that no breaking will occur for any of the simulations at the incoming boundary. The equation used to check this is as follows:

$$\frac{H_{max}}{d} = 0.78 \tag{11}$$

Where H_{max} is the maximum wave height that is possible to occur at a depth d before the wave experiences breaking. The value of 0.78 is recommended for non-linear wave theory and valid for shallow water (Bosboom and Stive, 2015). The chosen values for wave heights were checked to ensure that they produced a ratio below this value since breaking would occur if they were greater than 0.78. Wave periods corresponding to the wave heights were calculated based on the following equation[4] :

$$T_{rep} \approx 4.5 * \sqrt{H_{rms}} \tag{12}$$

where T_{rep} is the representative wave period and (H_{rms}) the root-mean-square wave height.

5.2.3 Conclusion

Recall from Figures 4 and 5 (Chapter 1) that many of the areas containing salt marshes often are impacted by the highest storm surges. Marsh preservation and understanding of the interaction between the salt marshes in these areas and the hydraulics during extreme storm events is crucial. Based on the recorded data obtained from this chapter, a combination of values was assigned for each of the eight categories (salt marsh characteristics and hydraulic conditions) for performance of the batch of XBeach-vegetation simulations (Chapter 5.3).

[4] Adjusted from T ≈ 4.5*$\sqrt{H_s}$ (A. Reniers, personal communication, May 13, 2016)

5.3 XBeach-Vegetation Simulations (for BN input)

5.3.1 Model Set-up

Based on the salt marsh and hydraulic data collected from various locations around the world, a batch of XBeach-vegetation simulations was generated in order to test all combinations defined in Table 9. In performing these simulations, a large dataset containing wave height values at various distances over a salt marsh platform could be obtained. These resulting wave heights at the various distances can be input into a BN for further analysis and quantification of wave attenuation (Chapter 5.4). In this subchapter, the methodology of the simulation process that was used will be explained. In viewing Figure 37, the computational domain for the batch of simulations can be seen.

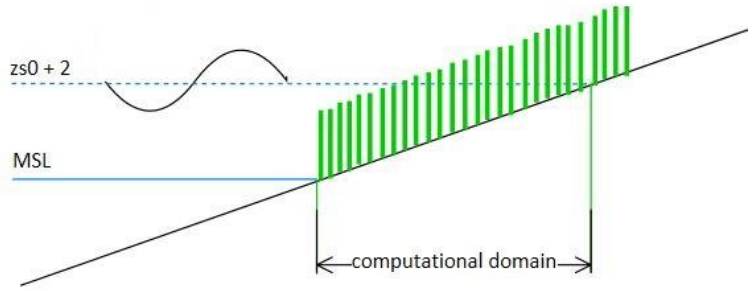

Figure 37: Definition of the computational grid for the batch of XBeach-vegetation simulations.

As displayed in Figure 37, the length of the model computational domain depends on the slope of the salt marsh and the water level (z_{s0}) plus run-up[5] height (2m). Run-up was added because although breaking does not occur at the incoming boundary, it will occur for various simulations as the depth is decreased across the salt marsh platform. The grid size (dx) varied based on the slope, where values of 2,5,10, and 25 meters corresponded to slopes of 1/20, 1/100, 1/500, and 1/2000, respectfully. This was arranged because a slope of 1/20 is too steep for a coarse grid size of 25 meters, and additionally this arrangement saved model computation time. The incoming boundary location was assigned at mean sea level (MSL), where the edge of the marsh is assumed to be located for all of the simulations. Since the main focus of this research is on wave attenuation by different characteristics of a salt marsh coastline, all of the hydraulic characteristics of waves from offshore to the marsh edge (e.g., refraction, shoaling, infragravity waves) can be ignored and the wave height (H_{rms}) from the marsh edge to a distance over the salt marsh platform can be obtained.

In Figure 38, a schematic is provided in order to show which parameters were used for the batch of XBeach-vegetation simulations. In addition, a short description of each parameter is listed below:

1. Stem height, ah [m]
   The average plant stem height of the salt marsh in relation to the bed.
2. Stem density, *N* [stems/m^2]
   The average plant stem density of the salt marsh.
3. Stem diameter, b_v [mm]
   The average stem diameter
4. Slope of salt marsh platform, *s* [1/value]

[5] Wave run-up is the highest water level occurring on a slope during a wave period (relative to the still water level) (Schiereck and Verhagen, 2012).

The slope of the salt marsh platform from the marsh edge until a water level of z_{s0} plus 2 meters for run-up.

5. Distance of wave travel over salt marsh platform, d_w [m]
   Distance of wave travel over the salt marsh platform beginning at the marsh edge (these values were assigned based on 'cross-shore width of salt marsh' in Chapter 5.2.1).
6. Wave height, H_{rms} [m]
   The root-mean-square wave height, located at the incoming boundary (seaward edge of salt marsh).
7. Wave period, T_{rep} [s]
   The representative wave period corresponding to the root-mean-square wave height.
8. Water level, z_{s0} [m]
   The water level relative to MSL.

A schematic is provided below in order to show the previously listed parameters (Figure 38).

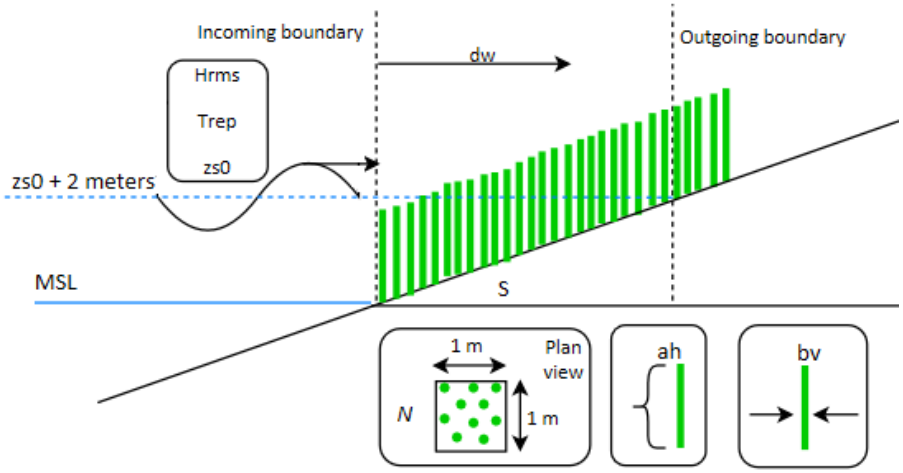

Figure 38: Visual description of the input parameters for the batch of Xbeach simulations.

Depending on the water level, wave height, slope, and stem height values used as input, the salt marsh platform could be partially or fully submerged for different simulations. Based on the obtained data for salt marsh characteristics and hydraulic conditions (Figure 30, 34, and 36), and the calculated wave heights and wave periods (eqns. 11 and 12), input values were assigned for the XBeach-vegetation model simulations. The chosen values used as model inputs can be viewed in Table 9.

Table 9: Selected parameters based on the data obtained for various salt marsh habitats around the world.

	Model input parameter	Input values
Salt marsh parameters	stem height [m]	0.4, 0.7, 1.3
	stem density [stems/m^2]	100, 500, 1000
	stem diameter [mm]	3.0, 6.0, 9.0
	marsh platform slope [m/m]	1/20, 1/100, 1/500, 1/2000
	distance of wave travel [m]	100, 250, 500, 1000, 2000
hydraulic parameters	wave height [m]	0.5, 1.0, 2.0, 2.5
	wave period [s]	3.2, 4.5, 6.4, 7.1
	water level (above MSL) [m]	3.2, 4.0, 5.0

As previously mentioned, the incoming boundary condition was set at the marsh edge, which has a vertical elevation that is assumed to be equivalent to MSL. The end of the computational domain is limited based on the water level (z_{s0}+2 m of run-up). In this way, unnecessary computations were avoided for the simulations having lower wave heights and water levels as input.

The drag coefficient was calculated at the marsh edge, and is based on the incoming wave height, water level, and stem diameter. In this way, a representative C_D can be calculated for each simulation based on the Möller *et al*. (2014) equation[6]. Values were extrapolated from this equation instead of using a constant C_D of 0.4, which was used for model calibration. It can be seen that the equation of Möller *et al*. (2014) gives reasonable results for the drag coefficients at different locations across the salt marsh at Hellegat polder for a range of hydraulic conditions (see Chapter 4.2). In Figure 39, the location where the extrapolated C_D value was calculated for all of the model simulations is shown.

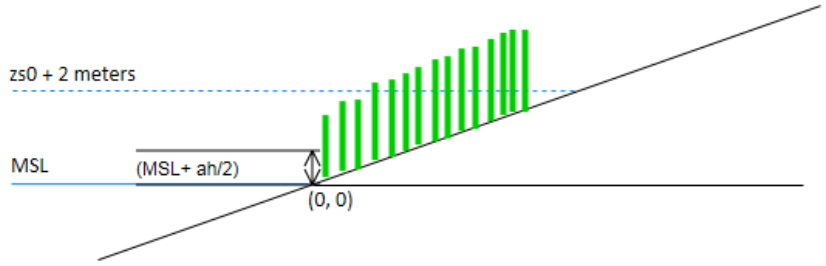

Figure 39: Location of the extrapolated drag coefficient (C_D) for the various input combinations.

This approach was chosen using the Möller *et al*. (2014) because a larger range of hydraulic conditions and salt marsh characteristics were simulated for this phase of simulations versus the simulations from the calibration phase (which only considered one set of salt marsh parameters and a more narrow range of hydraulic conditions). This equation produces values for the drag coefficient based on the hydraulic conditions and the stem diameter of each simulation. Since the drag coefficient depends largely on the wave height, water depth, and stem diameter, using an equation such as this is a more representative method of the varying conditions versus using a constant drag coefficient value (which was used in model calibration). This equation was created based on extreme hydraulic conditions (H_s up to 0.9 meters in wave height) which are among the highest recorded wave heights over salt marshes in the literature.

This method does provide a conservative approximation by only calculating the drag coefficient at the incoming boundary, and the reason is that it is known that the drag coefficient value changes constantly in the cross-shore direction. When a wave reaches the end of the computational domain, the water depth is decreased and drag coefficient value will be much higher (closer to 1), since the wave will be near full attenuation and the Reynolds number will be greatly decreased as a result. A conservative approximation was used so that the simulated wave heights would not be lower than those occurring in nature. If a method such as this one were to be applied to a given salt marsh coastline, a conservative approach would be used to account for uncertainty.

For the XBeach-vegetation simulations, the extrapolated values for the drag coefficient based on the parameter values in Table 9 ranged from approximately 0.16 to 0.30, which was found by obtaining the drag coefficient for the most extreme and least extreme combinations of hydraulic conditions and salt marsh characteristics. The results of these model simulations were first analyzed, and then input into the BN for further data analysis and sensitivity testing. An overview of the XBeach-

[6] Recall from Chapter 4: $C_D = (227/\mathrm{Re})^{1.62} + 0.16$

vegetation results can be found in the next paragraph, while the BN network construction can be viewed in Chapter 5.4.

5.3.2 XBeach Results

In reviewing the data before it was input into the BN, it can be seen that many of the wave heights are between 0 and 0.1 meters (Figure 40). This is because for many of the simulations, the waves did not reach the longer distances of 500, 1000, and 2000 meters. This indicates the occurrence of more dry cases (emergent salt marsh) for the longer distances over the salt marsh. This was especially the case for the simulations with a slope of 1/20.

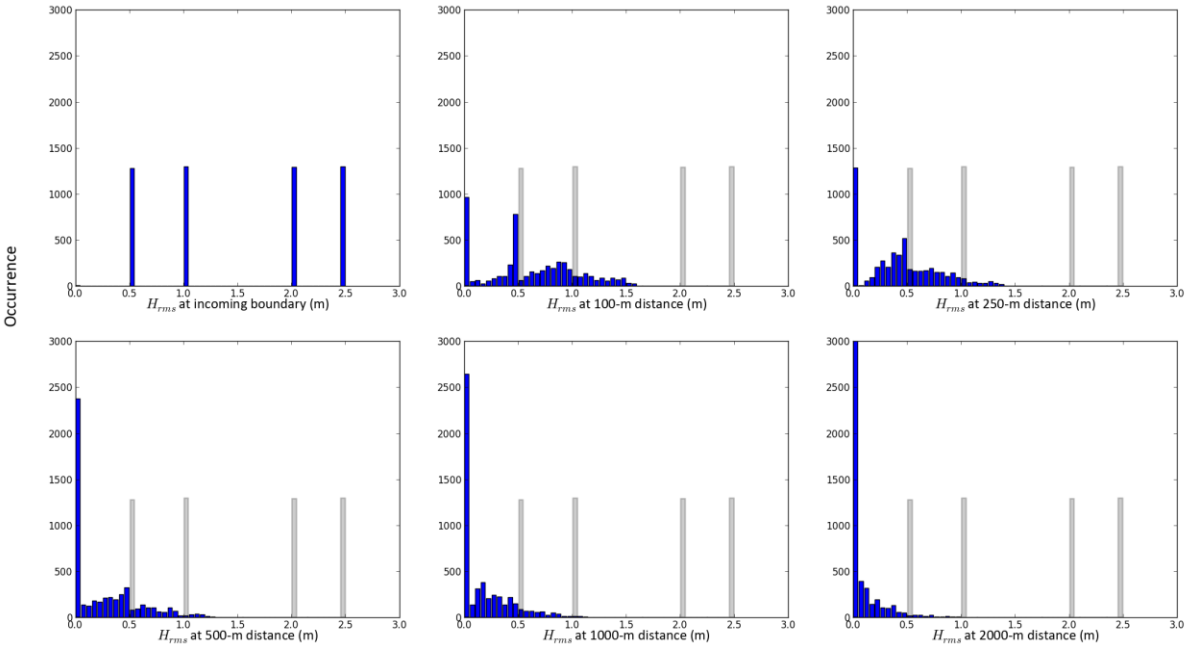

Figure 40: Resulting wave heights and their occurrence at the various distances for the batch of XBeach-vegetation simulations including results with values of zero. The gray bars in represent the wave height distribution at the incoming boundary (assigned input values) to show the shift in distribution from the beginning of the salt marsh platform until the end.

In reviewing Figure 40, the shift in wave heights can be seen from the incoming boundary to the 2000-meter distance over the salt marsh platform for all of the simulations. These distributions indicate that there is a reduction in wave heights occurring at each distance. At 100 meters, the wave heights range from approximately 0 to 1.6 meters, while at 200 meters the wave heights range from roughly 0 to 1.4 meters. At 500 meters the wave heights ranged from 0 to 1.2 meters, at 1000 meters the wave heights ranged from 0 to 1 meter, and at 2000 meters the range was 0 to 0.8 meters. A frequent value of approximately 0.5 can be noticed for the wave height distributions for the 100 and 200 meter distance. Once these values were checked, they could be analyzed in further detail by looking into results based on the various input parameters. By assessing the influence that the various salt marsh characteristics and hydraulic conditions, relationships can be obtained.

In Figure 41, the simulated wave heights based on the different stem properties used as input can be viewed.

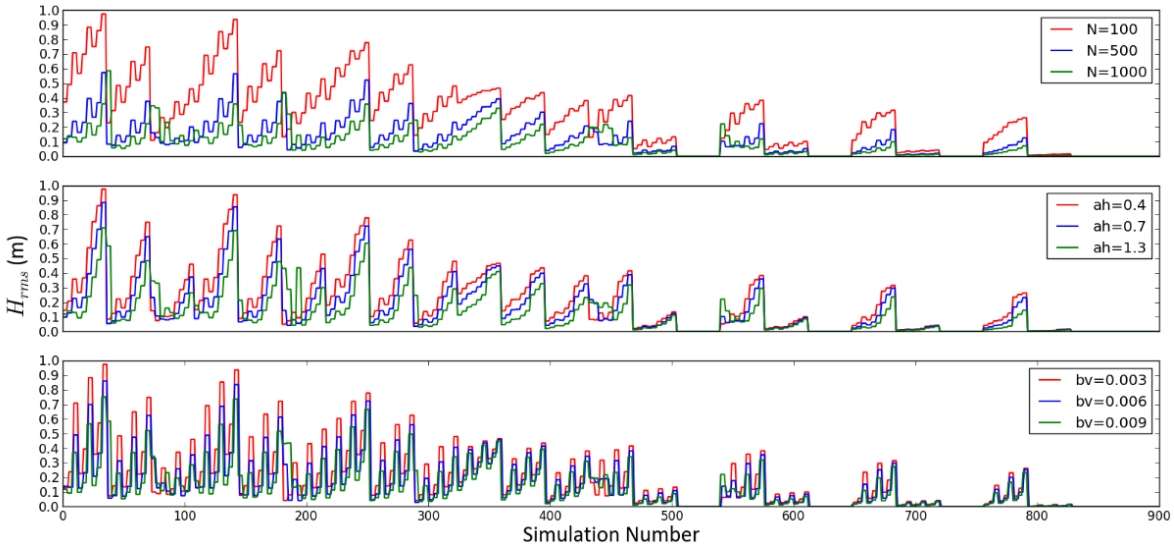

Figure 41: The resulting wave heights for all simulations at a 2000-meter distance for the various: stem densities (top image), stem height (middle image), and stem diameter (bottom image).

Figure 41 displays the wave heights at the 2000-meter distance resulting from the various values for: stem density (*N*), stem height (ah), and stem diameter (b_v) which were plotted in order to show their influence on the simulated wave heights. The wave heights were plotted at a distance of 2000 meters to amplify the influence that the various parameters have on the resulting wave heights.

In the following figure, a breakdown of the stem density is provided to show the results for the various slope values and incoming wave heights used as input.

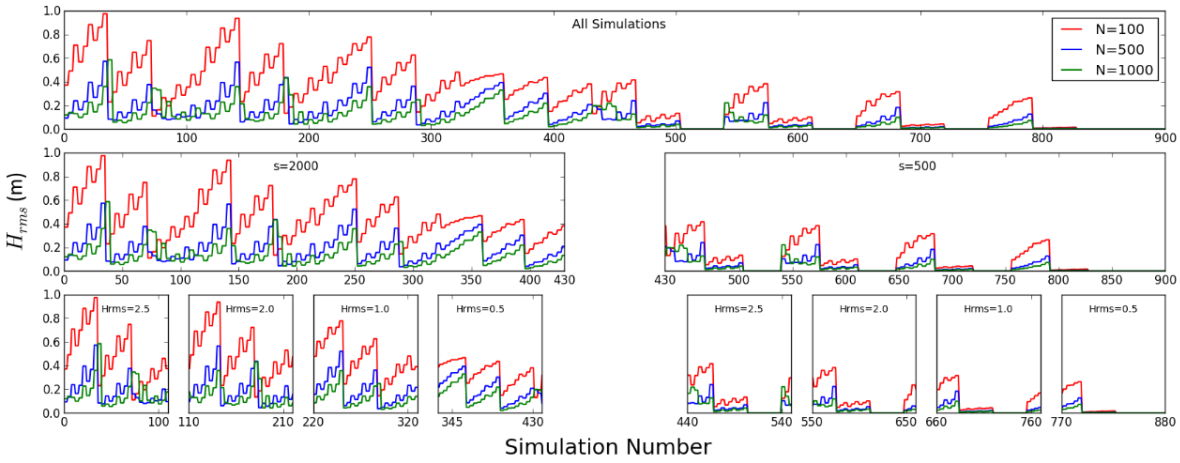

Figure 42: Stem density breakdown showing all simulations (top), simulations with a slope of 1/2000 (middle left), simulations with a slope of 1/500 (middle right), and the corresponding incoming wave heights for the two different slope values. Slope values of 1/100 and 1/20 did not produce waves at a 2000-meter distance, and therefore are not shown.

In viewing Figure 42, the lowest value used for stem density can be seen to produce the highest waves, while the highest value used as input for the stem density produces the lowest waves. Trends can be noticed based on findings from the literature, and these trends will be discussed further in the next chapter.

Similar to the breakdown of the stem density, the resulting wave heights based on the various stem heights were also studied in more detail for the various slope values and incoming wave height values. A visualization of this can be seen in Figure 43.

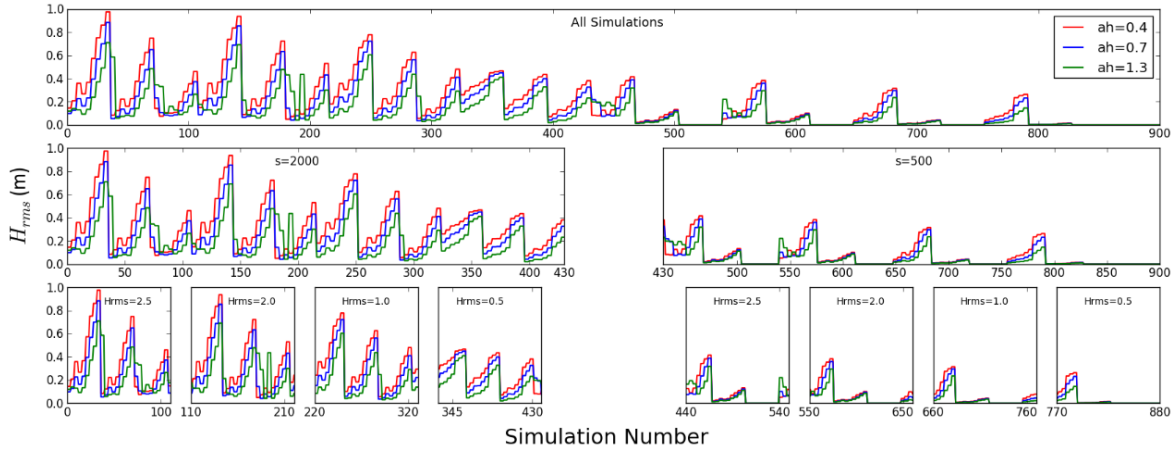

Figure 43: Stem height breakdown showing all simulations (top), simulations with a slope of 1/2000 (middle left), simulations with a slope of 1/500 (middle right), and the corresponding incoming wave heights for the two different slope values. Slope values of 1/100 and 1/20 did not produce waves at a 2000-meter distance, and therefore are not shown.

In Figure 43, the influence of varying the stem height shows similar trends as the influence of the stem density does, and differences can be noticed when studying the wave heights produced by the different slopes and incoming wave heights. Overall, the lowest stem height produces the highest wave heights, while the highest stem height produces the lowest wave heights.

Similar to the breakdown of the stem density and the stem height, the stem diameter was also studied for the various slope values and incoming wave height values. A visualization of this can be seen in Figure 44.

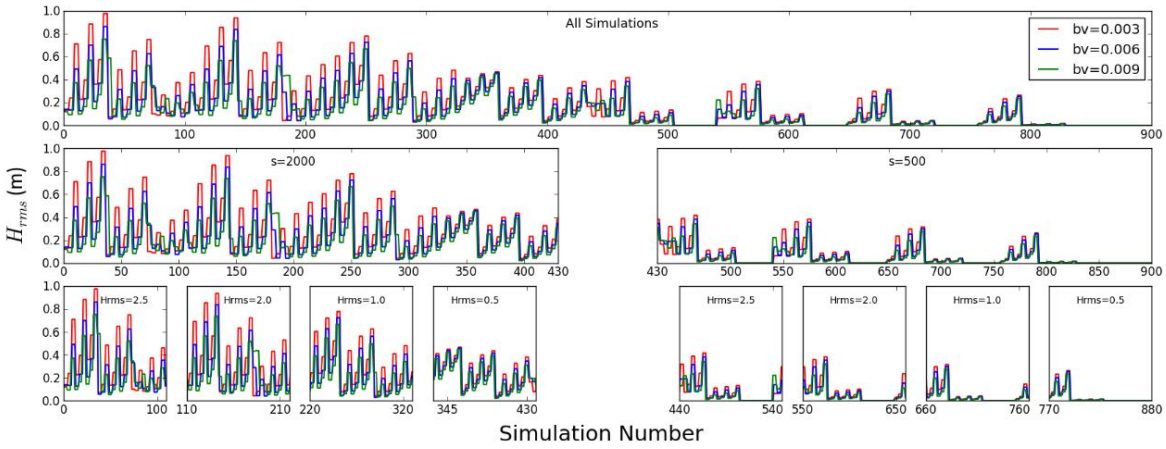

Figure 44: Stem diameter breakdown showing all simulations (top), simulations with a slope of 1/2000 (middle left), simulations with a slope of 1/500 (middle right), and the corresponding incoming wave heights for the two different slope values. Slope values of 1/100 and 1/20 did not produce waves at a 2000-meter distance, and therefore are not shown.

The trends realized from the stem diameter are similar to those found by looking at the resulting wave heights from the various stem density and stem height results. This is expected, since the stem diameter and the stem density are both part of the vegetation factor equation in the XBeach model.

Overall, the lower stem densities produce the highest waves while the highest value used for stem density produces the lowest waves.

Once a breakdown of the stem density, stem height, and stem diameter was plotted for analysis, an overview of the influence of the various slope, incoming wave height, and water level values was created (Figure 45).

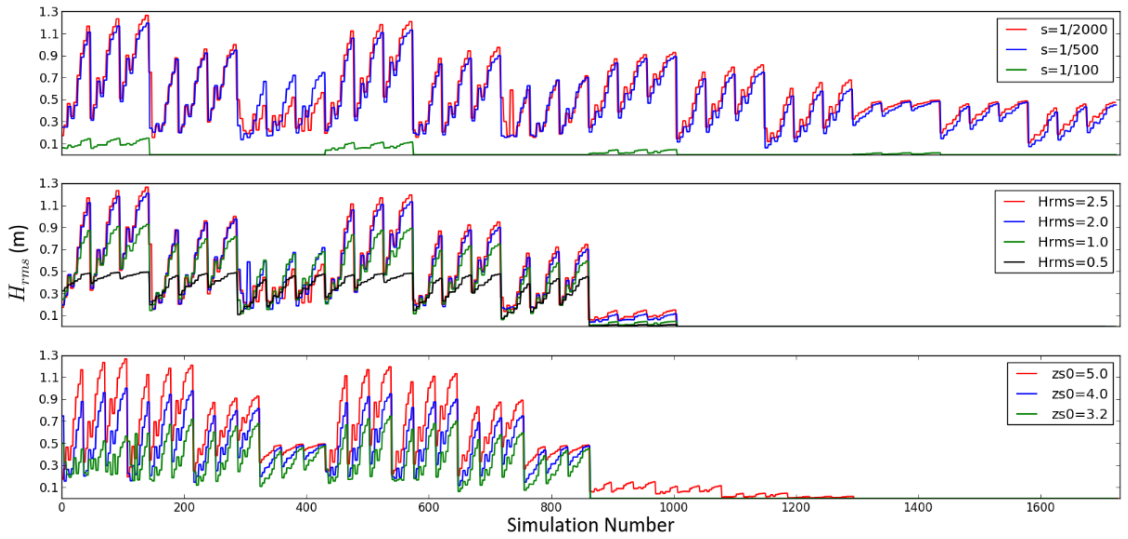

Figure 45: The resulting wave heights for all simulations at a 500-meter distance for the various: slopes (top image), incoming wave height (middle image), and water level (bottom image).

By studying Figure 45, several trends can be noticed. Overall, the highest waves are produced for a slope of 1/2000, a H_{rms} of 2.5 meters, and a z_{s0} of 5 meters. A slope of 1/20 was not included in this figure, since waves produced for that case did not reach the 500 meter distance. In order to display in more detail which input parameters create various wave heights, the simulation results for all slopes were plotted for review (Figure 46).

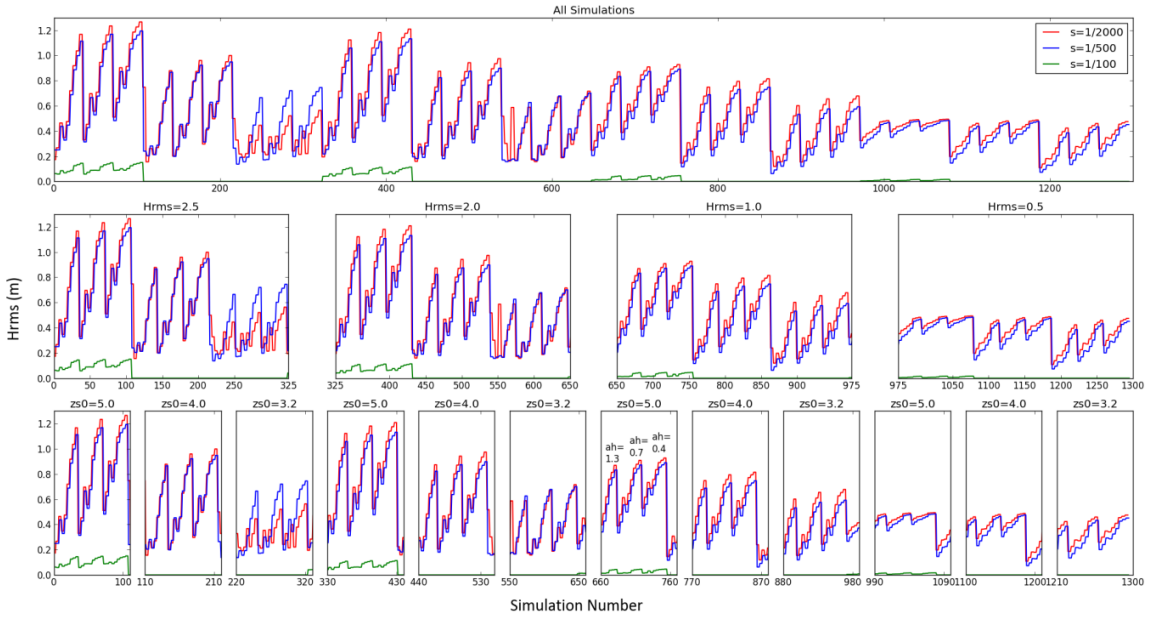

Figure 46: Slope breakdown for the resulting wave heights at 500 meters showing all simulations (top), simulations produced by the various incoming wave heights (middle images), and simulations produced by the various water levels (bottom images). Additionally, the stem height values (ah) are listed in the bottom row, seventh image from the left in order to show the influence on the wave height.

It can be gathered by looking at Figure 46 that for the cases resulting from a slope value of 1/20, no waves reached the 500-meter mark. Additionally, the various stem height values are listed in one of the plots located in the bottom row of Figure 46 to show the influence of the stem height on the wave heights. The results of this chapter will be discussed in further detail in Chapter 6. Once the data was plotted for review, it was input and compiled into the BN program Netica (Figure 47).

5.4 Bayesian Network Construction and Training

To construct the BN and handle the model results in a more organized and statistical manner, the Netica program was used. The Netica program is a statistical tool designed to work with belief networks and influence diagrams (Norsys, 2014). This program is useful for organizing large amounts of data into one system, and viewing the relationships between the different parameters (nodes). Netica has the ability to perform a sensitivity analysis based on the values of all the nodes, and also show dependencies between any of the nodes with each other. Specific values within the network can be selected in order to quickly obtain a resulting probability distribution based on the selected values.

Once the model runs were completed and input into Netica, the network must be compiled and trained before any action can take place. This step is necessary for connecting all of the nodes in the network properly, and refreshing them with the newly learned case file[7]. The network must then be trained once the data has been collected and the network has been constructed. This means that based on the collected data, conditional probabilities will be created for all of the child nodes. In this study, the child nodes were defined based on the distance of wave travel. Wave heights were obtained at five distances over the salt marsh platform (100, 250, 500, 1000, and 2000 meters), and input into the various child nodes based on the distance where the wave heights were obtained. The assigning of bins for each child node was performed based on the span of results at each distance (Figure 40). Initially, only five bins were assigned per node (Figure C-3). It was later decided to add more bins per node, and minimize the bin sizes in order to obtain a better distribution for the child node. After reviewing the results of the XBeach simulations, the data was input and compiled into the Netica program for further use of the BN (Figure 47).

[7] Netica has the ability to learn a new case file once excluding the previous one, or it can combine the previous case file with a newly produced one.

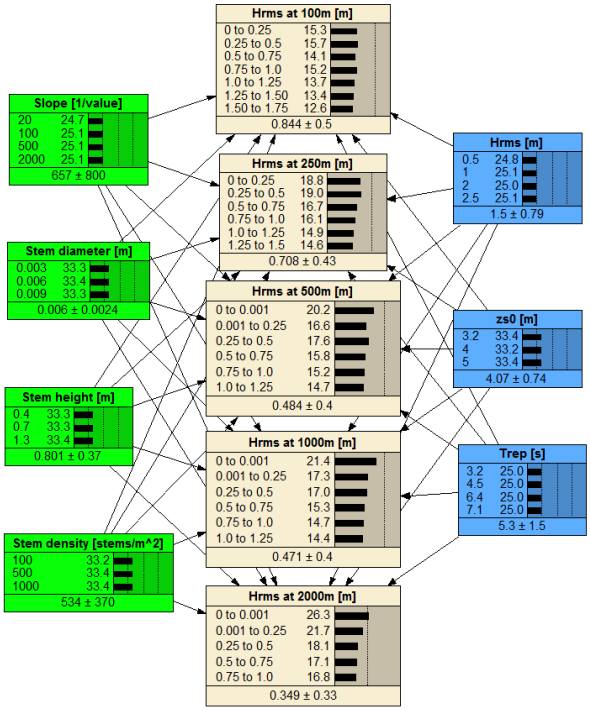

Figure 47: The compiled network with the salt marsh characteristics (strength variables) on the left in green (discrete nodes) the resulting wave heights in the middle (continuous nodes), and the hydraulic conditions (load variables) on the right in blue (also discrete nodes).

The load and strength variables (blue and green boxes) in Figure 47 are classified as discrete-type nodes, while the result nodes (tan boxes) are classified as continuous-type nodes. The discrete-type nodes could simply be assigned values based on previously defined parameters (Table 9), while the discretization of the bins for the continuous-type nodes was defined based on interpretation of model results (Figure 40). In addition, the mean and standard deviation values for each node can be found below all of the bins of a certain node. In the following chapter, results of BN testing will be presented and the influence of the different load and strength variables on the results will additionally be presented.

5.5 Netica (BN) Results and Sensitivity

The main purpose of this study is to simulate wave attenuation by global coastal salt marsh habitats for various salt marsh characteristics and hydraulic conditions. The development, calibration, and boundary condition orientation of the model used for measuring wave attenuation is explained in the previous chapters. The following chapters will provide an overview of the simulation results used to study wave attenuation by global coastal salt marsh habitats. The main components and some observations will be presented. Discussion of the results will occur in Chapter 6.

Once the network was compiled and trained (Chapter 5.4), the network can be used to obtain results using a large dataset. For this network, the various salt marsh characteristics and hydraulic conditions were tested by defining a wave height range (bin) at each child node. Figure 48 displays the results when selecting the highest bin and lowest bin for each resulting node.

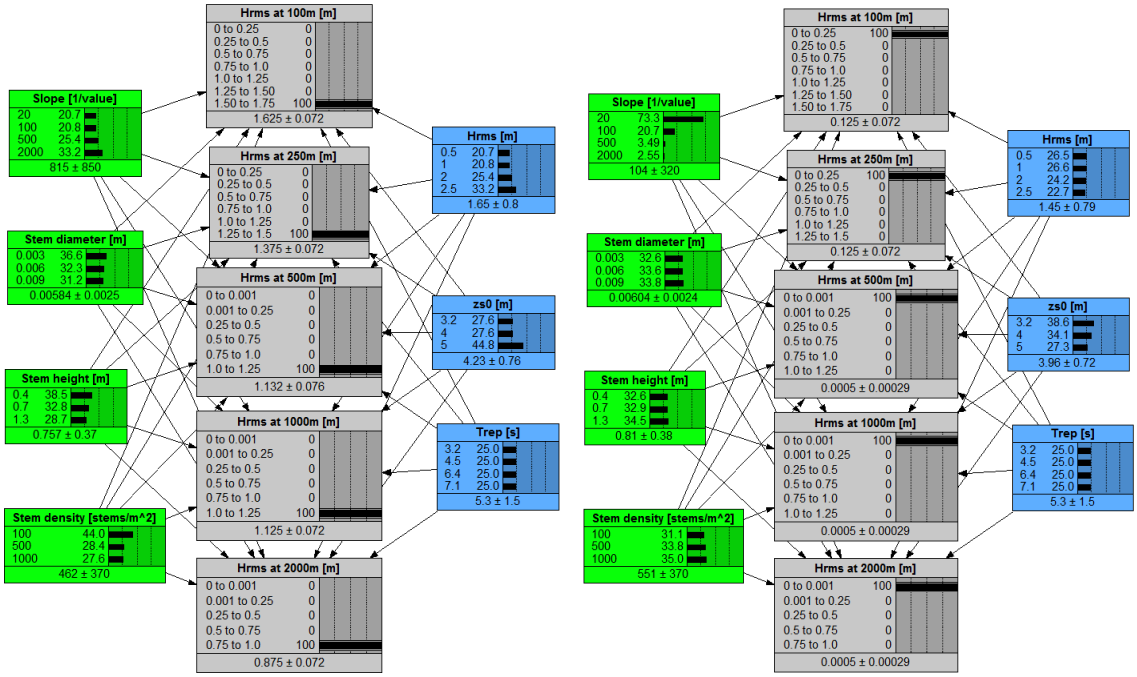

Figure 48: Selection of the highest and lowest hydraulic case for H_{rms} at each distance across the marsh platform transect. The results from selecting the most extreme case can be seen in the left image, while the results from the least extreme case can be seen in the right image.

By selecting the highest and lowest wave-height bin at each result node, it can be seen that the probability distributions for the various parent nodes change from the left image to the right image. Whenever the highest wave bins are selected at each distance, the probability is highest for the lower stem property values and the most gradual slope. For the hydraulic nodes, the probability is highest for the highest incoming wave height and water level. Whenever the lowest wave bins are selected at each distance, the probability is highest for the higher stem property values and the steepest slope. For the hydraulic parameters, the two lower wave heights show the highest probability and the lowest water level shows the highest probability.

5.5.1 Netica Sensitivity

In addition to analyzing the most and least extreme cases for the wave heights at each distance, the various stem properties were also isolated and analyzed to test their influence on the network. The various stem density values used as input were all tested in isolation in order to amplify their influence on the resulting wave height nodes. It was found that by isolating certain parent nodes (i.e., stem density, stem height, stem diameter, slope) and selecting the different values of that node, more information could be learned regarding a parent node's influence on the child nodes.

In Figure 49, the stem density influence on the nodes is shown for the wave height distributions at each distance.

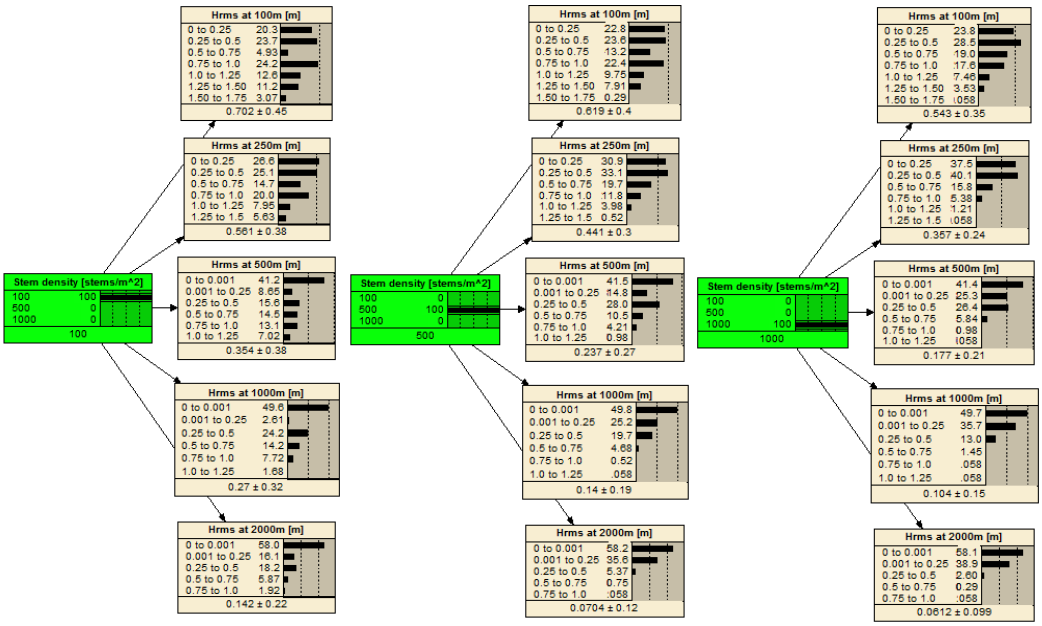

Figure 49: The resulting wave height distributions at the various distances for a stem density of 100 (left image), 500 (middle image), and 1000 (right image).

In viewing Figure 49, it can be seen that the distribution at each distance varies when different stem density values are selected. For a stem density of 100, the probability is greater for higher waves to occur, while for a stem density of 1000, the probability distribution shifts and hardly any waves are predicted for the two bins of highest value.

Similar to the stem density, the stem height was also isolated and analyzed with the result nodes alone. Although the probability values differ slightly when looking at the stem density versus the stem height, similarities in the trends can be noticed.

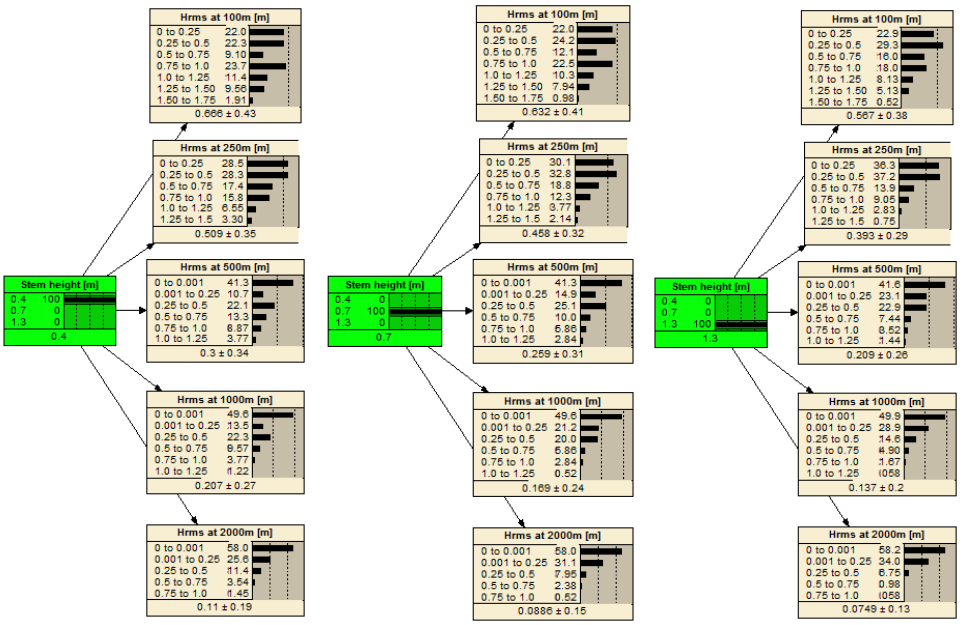

Figure 50: The resulting wave height distributions at the various distances for a stem height of 0.4 (left image), 0.7 (middle image), and 1.3 (right image).

In viewing Figure 50, it can be noticed that the higher the stem density, the higher the probability that the resulting wave height will be of lower value. Similar to analyzing the stem density and stem height, the stem diameter was also isolated to amplify its influence on the resulting wave heights at each distance (Figure 51).

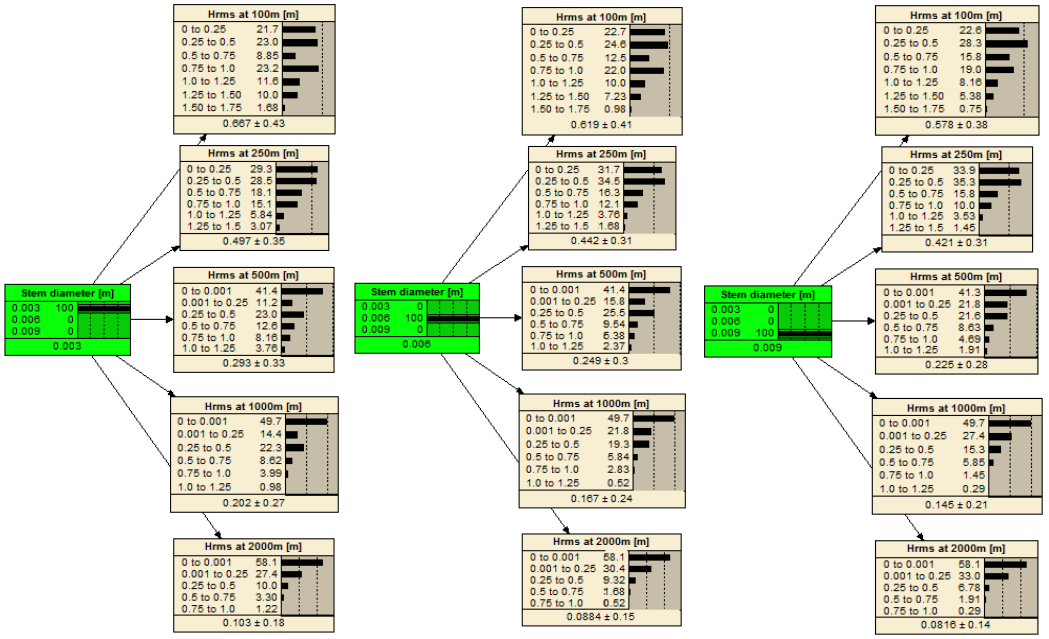

Figure 51: The resulting wave height distributions at the various distances for a stem diameter of 0.003 (left image), 0.006 (middle image), and 0.009 (right image).

The results of Figure 51 show similar trends to those of the stem height and the stem diameter. Finally, the salt marsh slope was isolated and studied (Figure 52) with the resulting wave heights at the various distances in order to see its influence.

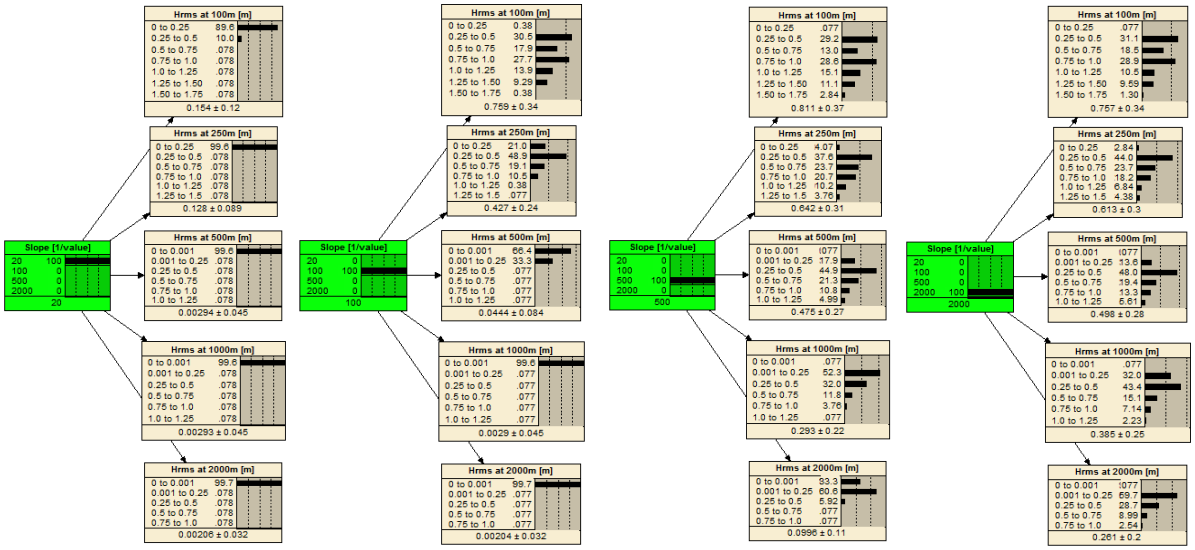

Figure 52: The resulting wave height distributions at the various distances for a salt marsh slope of 1/20 (left image), 1/100 (middle-left image), 1/500 (middle-right image), and 1/2000 (right image).

In viewing Figure 52, it can be noticed that the resulting wave heights are highly sensitive to the various slope values. Selecting a 1/20 value for the slope results in almost full certainty that the wave heights are never higher than 0.25 meters at each distance, while a slope value of 1/2000 shows higher probabilities for wave heights of greater heights occurring.

It is important to note an additional capability of Netica, which can give distributions for any parent node values as long as the desired value is between the lowest and highest of the defined values in the parent node. For instance, if it is desired to determine the probability of a 1/60 slope, or a 1/200 slope, this can be achieved. In Figure 53, examples of this can be noticed.

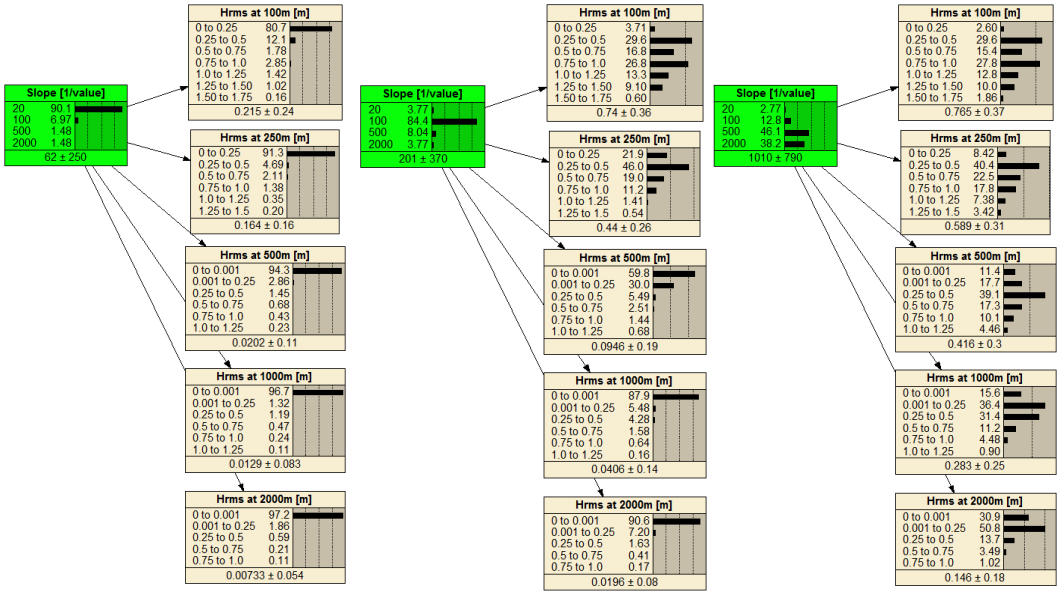

Figure 53: Probability distributions based on the assignment of parent node values which fall between the original values of 10, 100, 500, and 2000. Recall that the mean and standard deviation are provided at the bottom of each node, so for the parent nodes the values of roughly 60, 200, and 1000 can be seen.

In Figure 53, it can be noticed by viewing the green nodes that values of roughly 60, 200, and 1000 are all displayed for the mean value at the bottom of the node. This is a useful capability of Netica, which allows flexibility when it is desired to study a situation that falls within the dataset, but uses different input values than the original defined input values.

By repeating the above exercise for all of the salt marsh characteristics, probability distributions could be produced for a range of values and the sensitive parameters could be noticed. A sensitivity plot could be produced in order to see which parameters impact the results significantly, and this can be used for the improvement of future research in this field. In Figure 58, the sensitivity plot is provided.

5.5.2 Comparison of XBeach-vegetation with Netica

In addition to analyzing the different components of the BN and looking at their influence, the results can also be compared to the XBeach results for four cases. The highest and lowest hydraulic conditions and the highest and lowest stem property values will be checked by plotting both the XBeach results and the BN results separately.

In Figure 54, the highest hydraulic parameters are selected, and the two different cases are shown resulting from selecting the highest and lowest values for stem properties.

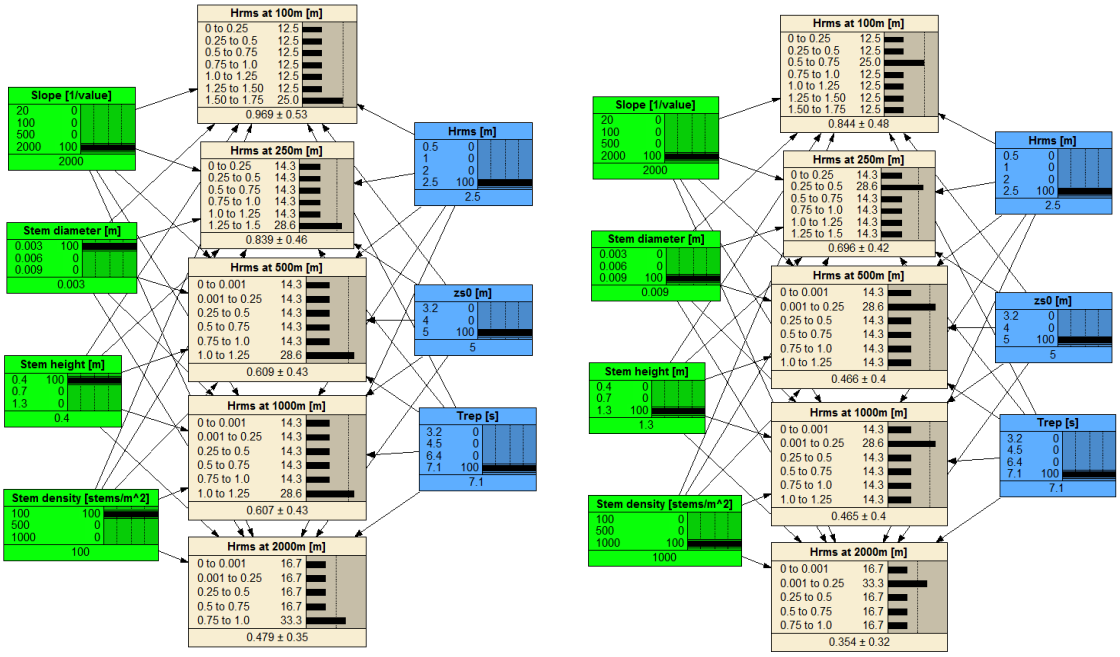

Figure 54: The probability distributions of the wave heights at each distance resulting from the most extreme hydraulic conditions and the weakest stem properties (left image) and the most extreme hydraulic conditions with the strongest stem properties (right image). A constant slope of 1/2000 was selected for both situations.

Based on Figure 54, higher probabilities can be noticed for certain bins for both cases, and these can be checked below by plotting the XBeach results using the same inputs from those cases. In Figure 55, the results from XBeach using the same input values as were used above in Figure 56 are plotted to show a comparison between the two different methods for predicting wave attenuation.

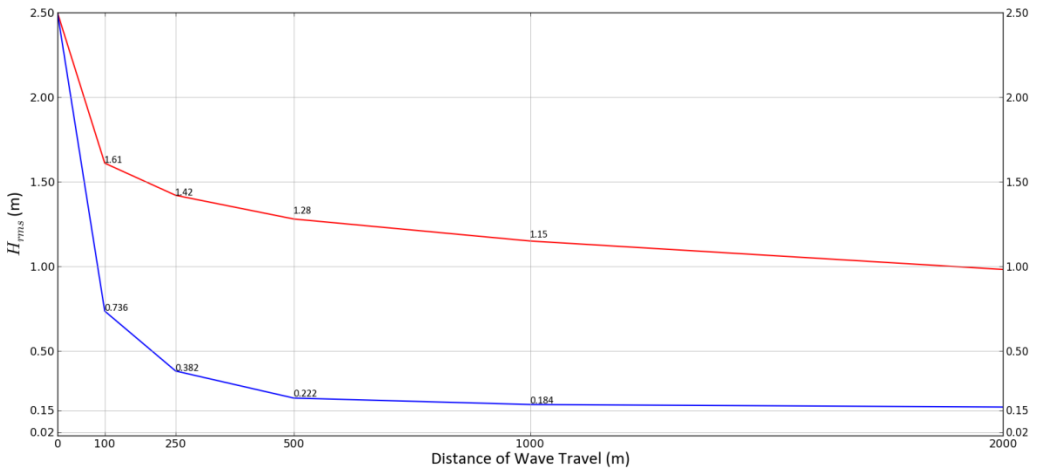

Figure 55: Highest hydraulic conditions for the strongest (blue line) and weakest (red line) stem properties.

In reviewing Figure 54 and comparing it to Figure 55, it can be noticed that the BN predicts the highest probability of occurrence for the bins which correspond to the XBeach results except for the value of 1.28, which falls just outside of the 1.0 to 1.25 bin at the 500 meter distance node. Similar to the most extreme hydraulic conditions, the least extreme hydraulic conditions were also compared between the BN and the Xbeach results.

In Figure 56, the lowest hydraulic values are selected, and the highest and lowest values for the various stem properties are also selected.

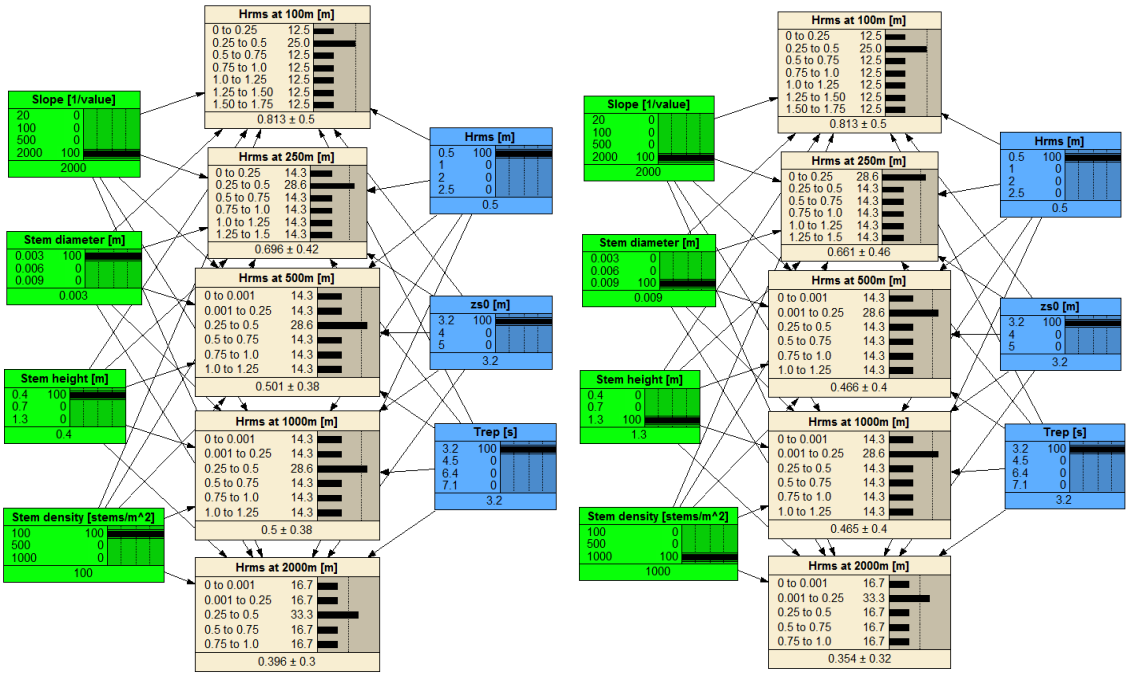

Figure 56: The probability distributions of the wave heights at each distance resulting from the least extreme hydraulic conditions and the weakest stem properties (left image) and the most extreme hydraulic conditions with the strongest stem properties (right image). A constant slope of 1/2000 was selected for both situations.

Based on Figure 56, the highest probabilities can be noticed for the resulting nodes, and these can be compared with the Xbeach results using the same input values. The Xbeach results for the same input values as used in Figure 57 are plotted below in order to show a comparison between the two methods.

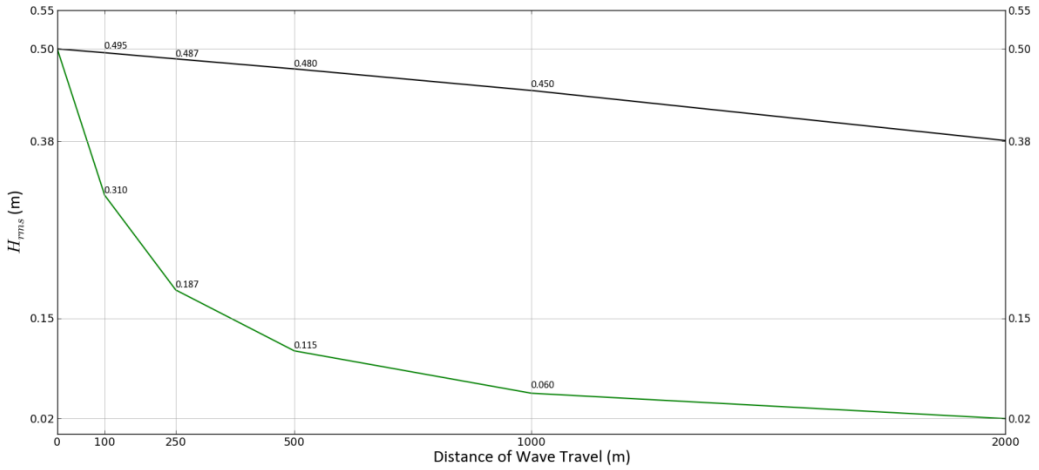

Figure 57: Lowest hydraulic condition with the strongest (green) and weakest (black) stem properties.

In comparing the results of Figure 56 with the results of Figure 57, the wave height values produced by XBeach fall within the bins predicted by the BN at all distances and for both cases. By first reviewing the results produced by the numerical model (Xbeach) and inputting those results into the BN (Netica), several trends were noticed that are consistent with findings in the literature. These trends and findings will be discussed further in the following chapter, along with results of the sensitivity analysis for the different salt marsh parameters, and conclusions and recommendations will follow in Chapter 7.

6 Discussion

6.1 Discussion of Results

Calibration and Validation Results

The numerical model performed well when tested with field results which recorded extreme wave heights (up to 0.69 m) during a winter storm at various locations along a marsh transect located at Hellegat Polder, Western Scheldt, the Netherlands. This shows promise for further application of the XBeach-vegetation model for use in analyzing salt marshes as nature-based and hybrid flood defense components, especially because the waves recorded at Hellegat are among the highest recorded over a salt marsh found in the literature. The drag coefficient and gamma (breaking parameter) were adjusted to form a close fit to data recorded in the field using values of 0.4 and 0.45, respectively. Additionally, based on the entire record of wave conditions at Hellegat, four drag coefficient equations found in the literature were plotted in comparison to each other and a common value that has been used (Figures 17 and 18). After analysis, it was decided to use the Möller *et al.* (2014) equation because it is best suited for reproducing drag coefficient values fit for extreme hydraulic conditions and a wider range of values. In testing the model further with the wave heights recorded at the Hannover Flume, it was found that the Paul and Amos (2011) equation produced acceptable results for less-extreme conditions. This could have resulted from the fact that this equation results from waves recorded over sea grass during calmer conditions (H_s= 0.1-0.18), or it could simply be a coincidence. However, overall the aim of this research was to analyze wave attenuation over salt marshes for extreme hydraulic conditions. Therefore, the Möller *et al.* (2014) equation equation was used in the batch of XBeach-vegetation simulations which obtained wave height results over an arbitrary salt marsh platform using various salt marsh characteristics and hydraulic conditions to produce results for the BN. The results of the XBeach-vegetation simulations will be discussed in the following paragraph.

XBeach-Vegetation Results

In looking at the results of the XBeach simulations, several findings are worth noting. By plotting the stem properties individually, common trends could be noticed for resulting wave heights (Figure 41). Overall, an increase in stem density resulted in a decrease in wave heights, which can be compared to an existing theory on this process. For instance, Lima (2006) found that increasing stem density resulted in a decrease in wave height. Additionally, the results in Figure 41 show that increasing the stem height produces lower wave heights overall. This can be compared to the idea of both Anderson *et al* (2011) and Yang *et al.*(2012) which stated that as stem height increases, wave attenuation increases. By increasing the stem diameter a decrease in wave heights can also be noticed in Figure 41. The stem diameter is known to increase proportional to the stem height (Figure 33), so this trend is expected.

Additional regimes can be noticed when looking at Figures 41-46. For a gradual slope (i.e., 1/2000), the stem properties have more influence on the resulting wave heights, since large variations can be noticed when looking at them separately. For a steep slope, (i.e., 1/100), the water level and incoming wave height have more influence, and have more importance. This is noticed especially when looking at Figure 46 for the simulations produced by incoming wave heights of 2.5 meters and a water level of 5 meters, since those conditions produce waves near 0.15 meters. Contrarily, wave heights produced by incoming waves of 0.5 meters and a water level of 3.2 meters are entirely attenuated (0 meters in height).

When viewing Figure 55 and 57, a relation can also be seen when looking at the most and least extreme hydraulic conditions produced for a slope of 1/2000 based on the finding of Tschirky *et al.*

(2000) that wave attenuation is larger for larger incident waves. For instance, when looking at the attenuation for the highest incoming wave height (2.5 meters) and water level (5 meters), the wave height reduction over a distance of 2000 meters is 1.5 meters for the weakest stem properties, and roughly 2.35 meters for the strongest stem properties. When looking at the wave height reduction for the lowest incident wave height (0.5 meters) and water level (3.2 meters), the wave height reduction over a distance of 2000 meters is 0.12 meters for the strongest stem properties, and 0.48 meters for the weakest stem properties. This implies that even for low rates of attenuation (.0125% wave height reduction per meter), if a wave propagates over a long section of salt marsh, the wave height reduction from the beginning (marsh edge) to the end of the salt marsh can be significant (total wave height reduction of 24%).

Additionally, pivot tables were created to look at average wave heights at each distance for the various salt marsh characteristics and hydraulic conditions (Appendix C). For instance, if the average wave heights produced by stem density values of 100 and 500 (stems/m^2) at 250 and 1000 meters, it can be noticed that increasing the stem density by a factor of 5 decreases the wave height by 25% at a 250-meter distance; at a 1000-meter distance, the average wave height is reduced by 48%. By looking at the slope values in Table C-5, it can be seen that the average wave heights produced by increasing the slope steepness by a factor of 5 decreases the average wave heights by 25% at 250 meters; at 1000 meters, the average wave height is fully attenuated (0 meters in height). The following paragraph discusses the BN results in more detail.

Netica Results

The purpose of the BN is to share the XBeach-vegetation results in order to efficiently quantify wave attenuation in a probabilistic manner. The BN proved to be useful in organizing the numerical model data, and showing dependencies of the various salt marsh components of the network (Figures 47-53). In analyzing the data both before and after input into the BN, the results from the BN show similar trends for dependencies as the XBeach results for the various stem properties, slope, incoming wave height and incoming water level. However, it is important to realize that Netica provides results for wave heights in a statistical manner (conditional probability distributions) instead of deterministic values. A sensitivity analysis was performed on the salt marsh components of the network, and additionally the BN was compared with XBeach results in order to show the two different forms of results and also to test if the BN could produce logical results. The results of these two performances will be mentioned in the following paragraphs.

An overall sensitivity analysis was performed for the BN to show the influence in changing the parent node values had on the child nodes (Figures 49-53). Additionally, values falling in between the ones originally defined values of these nodes could be tested, which is an advantage to using a program such as Netica. By changing the various values of slope, stem density, stem height, and stem diameter, knowledge could be gained on how the probability distributions of the child nodes (result nodes) vary.

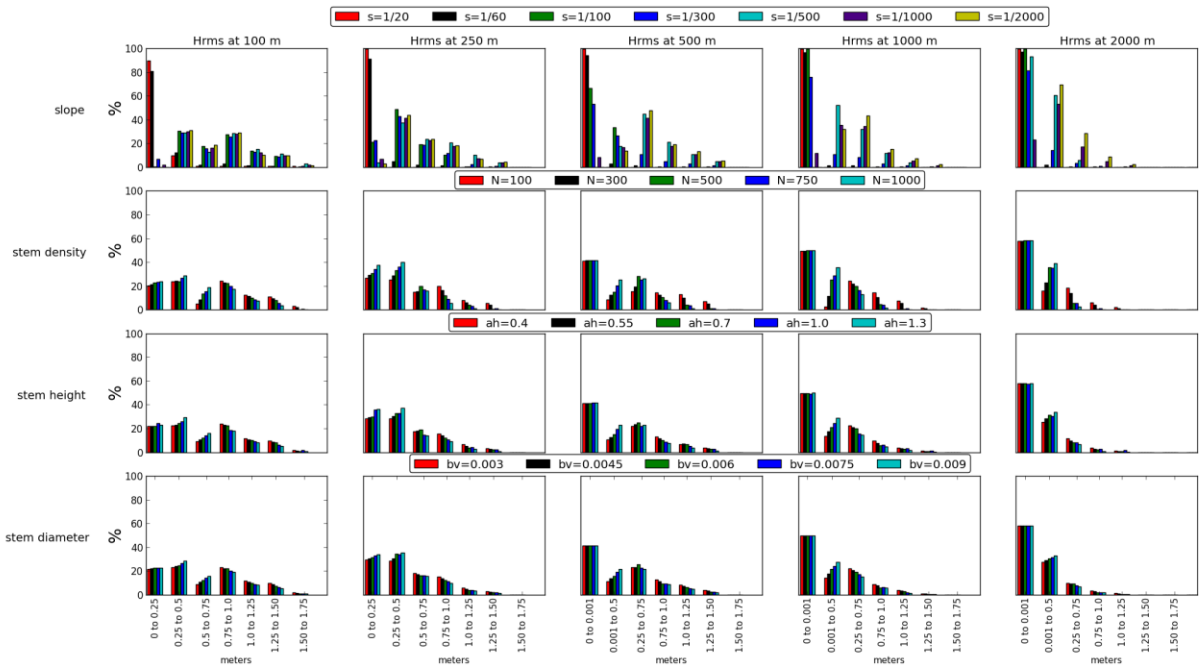

Figure 58: Overall Bayesian Network sensitivity obtained by isolating all of the salt marsh characteristics and plotting the probability distributions of the wave height bins at each distance.

By looking at Figure 58, several findings can be noticed. A large response was observed whenever the slope value was changed from a steep value of 1/20 to a gradual slope value of 1/2000. The slope values closest to 1/20 showed the most activity for the lowest wave bin, since often the steepness prevented waves from reaching their full potential in regards to wave height. The slope values closest to 1/2000 were responsible for producing values in the higher wave bins at all of the child nodes, since many the waves penetrated further over the salt marsh platform. The probability distributions produced from the various slope values show a large variation. The slope values of higher steepness have a higher probability of producing waves from 0 to 0.25 and 0.25 to 0.5 meters. As the slope values reduce in steepness, the probability of producing higher waves at further distances increases.

By looking at the probability distributions produced by the various stem density values, the variation is not as significant as the slope but still changes can be noticed. The highest stem density value of 1000 produces higher probabilities of waves occurring in the lower bins, while at the higher bins the lower stem density values produce a higher probability of occurrence. The same trend can be noticed for the stem height and stem diameter values, although the variation for these two values is less significant than the slope and stem density variation.

Overall, the stem density was not as sensitive as the slope when looking at the resulting probability distributions. Figure 49 shows that the stem density value of 1000 was the most probable to produce wave heights occurring in the two lowest bins of each child node. The values of 750 and 500 were seen to produce waves which most commonly occurred in the middle bins of each child node, while the values of 300 and 100 produced the highest probability of wave heights occurring in the highest 3 and 4 bins for the nodes of 250, 500, 1000, and 2000 meters. These findings are consistent with the findings when analyzing the XBeach results alone and the idea from Lima (2006), which stated that an increase in stem density results in a higher wave attenuation rate. Similar trends are expected for both stem density and stem diameter, since for the XBeach-vegetation mode these two values are components of the vegetation factor.

Since the results produced by the BN are provided in a statistical manner, they can be difficult to interpret in some instances. To show this, the BN was compared with the Xbeach results using the

same input values (Figure 54-57). The BN provides a probability which indicates that for a given set of input parameters, there is a percent probability that a wave height falls within a certain bin. Looking at the XBeach results alone, however, provides single, deterministic values for wave heights over a certain distance of salt marsh for a given set of input parameters. One important thing to note regarding the Netica program is that whenever all of the parent nodes have one defined value, often only one of the bins within a child node has a case from the large dataset used to build the network. The bin containing the case receives a high value for probability of occurrence, but the remaining probability is distributed to the other bins of that node. For instance, in viewing Figure 59 (a child node taken from Figure 57) it can be seen how Netica handles this situation.

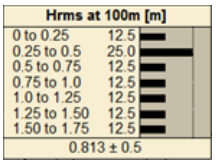

Figure 59: Example of a conditional probability distribution for a child node whenever all of the parent nodes have been confined to one value.

It can be noticed from Figure 60 that only data exists for the bin of 0.25 to 0.5 meters, and the remaining 75% of the distribution is allocated to the other 6 bins, automatically providing them with a 12.5% probability of occurrence. In reality, no data was produced for this specific case, but the bins still show a 12.5% probability which is incorrect. Figure 59 was provided in order to show the issue found from using the Netica program for quantifying wave attenuation. In the following chapter, the conclusions and recommendations gathered based on the entirety of this report will be provided.

6.2 Technical Discussion

In reviewing the results produced by both the numerical model XBeach and the statistical BN Netica, knowledge could be obtained based on the results of both methods. The initial research question was answered by reviewing the performance of the XBeach-vegetation simulations, which provided a table of wave heights over several distances of a salt marsh platform for a range of hydraulic conditions and salt marsh characteristics. This can be useful for obtaining wave heights for a given coastline if the given coastline's conditions fall within the range of hydraulic conditions and salt marsh characteristics that were used as inputs for the results produced in this study.

In an attempt to answer the second research question, the Xbeach results were implemented into the Netica, and a predictive network was created in order to attempt to forecast probability distributions for wave heights based on a given set of conditions. The results produced by Netica did represent those of Xbeach in probabilistic form by producing the highest probability in the bin where the Xbeach result was located for all distances except one when looking at the most and least extreme hydraulic conditions and the strongest and weakest stem properties. However, it is difficult to state if the second research question could be answered since accuracy was not quantified for the BN, and the validity check was not performed.

In order to answer the third and final research question and identify relationships between the various salt marsh characteristics, hydraulic conditions, and wave attenuation, both the XBeach results and the Netica results were reviewed. Netica was also used to identify dependencies within the network by isolating the different salt marsh components of the network to see the influence that each component has on the wave height distributions (Figure 58). By reviewing the XBeach results (Figures 41-46) and the Netica results (Figures 49-53, 58), trends were found and confirmed with those found in literature which relate salt marsh stem properties to wave attenuation. In addition, the importance of the salt marsh platform slope was realized. It is believed that the BN could be useful when studying seasonal changes of salt marsh characteristics and hydraulic conditions, since stem properties are weakened during winter months, and hydraulic conditions can

become more extreme as a result of winter storms in certain locations around the world. New values in Netica could easily be selected to produce new results for changing conditions. The following chapter will list conclusions and recommendations based on the work carried out in this report.

7 Conclusions and Recommendations

The quantification of wave attenuation by vegetation was carried out in order to test if this physical process could be performed efficiently by using both a numerical model (XBeach-vegetation) and a BN (Netica). Initially, the numerical model was calibrated based on recorded wave heights over a salt marsh in the Netherlands. Next, this model was tested based on flume data which recorded wave heights over natural salt marsh which was installed in one of the largest wave flumes in the world in Hannover, Germany. Once the model was calibrated, tested, and validated, it could be used to produce many different simulations using input parameters of various salt marsh characteristics and hydraulic conditions. The results of these simulations were analyzed and then input into a statistical BN. The salt marsh components of the network were compared through performance of a sensitivity analysis, and the resulting wave heights of before and after input in to the BN were compared. Finally, the results were discussed to highlight important findings produced by Xbeach and Netica.

7.1 Conclusions

It was found that by using the numerical model (XBeach-vegetation), wave attenuation by global coastal salt marsh habitats could be efficiently quantified for extreme hydraulic conditions. Once the proper input parameters were found in the calibration stage, the model was able to reproduce wave heights which were within several centimeters of those recorded in the field. Additionally, by using the stationary mode of XBeach and running it in its 1-dimensional form, thousands of simulations were performed in order to produce a table containing wave heights at various distances over a salt marsh. This method proved to produce results that are both efficient in regards to time and effective since they can be used for studies on coastlines whose salt marsh characteristics and hydraulic conditions fall between the ranges of the values used in this study. Even by running XBeach for many different combinations of salt marsh characteristics and hydraulic conditions, relationships between salt marsh characteristics and wave heights could be made similar to those found in the literature within this research field. For instance, by reviewing the XBeach results it was found that incoming wave height and water level were more influential and important for steep slopes (i.e., 1/20), while for gradual slopes (i.e., 1/2000) stem properties proved to be of higher importance when looking at resulting wave heights over a salt marsh platform.

By inputting the Xbeach results into Netica, a BN was formed in order to attempt to predict probability distributions for wave heights based on various salt marsh characteristics and hydraulic parameters. Once the numerical model results were reviewed and input into the BN, the network could be tested to see how using it compared to only looking at the numerical model results. Netica was successful in reproducing the behavior of the numerical model (XBeach-vegetation) results, and similar trends in the data could be noticed. By isolating the various salt marsh characteristic nodes and testing how different values produced different probability distributions in the child nodes, knowledge could be gained and relationships could be made on how dependent a certain wave height is at certain distances to the salt marsh components. It was found that the greatest variation occurs when looking at different slope values, followed by stem density, stem height, and stem diameter. By taking notice of this variation, the importance of the accuracy of salt marsh slope data was realized.

However, it should be noted that the use of the BN for producing accurate quantification of wave attenuation by salt marshes is still not well proven. The results produced by Netica represent the behavior of the Xbeach results, however the values provided do not appear to be ready for use in practical applications. Since the BN produces probabilistic results, the uncertainty must be quantified. In this report, quantification on uncertainty by the BN was not performed. Given the computational efficiency and accuracy of the XBeach-vegetation model, it is difficult to argue at this point that the BN is better equipped to predict wave attenuation by salt marsh habitats around the world. It is concluded at this point that the BN does not provide any new knowledge that cannot

already be obtained by using the XBeach-vegetation model in regards to quantifying wave attenuation by vegetation.

7.2 Recommendations

The numerical model XBeach-vegetation was successfully used to efficiently produce results for wave attenuation by vegetation and the statistical BN (Netica) was successfully used to represent the behavior of the XBeach results, but many opportunities exist for improvement of this method. These include:

- If the BN is a tool to be used for assessing the ability of a certain coastline to attenuate waves, then it is recommended to further validate it using the Log Likelihood Ratio (LLR) and the k-fold approach (seen in Gutierrez *et al.* (2015)) to quantify the uncertainty of the network, and score its predictive ability while quantifying its limitations. The overfitting ratio (calibration error rate/validation error rate) should be calculated in order to find the optimal number of bins necessary for creating a model that is not only well calibrated but also applicable to other locations around the world. If the uncertainty of the BN could be quantified, then perhaps it could be incorporated into the design of nature-based flood defense measures.

- It is also recommended to consider calculating wave run-up at the end of the end of the salt marsh platform as an output variable within the BN instead of wave heights at various distances over the salt marsh platform.

- The XBeach-vegetation results used as input for the Bayesian Network were produced using the stationary mode of XBeach, which neglects infragravity waves in the simulations. Furthermore, the consideration of infragravity waves when running a large-scale simulation to measure wave attenuation for various salt marsh characteristics and hydraulic conditions is recommended.

- It is additionally recommended to record wave heights over 1 meter and over-marsh water levels of 2.5 meters (produced by large winter storms and hurricanes) over distances of greater than 50 meters to be used for XBeach calibration and validation.

- An additional recommendation is to calculate the C_D using the Möller *et al.* (2014) equation not only at the start of the marsh edge, but also at each timestep of the model domain in order to reduce model error and uncertainty. As mentioned in Chapter 4.2, the drag coefficient can significantly vary from the seaward edge of the salt marsh to the most landward end of the salt marsh platform.

- It is also recommended to use a similar method as was used in this study, but look at salt marsh slopes in the range of 1/500 to 1/1500 in order to prevent a steep slope such as 1/20 slope from significantly impacting the results of the BN.

- If salt marshes are to be incorporated in to flood defense measures, then wave attenuation ability of salt marshes must be known when they are at their weakest state (winter season). A detailed seasonal variation study could be performed for regions which have harsh winters (e.g., England, the Netherlands, northeastern United States, and Canada). The BN could assist in showing seasonality differences for a given area if the stem properties in the area were recorded in both the summer and winter seasons.

8 References

About Ecosystems. (n.d.). Retrieved May 24, 2016, from http://www.unep.org/ecosystemmanagement/

Anderson, M.E., Smith, J.M. & Mckay, S.K. (2011). *Wave Dissipation by Vegetation*.US Army Engineer Research and development center.

Bosboom, J., & Stive, M. J. F. (2015). *Coastal Dynamics I*. Delft University of Technology.

Cain, J. L., & Cohen, R. A. (2014). Using sediment alginate amendment as a tool in the restoration of Spartina alterniflora marsh. *Wetlands Ecology and Management*, *22*(4), 439–449. http://doi.org/10.1007/s11273-014-9345-7

Coastal Ecosystems. (2015). Retrieved May 24, 2016, from https://maxwatsongeography.wordpress.com/section-a/coastal-environments/coastal-ecosystems/

Coastal Resilience. (n.d.). Retrieved May 31, 2016, from http://coastalresilience.org/our-approach/identify-solutions/coastal-defense/

Cronk, J. K., & Fennessy, M. S. (2001). Wetland plants : Biology and ecology. Boca Raton, Fla.: Lewis Publishers. http://www.crcnetbase.com/isbn/9781420032925

Dalrymple, B. R. a, Asce, M., & Kirby, J. T. (1984). Wave Diffraction Due To Areas, *110*(1), 67–79.

Dean, R. G., & Bender, C. J. (2006). Static wave setup with emphasis on damping effects by vegetation and bottom friction. *Coastal Engineering*, *53*(2-3), 149–156. http://doi.org/10.1016/j.coastaleng.2005.10.005

Delta Data Viewer. (n.d.). Retrieved May 25, 2016, from http://fast.openearth.eu/Discover Life. (n.d.). Retrieved May 24, 2016, from http://www.discoverlife.org/

Doody, P. (2008). *Saltmarsh conservation, management and restoration*. (B. Haq, Ed.). Brampton, UK: Springer.

Estuaries. (n.d.). Retrieved May 24, 2016, from http://oceanservice.noaa.gov/education/kits/estuaries/estuaries08_natdisturb.html

European Commission, Joint Research Centre (2016): European Extreme Storm Surge level - Historical. European Commission, Joint Research Centre (JRC). http://data.europa.eu/89h/0026aa70-cc6d-4f6f-8c2f-554a2f9b17f2

Gedan, K. B., Kirwan, M. L., Wolanski, E., Barbier, E. B., & Silliman, B. R. (2011). The present and future role of coastal wetland vegetation in protecting shorelines : answering recent challenges to the paradigm, 7–29. http://doi.org/10.1007/s10584-010-0003-7

Gutierrez, B.T., Plant, N. G., Thieler, E.R., & Turecek, A. (2015). Using a bayesian network to predict barrier island geomorphologic characteristics. J. Geophys. Res. Earth Surf., 120, 2452-2475, doi:10.1002/2015JF003671.

Hartig, E. K., Gornitz, V., Kolker, A., Mushacke, F., & Fallon, D. (2002). Anthropogenic and climate-change impacts on salt marshes of Jamaica Bay, New York City. *Wetlands*, *22*(1), 71–89. http://doi.org/10.1672/0277-5212(2002)022[0071:AACCIO]2.0.CO;2

Jadhav, R. S., & Chen, Q. (2013). Probability distribution of wave heights attenuated by salt marsh vegetation during tropical cyclone. *Coastal Engineering*, *82*, 47–55. http://doi.org/10.1016/j.coastaleng.2013.08.006

Jadhav, R.S., Chen, Q., Smith, J.M. (2013). Spectral distribution of wave energy dissipation by salt marsh vegetation. *Coastal Engineering*, 77, 99-107.

Knutson, P. L., Brochu, R. A., & See, W. N. (1982). Wave Damping in Spartina alterniflora Marshes, (1978), 87–104.

Leonard, L., Wren, P., & Beavers, R. (2002). Flow dynamics and sedimentation in *Spartina alterniflora* and *Phragmites australis* marshes of the Chesapeake Bay. *Wetlands*, *22*(2), 415–424. http://doi.org/10.1672/0277-5212(2002)022[0415:FDASIS]2.0.CO;2

Lovelace, J. K. (1994). Storm-Tide Elevations Produced By Hurricane Andrew Along the Louisiana Coast, August 25-27,1992. *U.S. Geological Survey*.

"National Hurricane Center." *National Weather Service*. N.p., 24 Apr. 2009. Web. 27 May 2016.

Mendez, F.J., Losada, I.J. (2004). An empirical model to estimate the propagation of random breaking and nonbreaking waves over vegetation fields. *Coastal Engineering*, 51, 103–118.

Mendez, F.J., Losada, I.J., Losada, M.A. (1999). Hydrodynamics induced by wind waves in a vegetation field. *Journal of Geophysical Research: Oceans (1978-2012), 104,* 18383-18396.

Minello, T.J., Rozas, L.P., Baker, R. (2012). Geographic Variability in Salt Marsh Flooding Patterns may Affect Nursery Value for Fishery Species Atlantic Ocean. *Estuaries and Coasts, 35,* 501–514.

Möller, I. (2006). Quantifying saltmarsh vegetation and its effect on wave height dissipation : Results from a UK East coast saltmarsh. , 69.

Möller, I., Kudella, M., Rupprecht, F., Spencer, T., Paul, M., van Wesenbeeck, B.K., Wolters, G., Jensen, K., Bouma, T.J., Miranda-Lange, M., and Schimmels, S. (2014). Wave attenuation over coastal salt marshes under storm surge conditions. Nature Geoscience. DOI: 10.1038/NGEO2251

Nepf, H. M. (2011). *Flow Over and Through Biota*. *Treatise on Estuarine and Coastal Science* (Vol. 2). Elsevier Inc. http://doi.org/10.1016/B978-0-12-374711-2.00213-8

Netto, S. A., & Lana, P. C. (1997). Intertidal zonation of benthic macrofauna in a subtropical salt marsh and nearby unvegetated flat (SE Brazil). *Hydrobiologia*, *353*, 171–180. http://doi.org/10.1023/A:1003090701675

Norsys Software Corp. (1997). *Netica - Application for Belief Networks and Influence Diagrams - User's Guide*.

Peek, K. M., & Young, R. S. (2013). Understanding the Controls on Storm Surge through the Building of a National Storm Surge Database. *Journal of Coastal Research*, *291*, 17–24. http://doi.org/10.2112/JCOASTRES-D-12-00249.1

Pennings, S. C., & Bertness, M. D. (1999). Salt Marsh Communities.

Portal:THESEUS. (n.d.). Retrieved May 24, 2016, from http://www.theseusproject.eu/wiki/

Raabe, E. A., & Stumpf, R. P. (2016). Expansion of Tidal Marsh in Response to Sea-Level Rise: Gulf Coast of Florida, USA. *Estuaries and Coasts*, *39*(1), 145–157. http://doi.org/10.1007/s12237-015-9974-y

Roelvink, D., van Dongeren, A., McCall, R., Hoonhout, B., van Rooijen, A., van Geer, P., … Quataert, E. (2015). XBeach Technical Reference : Kingsday Release.

Rupprecht, F., Kudella, M., Spencer, T., Paul, M., Wolters, G., Jensen, K., … Schimmels, S. (2014). Proceedings of the HYDRALAB IV Joint User Meeting, Lisbon, July 2014 Wave Dissipation and Transformation Over Coastal Vegetation Under Extreme Hydrodynamic Loading, (July), 1–6.

Schiereck, G. J., Verhagen, H.J. (2012). *Introduction to bed, bank and shore protection.*Delft: VSSD.

Simas, T., Nunes, J. P., & Ferreira, J. G. (2001). Effects of global climate change on coastal salt marshes, *139*, 1–15.

Spalding, M. D., Mcivor, A. L., Beck, M. W., Koch, E. W., Iris, M., Reed, D. J., … Woodroffe, C. D. (2014). Coastal Ecosystems : A Critical Element of Risk Reduction, *7*(June), 293–301. http://doi.org/10.1111/conl.12074

Spencer, T. et al. (1999). Wave Transformation Over Salt Marshes : A Field and Numerical Modelling Study from North Norfolk ,. , pp.411–426.

Sutton-grier, A. E., Wowk, K., & Bamford, H. (2015). ScienceDirect Future of our coasts : The potential for natural and hybrid infrastructure to enhance the resilience of our coastal communities , economies and ecosystems. *Environmental Science and Policy*, *51*, 137–148. http://doi.org/10.1016/j.envsci.2015.04.006

Suzuki, T. (2011). *Wave dissipation over vegetation fields*. Delft University of Technology, Delft.

Swales, A., MacDonald, I. T., & Green, M. O. (2004). Influence of wave and sediment dynamics on cordgrass (Spartina anglica) growth and sediment accumulation on an exposed intertidal flat. *Estuaries*, *27*(2), 225–243. http://doi.org/10.1007/BF02803380

Tonelli, M., Fagherazzi, S., & Petti, M. (2010). Modeling wave impact on salt marsh boundaries. *Journal of Geophysical Research: Oceans*, *115*(9), 1–17. http://doi.org/10.1029/2009JC006026

U. S. Fish and Wildlife Service. (2016). National Wetlands Inventory website. U.S. Department of the Interior, Fish and Wildlife Service, Washington, D.C. http://www.fws.gov/wetlands/

van Loon-Steensma, J. M. (2015). Salt marshes to adapt the flood defences along the Dutch Wadden Sea coast. *Mitigation and Adaptation Strategies for Global Change*, *20*(6), 929–948. http://doi.org/10.1007/s11027-015-9640-5

van Rooijen, A. A., van Thiel de Vries, J. S. M., McCall, R. T., van Dongeren, A. R., Roelvink, J. A., & Reniers, A. J. H. . (2015). Modeling of Wave Attenuation by Vegetation With XBeach, 1–7.

van Verseveld, H. C. W. Van, Dongeren, A. R. Van, Plant, N. G., Jäger, W. S., & Heijer, C. Den. (2015). Modelling multi-hazard hurricane damages on an urbanized coast with a Bayesian Network approach. *Coastal Engineering*, *103*, 1–14. http://doi.org/10.1016/j.coastaleng.2015.05.006

Vegetation–microclimate feedbacks in woodland–grassland ecotones - Scientific Figure on ResearchGate. Available from: https://www.researchgate.net/263369200_fig2_Figure-6-Global-distribution-of-mangroves-and-salt-marshes-Redrawn-after-Chapman-1975 [accessed 28 May, 2016]

Vuik, V., Jonkman, S.N., Borsje, B.W., & Suzuki, T. (2016). Nature-based flood protection: the efficiency of vegetated foreshores for reducing wave loads on coastal dikes. *Coastal Engineering* (accepted), http://doi.org/10.1016/j.coastaleng.2016.06.001

Wamsley, T. V., Cialone, M. A., Smith, J. M., Atkinson, J. H., & Rosati, J. D. (2010). The potential of wetlands in reducing storm surge. *Ocean Engineering*, *37*(1), 59–68. http://doi.org/10.1016/j.oceaneng.2009.07.018

Wood, N., & Hine, A. C. (2007). Spatial Trends in Marsh Sediment Deposition Within a Microtidal Creek System, Waccasassa Bay, Florida. *Journal of Coastal Research*, *23*(4), 823–833. http://doi.org/10.2112/04-0243.1

Yang, S. L., Shi, B. W., Bouma, T. J., Ysebaert, T., & Luo, X. X. (2012). Wave Attenuation at a Salt Marsh Margin : A Case Study of an Exposed Coast on the Yangtze Estuary, 169–182. http://doi.org/10.1007/s12237-011-9424-4

Appendix A: Calibration Data

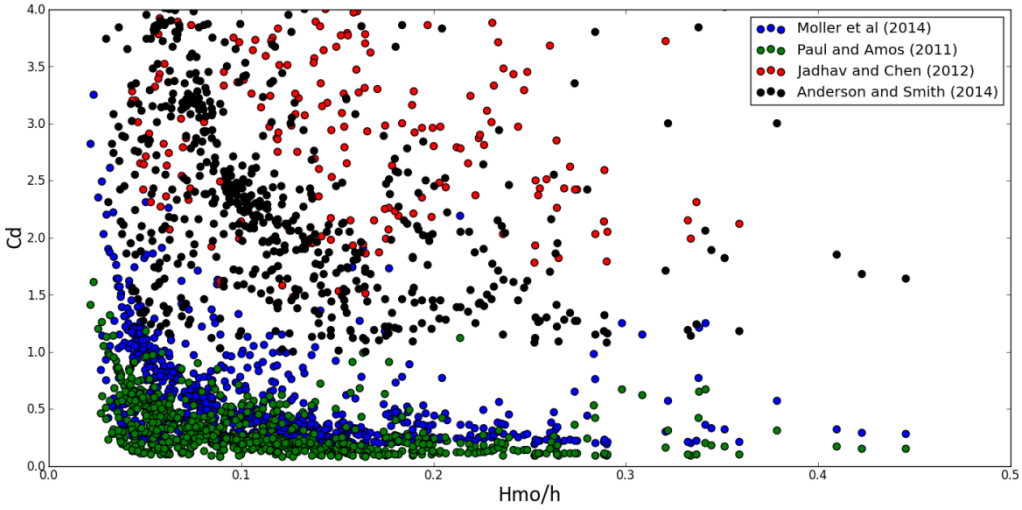

Figure A-1: The relation between the drag coefficient and the significant wave height to water depth ratio based on various equations in literature at wave sensor 3 for all bursts at Hellegat.

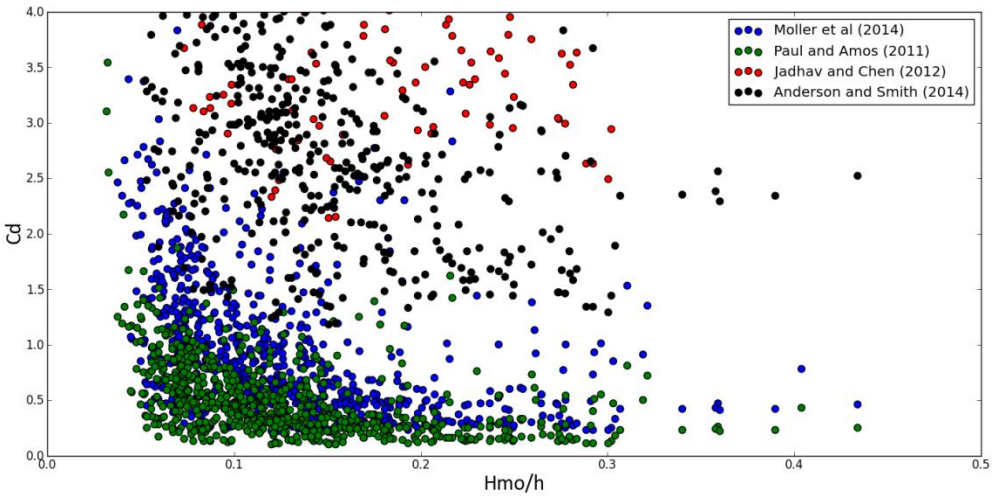

Figure A-2: The relationship between the drag coefficient and the significant wave height to water depth ratio at wave sensor 4 for all bursts at Hellegat.

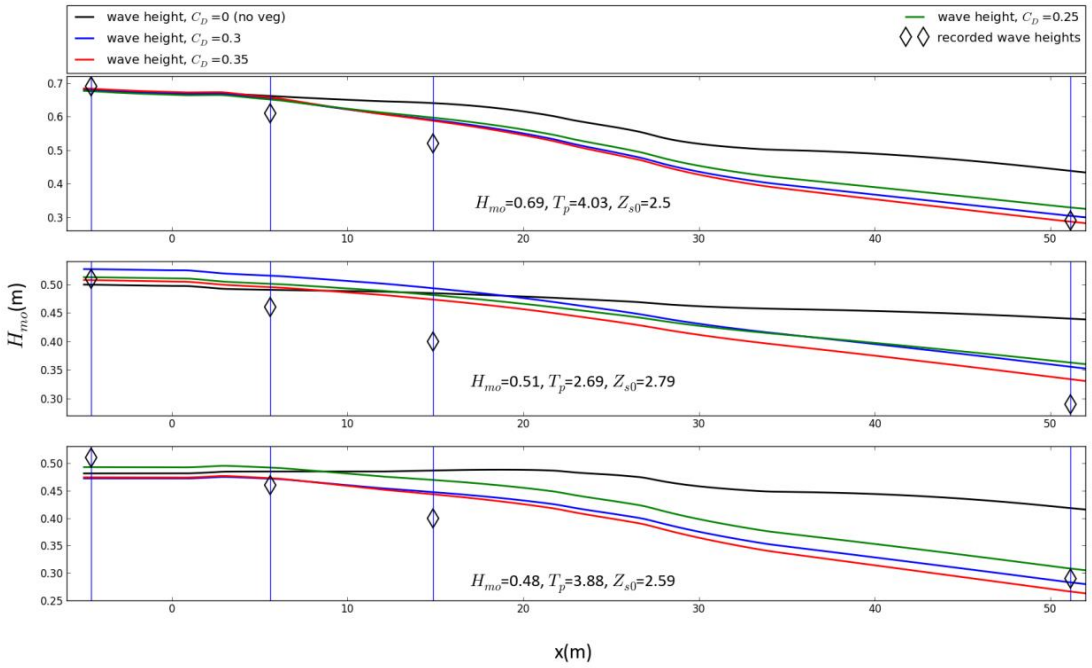

Figure A-3: Highest wave conditions analyzed for calibration using a gamma = 0.55.

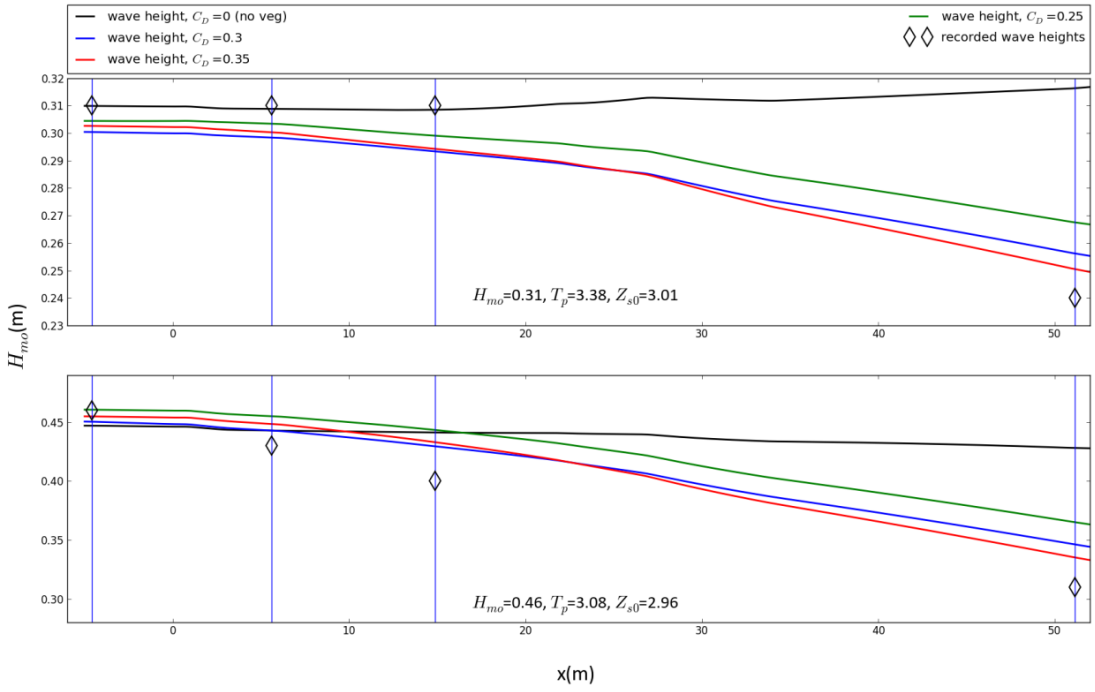

Figure A-4: Highest water level conditions analyzed for calibration using a gamma = 0.55.

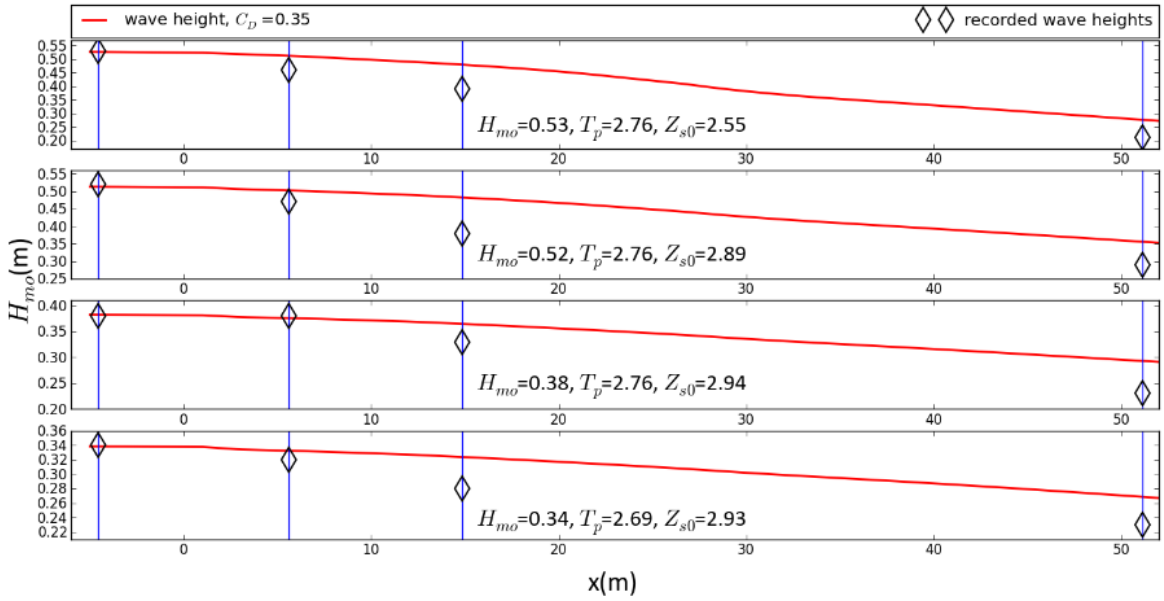

Figure A-5: Model results for the Hellegat site using a conservative value for C_D.

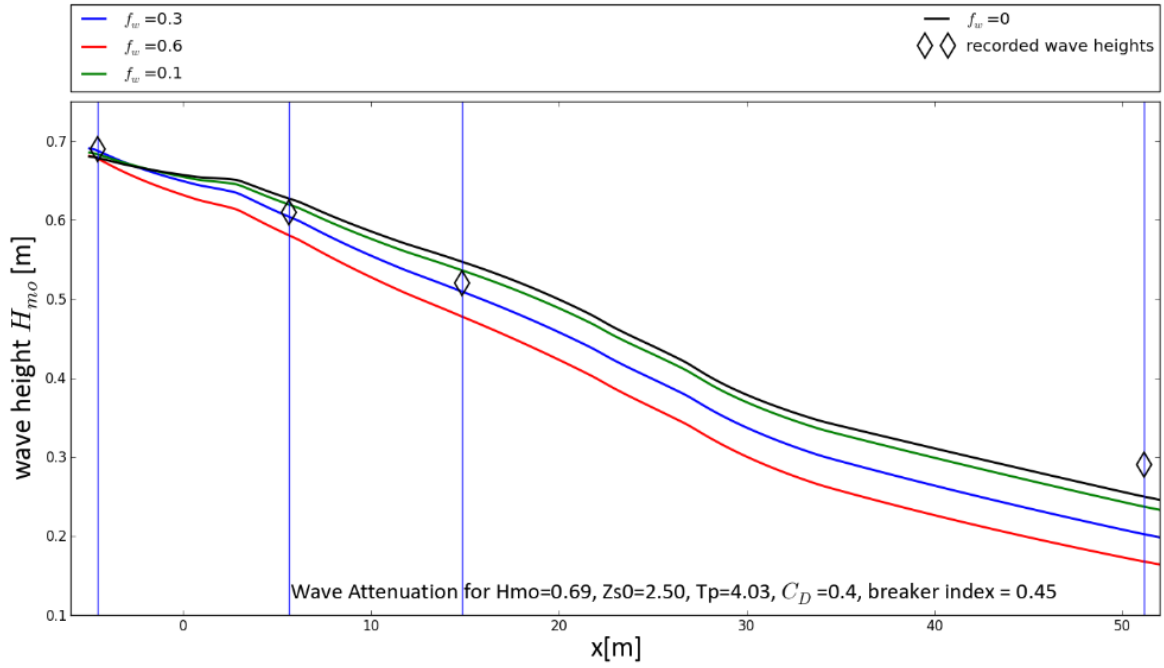

Figure A-6: Sensitivity for the bed friction (f_w).

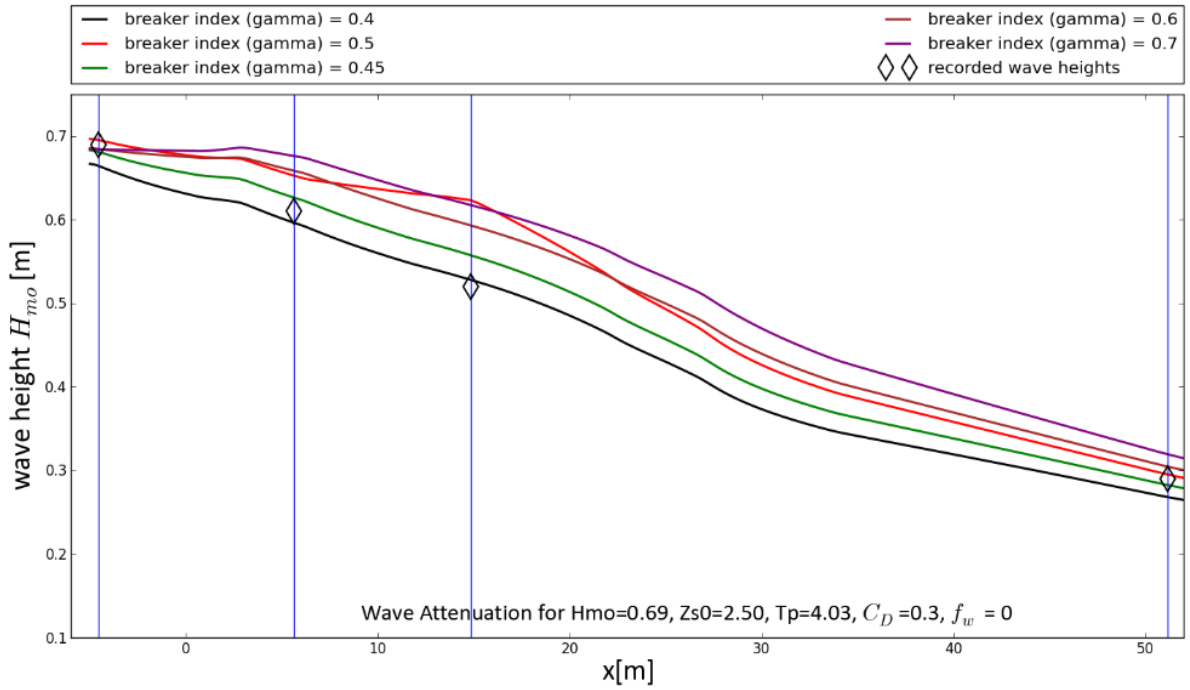

Figure A-7: Sensitivity testing for the breaker index (γ_{break}).

Table A-1: Hs and slope errors when varying the γ_{break} (gamma) parameter in XBeach.

		Difference (Hs model - Hs data)		Rms Error		Slope (data)	Slope (Model)	Rms Error
Run	γ	S2	S3	S2	S3			
1s	0.4	-5.62E-03	6.21E-03	1.58E-05	1.93E-05	-6.38E-03	-5.20E-03	1.18E-03
3s	0.5	3.34E-02	7.32E-02	5.57E-04	2.68E-03	-6.38E-03	-2.40E-03	3.98E-03
4s	0.45	1.64E-02	2.62E-02	1.34E-04	3.43E-04	-6.38E-03	-5.40E-03	9.83E-04
26s	0.55	3.34E-02	4.22E-02	5.57E-04	8.91E-04	-6.38E-03	-5.50E-03	8.83E-04

Table A-2: The calcluated mean, standard deviation, high and low values based on four drag coefficient values from the literature for the recorded wave heights at Hellegat.

	Cd	MÖller et al (2014)	Paul and Amos (2011)	Jadhav and Chen (2012)	Anderson and Smith (2014)
Sensor 3	Mean	0.62	0.33	6.87	3.08
	Std. Dev.	0.43	0.23	3.73	1.68
	High	1.05	0.56	10.6	4.76
	Low	0.19	0.1	3.14	1.4
Sensor 4	Mean	0.96	0.51	9.6	4.35
	Std. Dev.	0.72	0.35	4.88	2.44
	High	1.68	0.86	14.54	6.79
	Low	0.24	0.16	4.72	1.91

Appendix B: Data Collection for Salt Marshes

Figure B1: The National Wetlands Inventory (U.S. Fish and Wildlife Service)

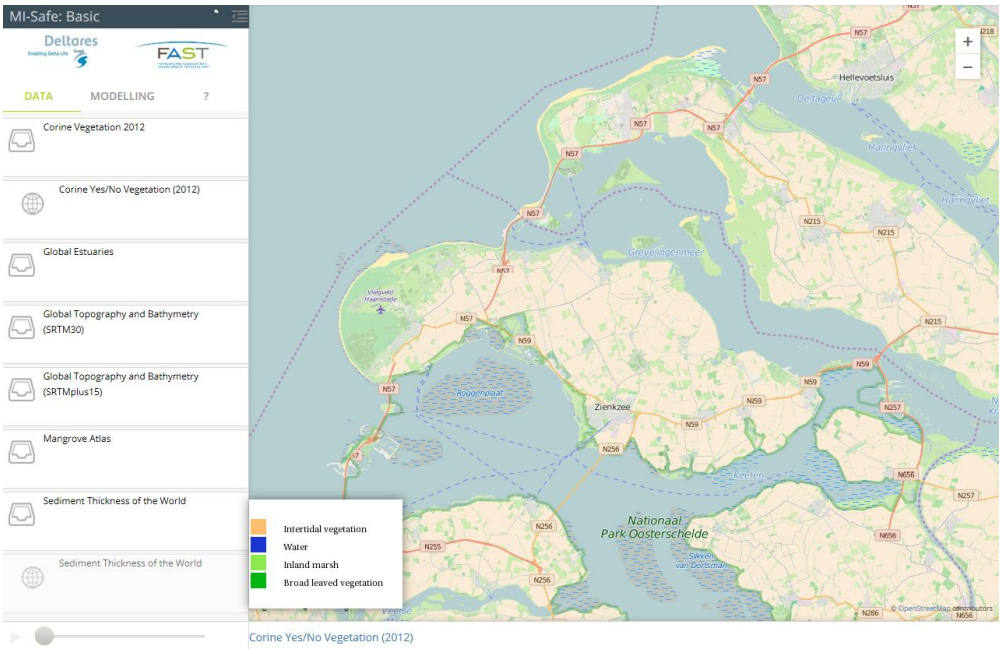

Figure B2: The Mi-Safe Basic viewer, part of the Delta Data Viewer (Deltares and EU-FAST project)

Table B-1: Collected salt marsh data from various sources.

Location	Source									
Europe		Slope	Slope (offshore only)	Slope (marsh only)	Marsh Width (m)	Stem ht (m)	Stem density (stems/m^2)	Stem diameter (mm)	Latitude	Longitude
Netherlands-Paulina					300	0.3-0.7	42, (40-600)	2.38	51°21'1.66"N	3°43'2.40"E
England-Tillingham (site 2)	FAST project data	1/500			1000		294		51°40'39.97"N	0°56'10.45"E
England-Donna Nook (site 1)	FAST project data	1/285			1200	0.185	10.32	3.53	53°30'33.77"N	0° 4'43.49"E
Spain-Cadiz	FAST project data	1/250				0.27	591	3.5	36°30'37.56"N	6°10'12.30"W
Romania-Danube	FAST project data	1/400			430	2.6	77	9.48	44°45'17.9"N	28°56'26.45"E
Hellegat, Western Scheldt, NL	Vuik, et al. (2016)	1/40			200	0.25	1200	3.0	51 21 58.31 N	03 57 04.13 E
Lisbon, Portugal	Simas and Ferreira, 2001				1000		480-2500		38 N	9 W
USA										
Ten Thousand Islands, FL		1/6000			5500					
Homosassa, FL	Raabe and Stumpf (2016)	1/2500			18000				25 51 35.36 N	81 28 52.76 W
Savannah River, GA, USA	Cain and Cohen (2014)				8530	0.56	370		28 48 12.80 N	82 39 32.78 W
Wescoat, Chesapeake Bay, VA	Leonard and Beavers (2002), Knutson et al. (1982)	1/30				0.52	214.25	3.93	31 59 27.29 N	80 54 25.70 W
Kings Creek, Chesapeake Bay, VA	Knutson et al. (1982)	1/100				0.40	299.67	3.8		
Cape Charles, VA, USA	Tonelli et al. (2010)				15000					
Cape Island, SC, USA					9000				37 20 49.79 N	75 47 15.46 W
Plaq. Parish/St. Bern. Par. LA					45000				33 03 38.32 N	79 24 42.18 W
Terrebonne Bay, Louisiana, USA	Jadhav and Chen (2013)	1/1000			30330	0.22	422	8	29 39 30.72 N	89 41 39.39 W
Waccasassa Bay, FL	Raabe and Stumpf (2016); Wood and Hine (2007)	1/4500			5250		400, 520		29°15'14.72"N	90°44'57.69"W
Kittery Point, ME									29 08 53 N	82 47 30 W
Ogunquit River, ME										
Jamaica Bay, NY	Hartig et al (2002)	1/400				1.0117				
Aransas Bay, TX	Minello et al (2012)	1/111	1/120	1/80						
Galveston Bay, TX	Minello et al (2012)	1/77	1/75	1/80						
Sabine Lake, TX/LA	Minello et al (2012)	1/111	1/120	1/100						
Timbalier Bay, LA	Minello et al (2012)	1/30	1/20	1/400						
Barataria Bay, LA	Minello et al (2012)	1/125	1/120	1/133						
Bay St. Louis, MS	Minello et al (2012)	1/45	1/35	1/67						
West Bay, LA	Minello et al (2012)	1/45	1/38	1/57						
Cedar Key, FL	Minello et al (2012)	1/50	1/86	1/30						
Chicopit Bay, FL	Minello et al (2012)	1/40	1/50	1/30						
St. Simons Sound, GA	Minello et al (2012)	1/12	1/10	1/20						
Charleston Bay, SC	Minello et al (2012)	1/12	1/6	1/27						
Wrightsville Beach, NC	Minello et al (2012)	1/37	1/30	1/57						
Newport River, NC	Minello et al (2012)	1/42	1/38	1/50						
Pamlico Sound, NC	Minello et al (2012)	1/63	1/60	1/67						
Lower Chesapeake Bay, VA	Minello et al (2012)	1/34	1/29	1/57						
Argentina										
Bahia Blanca Estuary									38 45 S	61 45 W
China										
Yangtze Estuary	Yang et al (2012)	1/80			3400	0.84, 0.38	334, 2352	5.2, 2.2	31 28 N	122 E
Quanzhou Bay						1.21	100	6.65	24 58 N	118 58 E
Brazil										
Paranagua Bay, Brazil	Netto and Lana (1997)	1/200								
New Zealand										
Manukau Harbor, Auckland, New Zealand					20	0.10625	2317			

Table B-2: Veg. factor calculations to ensure no combinations were repeated

ah	N	bv	Veg. factor
0.4	100	3	120
0.4	100	6	240
0.4	100	9	360
0.4	500	3	600
0.4	500	6	1200
0.4	500	9	1800
0.4	1000	3	1200
0.4	1000	6	2400
0.4	1000	9	3600
0.7	100	3	210
0.7	100	6	420
0.7	100	9	630
0.7	500	3	1050
0.7	500	6	2100
0.7	500	9	3150
0.7	1000	3	2100
0.7	1000	6	4200
0.7	1000	9	6300
1.3	100	3	390
1.3	100	6	780
1.3	100	9	1170
1.3	500	3	1950
1.3	500	6	3900
1.3	500	9	5850
1.3	1000	3	3900
1.3	1000	6	7800
1.3	1000	9	11700

Appendix C: Final XBeach Simulations and Bayesian Network Data

Table C-1: Preliminary sensitivity of the resulting wave heights at the various locations to the change in vegetation parameters.

	Hrms	Trep	zs0	dw	slope	stem height	stem density	stem diam	Hrms 100	Hrms 250	Hrms 500	Hrms 1000
	1	4.5	3.2	1000	500	0.4	100	0.003	0.808	0.708	0.592	0.364
	1	4.5	3.2	1000	500	0.4	500	0.003	0.772	0.643	0.492	0.244
	1	4.5	3.2	1000	500	0.4	1000	0.003	0.728	0.56	0.372	0.145
	1	4.5	3.2	1000	500	0.7	100	0.006	0.788	0.672	0.539	0.304
	1	4.5	3.2	1000	500	0.7	500	0.006	0.675	0.472	0.277	0.094
	1	4.5	3.2	1000	500	0.7	1000	0.006	0.557	0.325	0.165	0.049
	1	4.5	3.2	1000	500	1.3	100	0.006	0.76	0.62	0.454	0.202
	1	4.5	3.2	1000	500	1.3	500	0.006	0.56	0.33	0.167	0.05
	1	4.5	3.2	1000	500	1.3	1000	0.006	0.408	0.201	0.091	0.04
most extreme hydraulic condition	2.5	7.1	5	2000	2000	1.3	1000	0.009	0.736	0.382	0.222	0.184
least extreme hydraulic condition	0.5	3.2	3.2	2000	2000	1.3	1000	0.009	0.31	0.187	0.108	0.053
most extreme hydraulic condition	2.5	7.1	5	2000	2000	0.4	100	0.003	1.61	1.42	1.28	1.15
least extreme hydraulic condition	0.5	3.2	3.2	2000	2000	0.4	100	0.003	0.495	0.487	0.474	0.446

Table C-2: Stem density influence on the average wave heights across the salt marsh platform for all of the simulations

	Average of Hrms_100	Average of Hrms_250	Average of Hrms_500	Average of Hrms_1000	Average of Hrms_2000
100	0.707718423	0.545929552	0.36107361	0.271610344	0.138760287
500	0.61050038	0.413684519	0.232700451	0.141324324	0.058120935
1000	0.527096571	0.329061797	0.171935056	0.101222212	0.043542201
Grand Total	**0.614519068**	**0.429082011**	**0.254902992**	**0.171119268**	**0.079998329**

Table C-3: Stem height influence on the average wave heights across the salt marsh platform for all of simulations.

	Average of Hrms_100	Average of Hrms_250	Average of Hrms_500	Average of Hrms_1000	Average of Hrms_2000
0.4	0.665875134	0.486967656	0.301314693	0.209801566	0.10082691
0.7	0.624853729	0.434809191	0.256747935	0.170406327	0.078030514
1.3	0.554572144	0.366793748	0.207487738	0.133743778	0.061420976
Grand Total	**0.614519068**	**0.429082011**	**0.254902992**	**0.171119268**	**0.079998329**

Table C-4: Stem diameter influence on the average wave heights across the salt marsh platform for all of the simulations.

	Average of Hrms_100	Average of Hrms_250	Average of Hrms_500	Average of Hrms_1000	Average of Hrms_2000
0.003	0.66054063	0.479191963	0.295220405	0.20347147	0.097347262
0.006	0.610296425	0.42206614	0.24762552	0.163843157	0.07566088
0.009	0.574126598	0.386964251	0.222440534	0.146430554	0.067167739
Grand Total	**0.614519068**	**0.429082011**	**0.254902992**	**0.171119268**	**0.079998329**

Table C-5: Slope influence on the average wave heights across the salt marsh platform for all of the simulations.

	Average of Hrms_100	Average of Hrms_250	Average of Hrms_500	Average of Hrms_1000	Average of Hrms_2000
20	0.058234632	0	0	0	0
100	0.779306728	0.430725028	0.018083312	0	0
500	0.837357315	0.650094136	0.484339056	0.293476451	0.057640641
2000	0.777348086	0.630873735	0.514436019	0.389152111	0.261488494
Grand Total	**0.614519068**	**0.429082011**	**0.254902992**	**0.171119268**	**0.079998329**

Table C-6: Water level influence on the average wave heights across the salt marsh platform for all simulations.

	Average of Hrms_100	Average of Hrms_250	Average of Hrms_500	Average of Hrms_1000	Average of Hrms_2000
3.2	0.468106868	0.302893179	0.178610961	0.113707341	0.044110255
4	0.60123944	0.42849435	0.248778833	0.167496742	0.070454477
5	0.775186887	0.556554884	0.337683016	0.232387583	0.125455037
Grand Total	**0.614519068**	**0.429082011**	**0.254902992**	**0.171119268**	**0.079998329**

Table C-7: Incoming wave height influence on the average wave heights across the salt marsh platform for all simulations.

	Average of Hrms_100	Average of Hrms_250	Average of Hrms_500	Average of Hrms_1000	Average of Hrms_2000
0.5	0.349986761	0.287126924	0.185641994	0.136089969	0.066201086
1	0.58269592	0.421137932	0.25251483	0.167178216	0.075779844
2	0.74460226	0.496987368	0.288595211	0.189282789	0.087249316
2.5	0.780231883	0.511076265	0.293002469	0.192131901	0.090883312
Grand Total	**0.614519068**	**0.429082011**	**0.254902992**	**0.171119268**	**0.079998329**

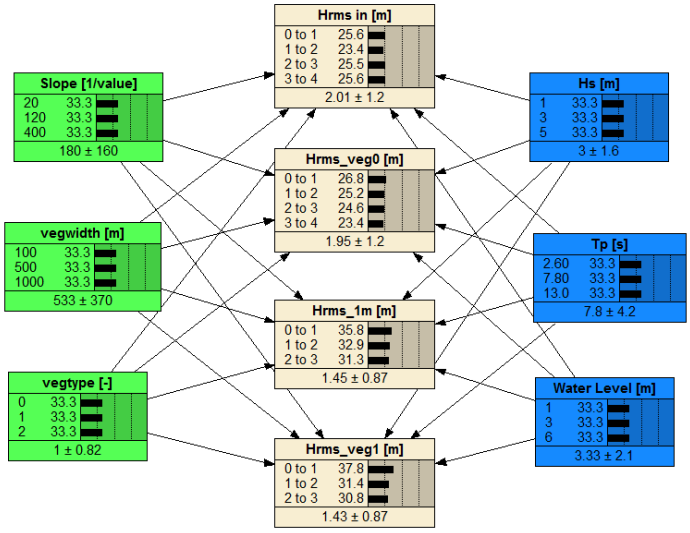

Figure C-1: The compiled network for the simple case of the Bayesian network.

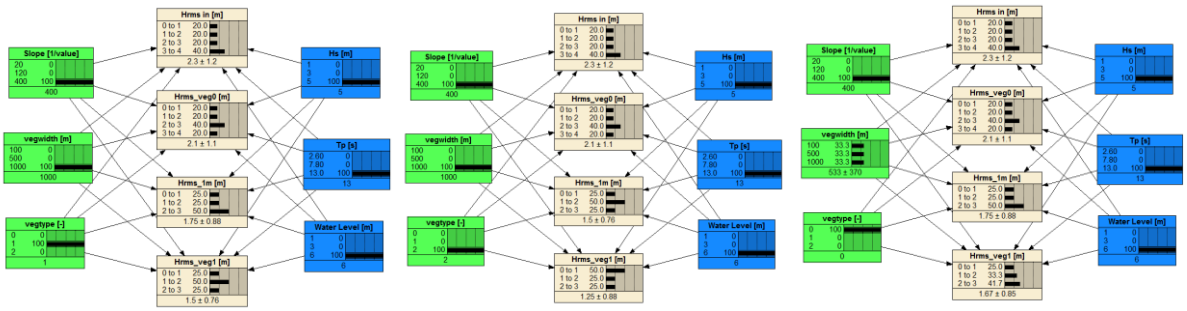

Figure C-2: The simple case when comparing vegetation type for the most extreme condition. A vegtype of 1 represents salt marsh (left figure), while a vegtype of 2 represents mangroves (middle figure), and a vegetation type of 0 mean there is no vegetation present. Hrms_veg1 represents the wave height at the end of the vegetation.

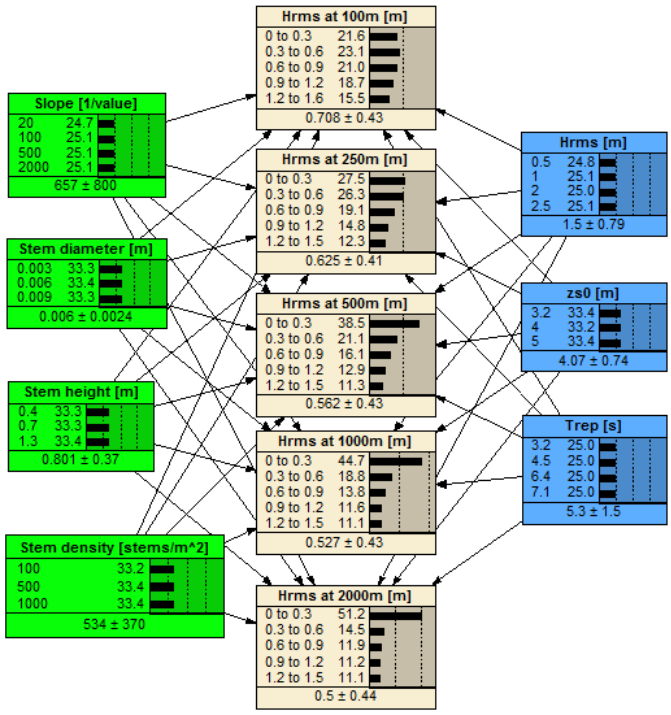

Figure C-3: The original compiled network using 5 bins in the result nodes.

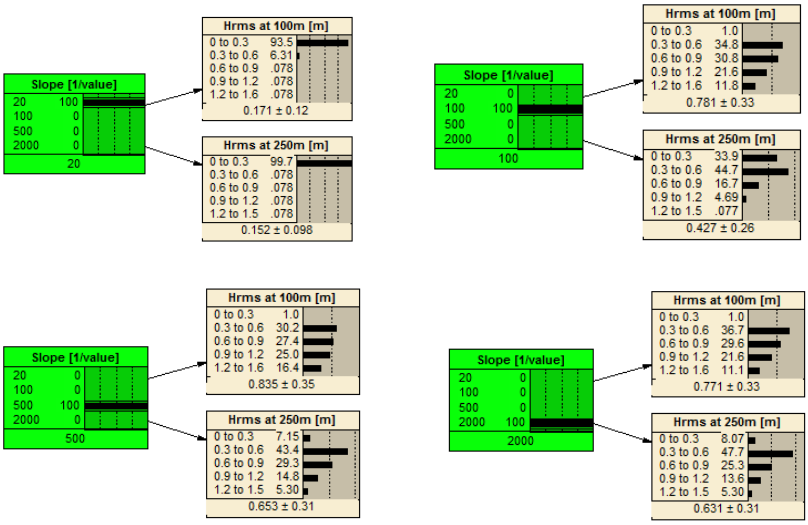

Figure C-4: The probability distributions of the various slopes when only considering the slope, Hrms at 100, and Hrms at 250 nodes as a network.

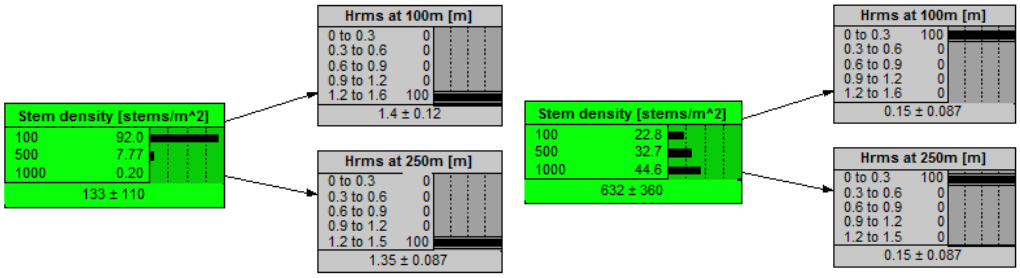

Figure C-5: Stem density sensitivity

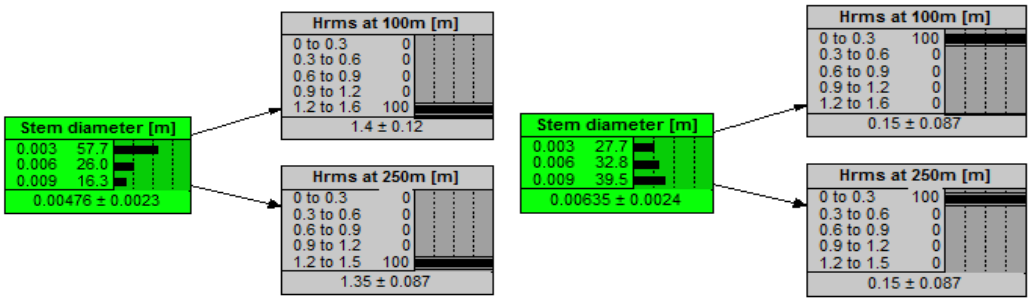

Figure C-6: Stem diameter sensitivity

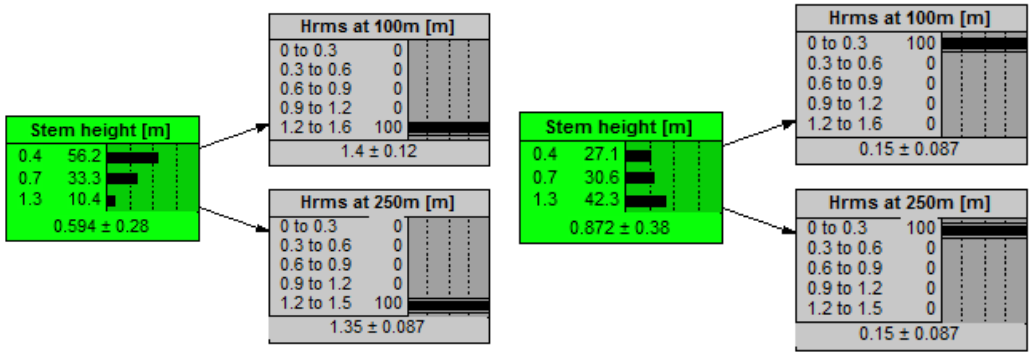

Figure C-7: Stem height sensitivity

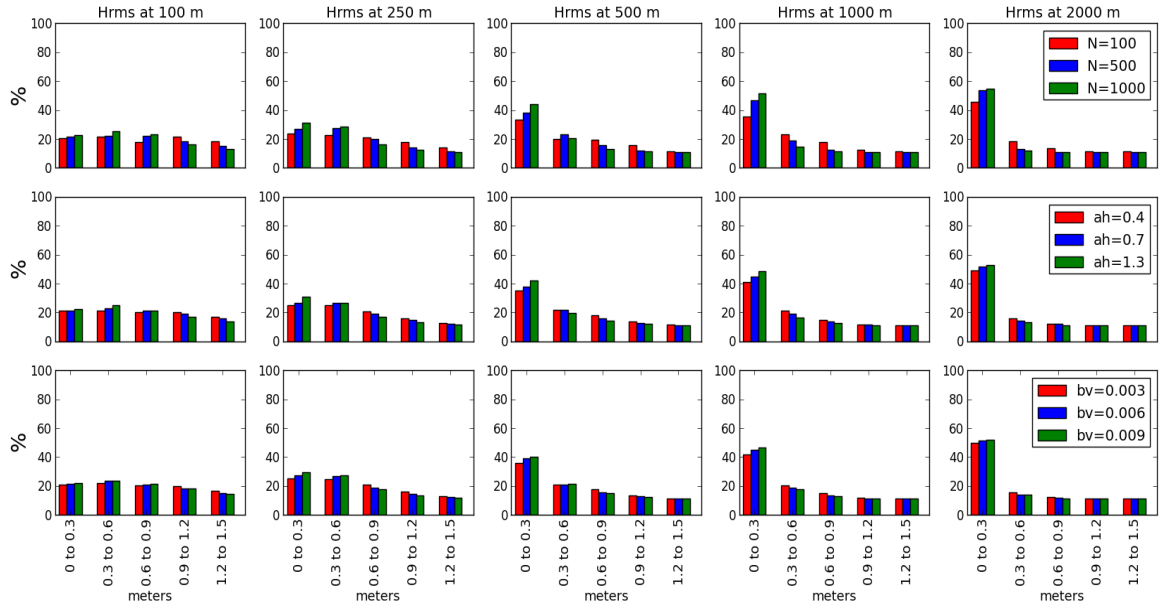

Figure C-8: Sensitivity for stem density (top row), stem height (middle row), and stem diameter (bottom row).

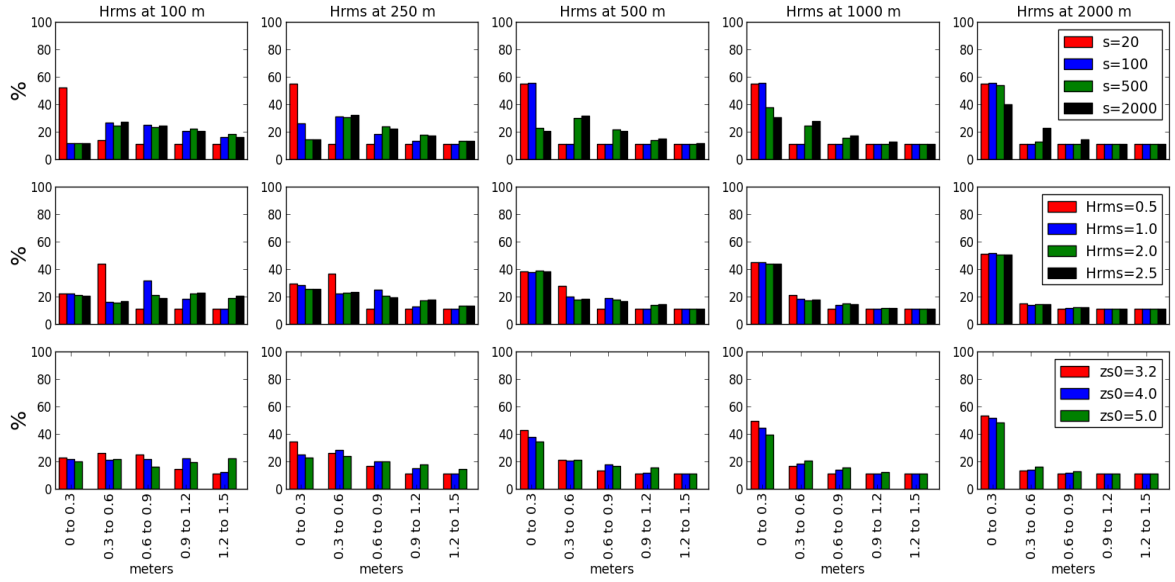

Figure C-9: Sensitivity for slope (top row), incoming wave height (middle row) and incoming water level (bottom row).